The influence of core permeability on armour layer stability

A theoretical research to give the 'notional' permeability coefficient P a more physical basis

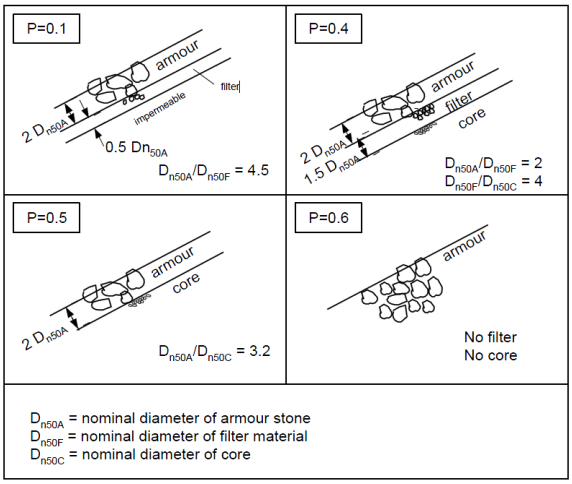

Master of science thesis
by
H.D. Jumelet

Delft
June 2010

Delft University of Technology
Faculty of Civil Engineering and Geosciences
Section of Hydraulic Engineering

DEME
Dredging, Environmental & Marine Engineering
Hydronamic bv

The influence of core permeability on armour layer stability

A theoretical research to give the 'notional' permeability coefficient P a more physical basis

Master of science thesis
by
Daan Jumelet

Delft
June 2010

This research is done for the partial fulfillment of requirements for the Master of Science degree at the Delft University of Technology, Delft, the Netherlands

Graduation Committee:

Prof.dr.ir. M.J.F. Stive	Delft University of Technology / Hydraulic Engineering Section
Ir. H.J. Verhagen	Delft University of Technology / Hydraulic Engineering Section
Prof.dr.ir. W.S.J. Uijttewaal	Delft University of Technology / Environmental Fluid Mechanics Section
Ir. M. van den Broeck	DEME / Head / Research, Method, Production and Engineering Department
Ir. J. Maertens	DEME / Coastal Engineer/ Research, Methods, Production and Engineering Department

Preface

This thesis is presented in order to obtain the Master of Science degree at the Delft University of Technology, faculty Civil Engineering & Geosciences, section Hydraulic Engineering.

I want to take this preface as an opportunity to thank all the people who cooperated in my student time to obtain the degree of Master of Science at Delft University of Technology. At first I want to thank my family, for their unconditional support during my student time. I would also like thank my friends and roommates. Especially Pieter and Emiel, who I have shared my entire study with. The joint preparation for exams, group working and having discussions about our thesis's gave me much support to complete my student time.

From BAM infra consultant I want to thank Markus Muttray. Your enthusiasm for my research, input and experience helped me extraordinary with my thesis. I want to thank my graduation committee for their advice and supervision of my research process. I am very grateful for the guidance and supervision of Henk Jan Verhagen and Wim Uijttewaal. Besides I want to thank my Professor Marcel Stive for leading my graduation committee and also for his guidance during the graduation period. From DEME I want to thank Marc van den Broeck, Geert Vanneste and Jonas Maertens for their advice and support. Finally, I am thankful for the specialists Marcel van Gent (Deltares) and Jentsje van der Meer (Van der Meer Consulting B.V.) for investing their valuable time in my project.

I would like to end this preface with an anecdote about the changing view that I get from a coastal defense system during my life:

My hometown is a small village in the province of Zeeland, Bruinisse, and is surrounded by water (Lake Grevelingen and the Eastern Scheldt). During my childhood, my friends and I were always in the vicinity of the water. Fishing in the winter season and swimming in the summer season. Our regular spot was a pier built of rock (i.e. breakwater) at a harbor inlet in the Eastern Scheldt. The composition of the upper layer (i.e. armour layer) of this pier was everything but comfortable, because the stones were large and sharp. To benefit our comfort we removed this upper layer from our regular spot, with the result that a comfortable finer material (i.e. filter layer) emerged. With this finer material it was much easier to put down your seat while you were fishing and to lay down your towel while you were swimming. We have dropped the stones of the upper layer a few meters from the spot, because we weren't intended to enable the function of these bunch of stones…….

I think I should visit this place soon again and replace the moved stones, because it seems that this top layer plays a quite substantial role.

Daan Jumelet

Delft, June 2010

Abstract

This study describes a theoretical approach of a physical description of the notional permeability factor in the stability formulae of VAN DER MEER [1988]. Caused by the empirical character of these stability formulae a physical description is not available for the notional permeability factor. In practice this leads to ambiguities in determining the value of this factor. To give this factor a physical description a volume-exchange-model was introduced to express the effect of core permeability on the external wave run-up process. This volume-exchange-model couples the external with the internal process. The external process is described by a wave run-up model. In this model the wave run-up wedge approach of HUGHES [2004] is linked to the wave kinematics in front of the structure. The internal process is described by the 'Forchheimer' equation for the water flow through a porous medium.

In this study it is assumed that the notional permeability factor P is highly related to the volume-exchange-model. By coupling the volume-exchange-model with the notional permeability factor this relation is investigated. This coupling is realized by work out the volume-exchange-model for the four defined 'notional permeability structures'. In case of a vertical structure transition the elaboration of the volume-exchange-model works well. For a sloped structure transition the volume-exchange-model is subject to a phase difference between the separate layers. This phenomenon should be studied more extensively. However, in both cases (sloped and vertical structure transition) the correlation between the P-factor and the so-called run-up reduction coefficient c_r (followed from the volume-exchange-model) is clearly visible. With this correlation it is possible to choose a value of the notional permeability factor P that is based on a physical description. Besides this, the study also shows that the permeability of the structure not only depends on structural properties, as stated by VAN DER MEER [1988], but also on the hydraulic parameters. With this consideration the dual permeability notation in the stability formula (for surging waves) is explained.

This report gives a proposal to separate the P-factor from the stability formulae by incorporating the influence of the permeability in the stability formulae in the run-up reduction factor. However, without an additional test program this is in the present form of the volume-exchange-model not possible. Therefore, this report ends with suggestions for recommended tests.

Keywords

Rubble mound breakwater

Core permeability

Notional permeability

Porosity

Turbulent coefficient

Run-up reduction coefficient

Volume-exchange-model

Index

List of Figure

List of Table

Notation

a	1. Amplitude of incident regular wave	[m]
	2. Porous friction coefficient in the Forchheimer equation	[s/m]
a_1-a_4	Empirical curve fitting coefficients	[-]
a'	Porous friction coefficient in the Forchheimer equation (fully turbulent)	[s/m]
a''	Porous friction coefficient in the Darcy equation	[s/m]
A	Fitting coefficients in the run-up formula (CUR/CIRIA [2007])	[-]
b_1	Empirical curve fitting coefficient	[-]
b	Turbulent friction coefficients in the Forchheimer equation	[s^2/m^2]
b'	Porous friction coefficient in the Forchheimer equation (fully turbulent)	[s^2/m^2]
B	Fitting coefficients in the run-up formula (CUR/CIRIA [2007])	[-]
c	Dimensionless friction coefficients in the Forchheimer equation	[m^2/s]
c_g	Group velocity	[m/s]
c_r	Run-up reduction coefficient	[-]
C_D	Drag coefficient in the Morison-type equations	[-]
C_L	Lift coefficient in the Morison-type equations	[-]
C_M	Interia coefficient in the Morison-type equations	[-]
C_{pl}	Coefficient for plunging waves in the Van der Meer formula	[-]
C_r	Wave reflection coefficient, ratio of reflected and incoming wave	[-]
C_s	Coefficient for surging waves in the Van der Meer formula	[-]
d	1. Water depth from bottom to still water level	[m]
	2. Base of a the run-up triangle in the 'new' wave run-up wedge approach	[m]
D	Coefficient to account for seapage length as a result of the deviation of the flow path caused by grains	[m]
D_{15}	Diameter of rock that exceeds the 15% value of sieve curve	[m]
D_{85}	Diameter of rock that exceeds the 85% value of sieve curve	[m]
D_{n50}	Median nominal diameter$\left(= (m_{50}/\rho_s)^{1/3}\right)$	[m]
E_d	Dissipated energy	[J]
E_d	Dissipated energy in body	[J]

$E_{d,s}$	Dissipated energy on slope	[J]
E_i	Energy of the incoming wave	[J]
E_k	Kinetic energy	[J]
E_p	Potential energy	[J]
E_r	Energy of the reflective wave	[J]
g	Gravitational acceleration	[m/s^2]
h	1. Water depth from bottom to still water level	[m]
	2. Water depth from bottom to instantaneous sea surface elevation η	[m]
h_0	Water depth from bottom to still water level	[m]
H	Water depth from bottom to still water level in energy balance of Van der Meer	[m]
H_b	'Body' wave height	[m]
H_r	Wave height of the reflection wave	[m]
H_{slope}	Wave height on the slope	[m]
H_S	Significant wave height, $H_S = H_{1/3}$	[m]
$H_{2\%}$	Wave height, wave height exceeded by only 2% of the waves	[m]
I	Hydraulic gradient	[-]
I_y	Hydraulic gradient in the vertical direction	[-]
k	Wave number, $k = 2\pi/L$	[m^{-1}]
K	Darcy permeability coefficient, hydraulic conductivity	[m/s]
K_P	Reduction factor to account for slope porosity ($K_p = 1$ for impermeable slopes)	[-]
K_M	Unknown constant of proportionality	[-]
K_r	Wave reflection coefficient, ratio of reflected and incoming wave	[-]
L	Local wave length	[m]
L_0	Deep water wave length, $L_0 = gT^2/2\pi$	[m]
m	Mass of water particle	[kg]
m_{50}	Average mass of rock grading, determined by the 50% value on the mass distribution curve	[kg]
M_F	Depth-integrated wave momentum flux across a unit width	[N]
$(M_F)_{max}$	Maximum depth-integrated wave momentum flux across a unit width	[N]

n	Porosity	[-]
n_0-n_1	Empirical curve fitting coefficients	[-]
N	Number of waves in the Van der Meer formula	[-]
P	Notional permeability factor	[-]
R_c	Crest height	[m]
R_D	Run-down level, relative to SWL	[m]
R_e	Reynolds number (UD/ν)	[-]
R_{ep}	Reynolds number related to the diameter of the pores $\left(UD_p/\nu\right)$	[-]
R_u	Run-up level, relative to SWL	[m]
$R_{u,f}$	Run-up level with slope friction included, relative to SWL	[m]
$R_{u,r}$	The reduced run-up level with slope friction and permeability included, relative to SWL	[m]
$R_{u2\%}$	Run-up, run-up level exceeded by only 2% of run-up tongues	[m]
s	1. Slope (gradient) , cot (α)	[-]
	2. Wave steepness, $s = H/L$	[-]
su	Internal set-up height	[m]
su_{max}	Maximum internal set-up height	[m]
S	Damage level in the Van der Meer formula	[-]
T	Wave period	[s]
T_m	Mean wave period	[s]
u	Horizontal velocity, for a porous medium the filter velocity	[m/s]
u_i	Inflow velocity	[m/s]
u_w	Orbital velocity	[m/s]
u_{slope}	Slope velocity	[m/s]
u_{rms}	Horizontal root mean square velocity	[m/s]
U_δ	Flow velocity above the boundary layer	[m/s]
$\widehat{U}_\delta$	Maximum orbital velocity above the boundary layer	[m/s]
u	Vertical velocity	[m/s]
v_f	Filter velocity	[m/s]
v_{Rd}	Run-down velocity in the energy balance of VAN DER MEER [1995]	[m/s]

v_{Ru}	Run-up velocity in the energy balance of VAN DER MEER [1995]	[m/s]
V	Volume	[m^3]
V_i	Volume that flows into the structure	[m^3]
V_{Rd}	Volume of the run-down	[m^3]
V_{Ru}	Volume of the run-up	[m^3]
$V_{Ru,f}$	Volume of the run-up with slope friction included	[m^3]
$V_{Ru,r}$	Volume of the reduced run-up with slope friction and structure permeability included	[m^3]
$(W)_{ABC}$	Weight of water per unit crest width in area ABC	[N]
x	Horizontal coordinate positive in the direction of the wave propagation	[m]
z	Vertical coordinate directed positive upward with origin at the SWL	[m]

Greek letters

α	1. Angle of slope of breakwater	[rad] or [°]
	2. Coefficient dependent on the Reynolds number and the grain shape and grading used in the friction coefficient a in the Forchheimer equation	[-]
β	Coefficient dependent on the Reynolds number and the grain shape and grading used in the friction coefficient b in the Forchheimer equation	[-]
γ	Coefficient dependent on the Reynolds number and the grain shape and grading used in the friction coefficient c in the Forchheimer equation	[-]
γ_f	Roughness reduction coefficient	[-]
Δ	Relative density of rock in water	[-]
η	Instantaneous sea surface elevation relative to still water level	[m]
θ	1. Reflection phase angle of a regular wave	[-]
	2. Unknown angle between still water level and run-up water surface	[-]
κ	Spectral shape parameter	[-]
ν	Kinematic viscosity	[m^2/s]
ξ	Surf similarity parameter, Iribarren number $\xi = tan\alpha\sqrt{s}$	[-]
ξ_0	Surf similarity parameter based on calculation with $L_0 = gT^2/2\pi$	[-]
ξ_m	Surf similarity parameter for mean wave period T_m	[-]

ξ_p	Surf similarity parameter for peak wave period T_p	[-]
ρ_s	Density of rock material	[kg/m3]
ρ_w	Density of water	[kg/m3]
τ_o	Shear stress	[N/m2]
τ_{sl}	Shear stress on slope	[N/m2]
ω	angular frequency of waves, $\omega = 2\pi/T$	[s^{-1}]

Abbreviations

RMS	Root-mean-square
SWL	Still water level
$L.W.T$	Linear wave theory

Chapter 1
Introduction

1.1 General

Coastal structures are used in coastal defense schemes with the objective of preventing shoreline erosion and flooding of the hinterland. Other objectives include preventing siltation of navigation channels at inlets and protecting of harbor entrances against waves. Examples of these coastal structures are breakwaters, revetments and dykes. In general, revetments and dykes have an impermeable core, because the principal function of these structures is protecting low-lying areas against flooding. These coastal structures are usually built as a mound of fine materials like sand and clay. These materials can be seen as impermeable. In contrast, the principle function of breakwaters is to dissipate wave energy. This type of structure has a permeable character, because this function allows a water flow through the structure. In this study, the influence of the permeability on the armour layer stability will be examined. Therefore, within the framework of this research, only the rubble mound breakwaters will be further investigated.

Rubble mound breakwaters are the most commonly applied type of breakwater. In its most simple shape, a rubble mound breakwaters is a mound of quarries rock, usually protected by a cover layer of heavy armour stones or concrete armour. A homogeneous structure of stones, large enough to resist displacements due to wave forces, is not often used because of the high permeability. It also might cause too much penetration not only of waves, but also of sediments if present (in the area). Besides, large stones are expensive because of the higher placing costs and quarries produce mainly finer material (quarry run) and only relatively few large stones. Therefore, the conventional rubble-mound structures consist of a core of fine material covered by big blocks forming the so-called armour layer.

To prevent finer materials to be washed out through the armour layer, filter layers must be applied Structures consisting of an armour layer, filter layer(s) and a core are referred to as multilayer structures. The lower part of the armour layer is usually supported by a toe berm except in cases of shallow water structures. Figure 1.1 shows a conventional type of rubble mound breakwater. Normally, quarry armour units are used, but at sites where a sufficient amount of large quarry stones is not available, or in areas with rough wave climates, artificially manufactured concrete blocks are used.

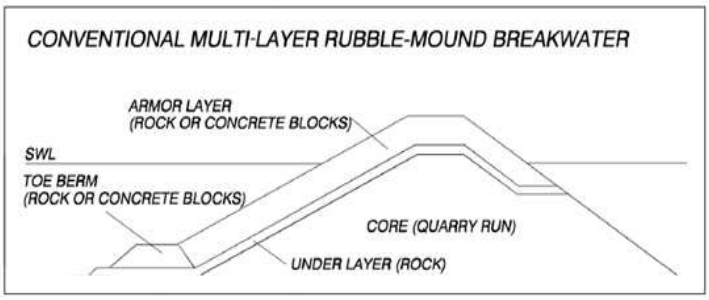

Figure 1.1 - Conventional multilayer rubble-mound breakwater

The interaction between the waves and the rubble mound breakwater is described by a large number of related physical processes. The waves that run into the breakwater slope are running up or down (wave run-up and wave run-down) with periodic movements (non-permanent flow). A part of the wave energy is reflected back to sea (wave reflection), the remaining wave energy is dissipated in the breakwater or transmitted through the structure to the leeside of the structure (wave transmission). The flow through the pores of the core material (porous flow) exhibits laminar and turbulent characteristics and is linked to the wave motion via the in- and outflow through the armour and filter layer(s). The flow associated with these hydrodynamic pore pressures (i.e. the water pressure in the pores of the grain structure due to the wave effect) slowly decreases to the rear of the core.

If the crest is sufficiently high, a part of the water run-up volume flows over the crest (overtopping), and through the crest and landward slope to the rear of the breakwater. The waves penetrate through the porous armour layer to the core and cause a cyclic in and outflow of water. This interaction process of a wave with rubble mound breakwater results in a complex flow which is both non-linear and turbulent. As a result of the complexity of this interaction process, it is in present time not possible to give an accurate description of the wave-structure-interaction. Therefore, the design of such structures is often based on empirical relationships, scale tests out of research laboratories and a synthesis of knowledge from different disciplines.

The most important part in designing the breakwater is the prediction of the rock-size of the armour units (D_{n50}), to withstand the wave attack. Many methods in predicting rock-size armour units designed for wave attack, have been proposed in the last half century. Examples of these are the stability formulae by IRIBARREN [1938, 1953], HUDSON [1953, 1959], VAN DER MEER [1988], a modification of the formulae of VAN DER MEER [1988] by VAN GENT ET AL. [2003] and a formula by VAN GENT ET AL. [2003].

The formula of Iribarren is based on the equilibrium of the forces acting on blocks placed on the slope. A comparable equation was been developed by HUDSON. He performed many tests to find the constants of the Iribarren formula. For rock, this formula is not often used any more, but this relation can be found in design formulae for concrete armour units. The formulae of VAN DER MEER [1988] are a step forward compared to Hudson's equation, because more relevant parameters are included. The last two stability formulae (the modified Van der Meer and VAN GENT ET AL. [2003]) were developed to extend the field of application of stability formulae, so they can be applied not only for deep water at the toe but also for shallow water at the toe of non-overtopped rubble mound structures.

By reason of the wide applicability, the stability formulae of VAN DER MEER [1988] are often used as the design formulae. These design formulae can be described as follows:

$$\frac{H_s}{\Delta D_{n50}} = c_{pl} P^{0.18} \left(\frac{S}{\sqrt{N}}\right)^{0.2} \xi_m^{-0.5} \qquad \text{for plunging waves} \qquad (1.1)$$

$$\frac{H_s}{\Delta D_{n50}} = c_s P^{-0.13} \left(\frac{S}{\sqrt{N}}\right)^{0.2} \sqrt{cot\alpha} \cdot {\xi_m}^P \qquad \text{for surging waves} \qquad (1.2)$$

Besides the wave height (H_s), design criteria for damage (S), the Iribarren number (ξ), the relative mass density, the number of waves (N) and the slope steepness, the stability is strongly related to the

notional permeability factor (P). The value of this factor is based on curve fitting results of the test program of VAN DER MEER [1988]. This test program includes three structure types. For that reason, the notional permeability is only defined for three structure types, whilst a fourth value (P=0.4) has been assumed, see Figure 1.2. The notional permeability coefficient has no physical meaning but was introduced to ensure that the permeability of the structure is taken into account.

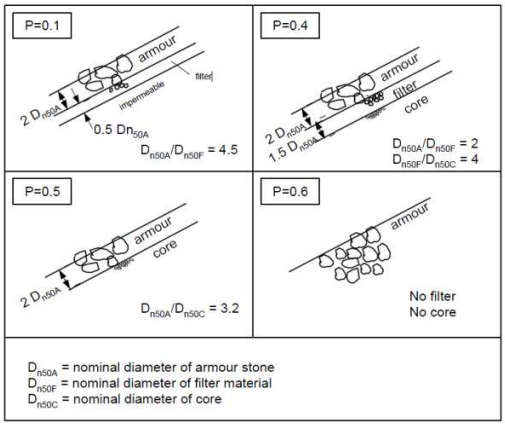

Figure 1.2 - Notional permeability P according VAN DER MEER [1988]

Caused by the absence of a physical description it is not possible to determine the notional permeability factor for different types of structure. In practice this leads to ambiguities in determination of the value of this factor, which results in overdesigned size of the D_{n50}. In practice, usually a P-value for non-standard designs (0.1 <P <0.4) is selected, based on experience and a sensitivity analysis is done to determine the design margin. It is clear that the permeability parameter has a significant influence on the outcome. Figure 1.3 shows the influence of the permeability on the D_{n50} for surging and plunging waves. The influence for the plunging waves is lower, since this wave breaking process will mainly take place in the armour layer. For the example below, only the permeability has been apprehended as a variable, so this plot only reflects the general trend in the stability curves.

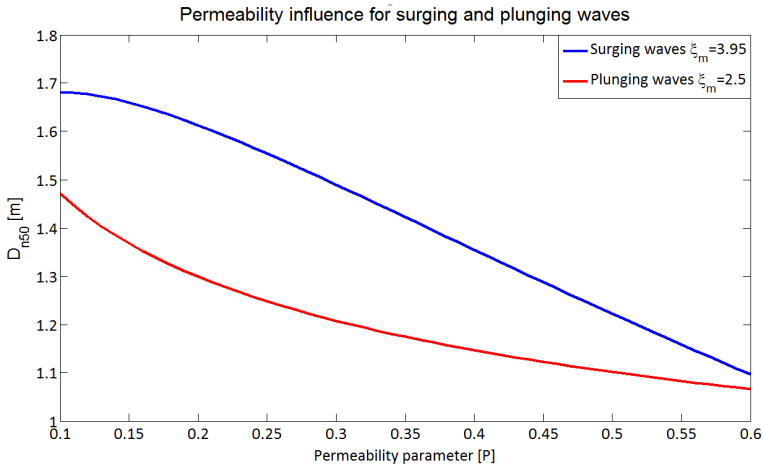

Figure 1.3 - Example of the influence of the notional permeability coefficient P on the D_{n50} of the armour unit

As already mentioned, the permeability parameter P is only defined for a fixed number of structure compositions. Therefore an accurate application, for different kind of structure compositions, is not possible. In practice this leads often to the use of values that do not correspond to the actual value, which results in overdesigned sizes of the D_{n50}.

In general, for the construction of a breakwater it can be supposed that if the quarry run percentage of the total breakwater volume is high, the total costs are low. This is because the total costs (placing, transport and the price of the rock) of the quarry run are significantly lower than for higher D_{n50} classes. Mainly the placing costs are determining this significant difference. In case of a higher D_{n50}, the quarry run rate is lower, since not only the armour layer occupies a greater volume, but the volume of the filter(s) layer will also increase.

By means of these considerations it is clear that the influence of the core permeability on armour layer stability is of both academic and practical importance. This study has the aim to investigate whether more physical basis can be given to the influence of core permeability on the armour layer stability. A more physical background on this field can result in a more precise choice of the notional permeability coefficient P in the calculation of the breakwater design. While the understanding of the problem is still far from complete, its application in coastal defense systems is extremely common.

1.2 Problem definition

In the previous section the influence of core permeability on armour layer stability was illustrated. Due to the absence of a physical permeability description it is not possible to determine this influence. The problem of this thesis research is therefore defined as follows:

> *The influence of the core permeability on armour layer stability is not completely described in literature. In the widely used stability formulas of VAN DER MEER [1988] the influence of the core permeability is described by a coefficient (notional permeability coefficient P) that has no physical basis. Since the permeability has large influence on the stability relation, a more precise description of the core permeability influence is important.*

1.3 Research objective

With this problem definition the main objective of this study can be defined as follows:

> *Improving the insight in the physical process related to the core permeability influence on the armour layer stability. Particularly focusing on the research of concretization of the 'notional' permeability coefficient P in the formulae of VAN DER MEER [1988]. Aim is to investigate whether more physical basis can be given to the 'notional' permeability coefficient, which ultimately should lead to more adequate guidance for breakwater design practice.*

1.4 Methodology and report outline

The methodology used in this report can be divided into the following steps, which can be seen as the underlying structure of the report.

Chapter 2: Theoretical background of the problem description and formulating a hypothesis for this research

Chapter 3: Literature study to analyze this hypothesis and setting-up conceptual methods

Chapter 4: Detailed description of the conceptual methods

Chapter 5: Elaboration of the selected method

Chapter 6: Practical application of the method

Chapter 7: Drawing conclusions and recommendations

The approach for this research is based on these sequencing steps. The steps are not directly used in the chapter titles, therefore follows a brief outline of each chapter:

The second chapter presents a comprehensive description and analysis of the problem. This is done by an investigation of the (de)stabilization process. Thereafter, the influential parameters on this process are described briefly with the exception of the permeability, which is described in detail. Since the influence of the core permeability on armour layer stability only depends on the 'notional permeability parameter of VAN DER MEER [1988], this parameter is discussed and analyzed. With this background a hypothesis is formulated for the remaining part of the research.

Chapter 3 presents descriptions of the external and internal motions. This aims to draw some conceptual coupling functions between both motions. For the external motion, energy approaches, momentum approaches and volume approaches, are given. The Forchheimer equation is described for the internal water flow. Due to the time dependence of the friction in the porous medium also this dependency of the internal process will be described. With the insight of the internal and external process some conceptual coupling methods are drawn.

The transfer functions (coupling methods) for the wave-structure-interaction process are further elaborated in the fourth chapter. Based on this elaboration one method is chosen which will be further worked out. Partly by the straight forward approach and its simple principle, the volume-exchange-model is selected.

In the fifth chapter follows the development of the volume-exchange-model. This should lead to a method that is able to determine the core permeability on the armour layer stability. This volume-exchange-model links the external with the internal process. The external process is described by a wave run-up description. In this description the wave run-up wedge approach of HUGHES [2004] is linked to the wave kinematics in front of the structure. The internal process is described by the 'Forchheimer' equation for the water flow through a porous medium.

In chapter 6 a practical application of the volume-exchange-model is given. First, a sensitivity analysis is done to investigate the influence of each variable in the model. Then the volume-exchange-model is

coupled with the notional permeability factor of VAN DER MEER [1988]. This is done for a vertical transition and a sloped transition. For both elaborations a notional permeability formula is derived from a curve fitting. With these elaborations and formulae a suggestion is given to replace the notional permeability factor in the stability formulae of VAN DER MEER [1988]. The chapter ends with a hypothesis for further research and an associated recommended test program.

Conclusions and recommendation for further research are given in Chapter 7.

Chapter 2

Theoretical background of the problem with associated hypothesis

2.1 Armour layer stability

2.1.1 General

Before to proceed to a more detailed description of the problem, first a general description of the armour layer stability follows. The armour layer stability is determined by the hydraulic and structural parameters. The main hydraulic parameters are the wave height and wave period. The main structural parameters are the porosity, stone diameter and the slope angle. In general, the hydraulic parameters are variable and the structural parameters are determined by these hydraulic parameters. However, based on economic motives the range of the overall breakwater geometry is fixed. In fact, a large area of the breakwater cross section results in a larger quantity of material. It is therefore important that this area should be designed as small as possible. An important point here is the angle of the structure slope. The quantity of material will be smaller if the structure slope is steep. Since the slope of the breakwater is steep, and the slope of the foreshore is mainly flat, there will be much energy left for the wave-breakwater interaction. Caused by this large amount of wave energy, the structure slope is subject to severe wave attacks. This results in large forces on the breakwater slope that should be absorbed to counteract destabilization. This interaction process is determined by the type of wave that is being developed during this process. The next section gives a relationship to indicate the type of wave.

2.1.2 Types of wave breaking

The kinematics of waves breaking on smooth, impermeable slopes can be qualitatively described by the so-called surf-similarity or Iribarren number, introduced by BATTJES [1974] (reference BATTJES [2006]). If viscous forces are neglected, dimensional analysis shows that the flow characteristics are a function of the parameters $(gT^2)/H$ and α, where α is the slope angle. Using the expression for the deep water wave length $L_0 = (g/2\pi)T^2$, the parameters can be combined into the surf-similarity parameter, originally defined for regular waves as $\xi_0 = \tan\alpha\,(\mathrm{H_0/L_0})^{-0.5}$, where $\mathrm{H_0/L_0}$ is the deep water wave steepness. The surf-similarity parameter is a relation between the hydraulic parameters and the structural parameter α and gives answers to the question whether the waves will break and how the waves will break. Figure 2.1 shows the main breaker types, which are surging, collapsing, plunging and spilling. This study focuses on breakwaters with a steep front face, so only the first three breaker types are interesting.

The similarity parameter can also be expressed for irregular waves as a function of the average wave period (ξ_m) or as a function of the peak wave period (ξ_p). With the breaker type description it is possible to describe the influence of the environmental parameters on the wave process close to a sloped structure.

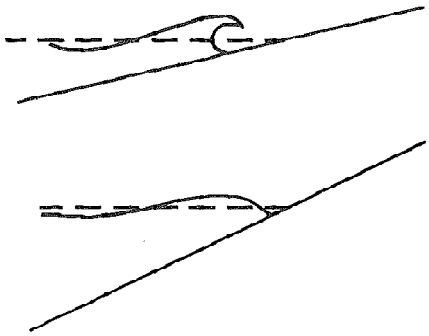

Plunging: $0.5<\xi<3.3$

Surging or collapsing: $\xi>3.3$
(no real wave breaking on the slope)

Figure 2.1 - Breaker types

2.1.3 Influence of structural and hydraulic parameters

Besides the three parameters expressed in the Iribarren parameter, the wave-interaction process depends also on the permeability and the roughness of the structure (slope). Those two parameters can be expressed respectively in *P* and the D_{n50}. In particular, the run-up process is an important component for describing the wave-structure-interaction and therefore the armour layer stability. Wave run-up is the extreme level of water oscillation that is reached in each wave caused by wave action. A simple description of the relation between the run-up process and the armour stability can be given as follows:

> *When the extreme level of water oscillation is 'small', the up-rush and down-rush velocity are small. This is because the slope velocities are determined by the extreme water level oscillation and the wave period. In general, the stability of the armour layer is larger in case of smaller slope velocities.*

The wave run-up strongly depends on the structural and hydraulic parameters mentioned above. Below a short overview of the influence of each parameter on the run-up is shown. When analyzing one parameter, all others are taken constant.

Hydraulic parameters

Wave height: when the wave height H_s is increasing, the run-up height is also increasing**.** Waves are the main driving force for run-up, so there has to be a direct relation between run-up and wave height.

Wave period: a shorter wave period result in a steep wave, this wave will break faster. By wave breaking there is a lot of energy dissipation on the slope, this will lead to a lower run-up level. Due to the various types of breaking a direct relationship of the period and run-up cannot be expressed. Therefore, the types of wave behaving have to be dealt separately.

'Joint' parameter

Slope angle: this parameter is a combination of environmental and structural properties. The influence of the slope can be explained in two ways. The first is when the waves pass over a gentle slope, the roughness of this slope will have a longer path to interact with the waves. The other influence is the

difference in breaker type for a different slope angle. These two effects provide more energy dissipation to the slope, leaving less energy available for the run-up.

Structural parameters

Slope roughness/Stone diameter: the roughness is related to the diameter of the armour unit. For a larger diameter the roughness becomes higher and therefore the run-up will be less. The influence of the armour unit diameter in the run-up can be found in two factors. The first reason is the increasing of resistance by increasing the roughness of the slope, thus more energy dissipation. The second reason is the proportionality of armour diameter with the size of the pores. When the size of the pores is larger, more space for the waves is available to dissipate energy. The energy loss will lower the wave run-up level. In literature these two factors are expressed in one roughness coefficient, but in this study those two factors would be described separately.

Porosity: If the porosity of the structure increases, the run-up will decrease. A higher permeability of the structure reduces the flow velocities along the slope surface, because a large proportion of the flow takes place within the slope. Since the focus of this research lies especially on the influence of the porosity or permeability, the following sections will describe this topic in more detail.

2.2 Relation of structure permeability with armour layer stability

2.2.1 Definition of the permeability

In literature different expressions exist for the term permeability. For an unambiguous description of the permeability in this study, the used definitions in this study are described below. When a different definition is used this will be mentioned explicitly.

Porosity or permeability

The permeability is the property of bulk material (sand, crushed rock, soft rock) which permits movement of water through its pores. The porosity, *n*, is usually defined as the ratio of the pore volume with the total volume. The parameter is therefore dimensionless. For a normal grain-structure, *n* can be used also as a permeability parameter.

Notional permeability

A ratio between the size of the filter layers and the core is known as the notional permeability. This definition is introduced by VAN DER MEER [1988] and is an expression for the influence of the permeability or porosity of the breakwater structure on the dimensionless number $H_s/\Delta D_{n50}$. The expression indicates the composition of the breakwater in terms of the mutual relation of the grain sizes in subsequent layers.

Note 2.1: *The dimensionless permeability description in this report should not be confused with the hydraulic conductivity (K), which in literature is also expressed as permeability.*

2.2.2 General description of the permeability influence on the armour layer stability

As mentioned before, the permeability of the structure can be divided into two different areas. This is the permeability of the armour and the permeability of the core (and filter). The influence of increasing the armour permeability is the reducing of flow velocities along the slope surface because a large proportion of the flow takes place within the slope. When the permeability of the core (and filter) is increased, the amount of water that flows into the structure can be stored within a larger area of the cross section. It can be seen that both have a different effect on the wave process. Where the change in the D_{n50} of the armour layer (increasing armour permeability) has a strong relation with energy dissipation and the permeability of the core structure gives also a water volume reduction. Below follows a more detailed description of the permeability influence on the wave process.

(The following text and illustration is based on or taken from BURCHARTH [1993] and BURCHARTH ET AL. [1998]*):*

The velocity varies in case of a impermeable slope and a permeable 'structure' (see Figure 2.2). Both the size and the direction of the velocity vectors are important for the stability of the armour units. For a slope with an impermeable core the flow is concentrated in the armour layer, causing large forces on the stones during run-down. The reason for generally smaller stability in case of fine core material is because of the relatively impermeable core where the water cannot percolate into the voids of the core. If no water is allowed to percolate into the voids of the structure, the long waves will be more damaging than the short waves, since each wave carries more water into the structure than for short waves. For a slope with a permeable core, the water dissipates into the core and the flow becomes less violent. With longer waves periods (larges ξ_m) more water can percolate and flow down through the core. This reduces the forces and stabilizes the slope. In the case of coarse core material, the long waves have time enough to penetrate deep into the structure, and thereby reduce the flow in the armour layer. The short waves have less time to penetrate into the core, and hence a larger amount of the flow is situated in the armour layer, and thereby reduces its stability.

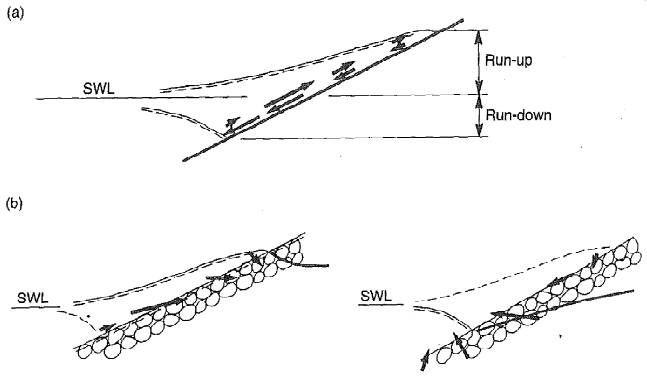

Figure 2.2 - Up/down-rush on a impermeable slope (a) and permeable slope (b), BURCHARTH [1993].

According to BURCHARTH [1993], the degree of the permeability determines not only the velocity vectors in and on the structure but also the internal water table is affected, as is indicated in the

illustration of BURCHARTH [1993] (Figure 2.3). Due to the wave action, the internal water level will rise and therefore the mean pore pressure will rise. This internal set-up is caused by a higher water level that is reached during up-rush than during down-rush. The mean flow path for inflow is also shorter than that for outflow. The destabilizing forces on armour units are thereby reduced. This positive reservoir effect is reduced in the case of a large internal set-up of the water table. The rise of the phreatic line will continue until the outflow balance the inflow.

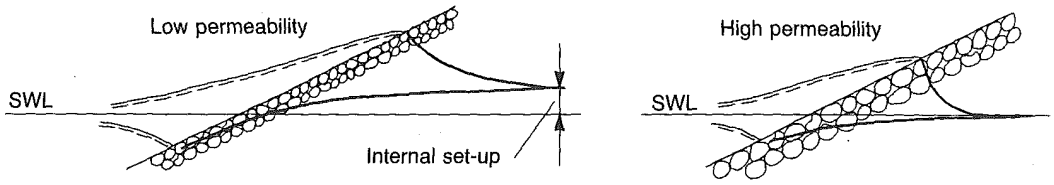

Figure 2.3 - Illustration of variation in internal water table (BURCHARTH [1993])

Note 2.2: *The correctness of the internal set-up illustration (Figure 2.3) is questionable. This will be discussed in detail in Chapter 5.*

The difference in run-down between a permeable and an impermeable structure will cause also a difference in the breaker type. The waves on an impermeable structure will be relatively steeper compared to the waves that break on a permeable structure. The transition between plunging and surging breakers will therefore move to lower values of the surf similarity, if the permeability of the structure is increased. This is illustrated in Figure 2.4.

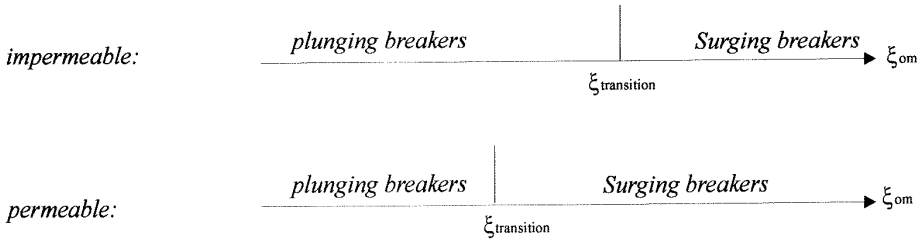

Figure 2.4 - Breaker type regions for different permeability

2.2.3 Introduction of the notional permeability coefficient

The foregoing shows that the permeability of the structure has a major impact on the external process, and therefore on the stability of the armour layer. Many descriptions of these physical effects are described in the literature, see for example BURCHARTH [1993] and BURCHARTH ET AL. [1998] in the previous section. However, expressions in the form of a coefficient or variables, are limited. Actually only the notional permeability coefficient P in the stability formulas of VAN DER MEER [1988] is an expression, for it is assumed that this parameter describes the influence of the core permeability. The extra term 'notional' in the definition, indicates explicitly that there cannot be directly assumed that this term exactly describes the permeability. Before this coefficient can be discussed, first the way of the introduction is described. This is only possible when the full derivation of the 'Van der Meer'- formulas is considered. Next, a brief overview of the derivation of these stability formulae follows.

Derivation of the stability formula

Below follows a derivation of the stability formula of VAN DER MEER [1988] for surging waves. The same principle is applied in the derivation of plunging waves, but given that a surging wave is more influenced by varying permeability, only this derivation is described. The list below was provided for governing variables for static stability.

Table 2.1 - Possible range for application of the governing variables

Variable	Expression	Range
The wave height parameter	$H_s/\Delta D_{n50}$	1-4
The wave period parameters, wave steepness,	s_m	1-4
and surf similarity parameter	ξ_m	0.01-0.06
The damage as a function of the number of waves	$S/N^{0.5}$	0.7-7
The slope angle	cotα	<0.9
The grading of the armour stones	D_{85}/D_{15}	1.5-6
The permeability of the structure	P	1-2.5
The spectral shape parameter	κ	imperm.-hom.
The crest height	R_c/H_s	0.3-0.9

The above mentioned range of possible application is almost completely covered by the test program of VAN DER MEER [1988]. The list of variables can be shortened using the qualitative results of the tests by VAN DER MEER [1988]:

- The spectral shape parameter is, by using the average period, quite small and can be ignored;
- Armour grading has practically no influence on the stability, and the stone class can be described by the nominal diameter D_{n50};
- Crest height – to be researched;
- Roundness and surface texture of the stones – to be researched (see LATHAM ET AL. [1988]);

With these assumptions the stability of rubble mound revetments and breakwaters can then be described by the following dimensionless variables:

$H_s/\Delta D_{n50}$; ξ_m; $S/\sqrt{N}$; P and $cot\alpha$

The test results on stability were shown in $H_s/\Delta D_{n50}$ - ξ_m plots. In these plots the trends of the curves are clearly visible. For example in the surging region; the $H_s/\Delta D_{n50}$ is increasing with decreasing ξ_m-values, regardless of the other variables, such as damage level, storm duration and permeability.

VAN DER MEER uses a curve to derive a stability relation. For this curve fitting he used a power function, because this function has the advantage that the power coefficient describes the trend of the results (curved, increasing or decreasing) and the other coefficient describes the location of the curve, so the function has only two coefficients.

As mentioned before only the derivation of the stability formula for surging waves is described. VAN DER MEER [1988] has also elaborated the plunging and the surging wave region separately, because the two different regions have two complete different trends. The intersection between the two functional relationships will give the transition from plunging to surging waves. The influence of the wave steepness can be described in the following way:

$$H_s/\Delta D_{n50} = a_1 \xi_m^{b_1} \qquad \text{with} \qquad a_1 = f(\frac{S}{\sqrt{N}}, P, cot\alpha)$$

For the three tested structures, impermeable core, permeable core and homogeneous structure, the values of the coefficient b_1, were 0.1, 0.5 and 0.6, respectively. The increasing value of b_1 shows the increasing influence of wave steepness with increasing permeability. This reflected in the steeper curves found on the $H_s/\Delta D_{n50}$-ξ_m - plot, see Figure 2.5. In Figure 2.6, the curve fitting for the three different permeabilities is showed. The equations for the three different types of compositions can be described as follows:

$$H_s/\Delta D_{n50} = a_2 \xi_m^{0.1} \qquad \text{with} \qquad a_2 = f\left(\frac{S}{\sqrt{N}}, P, cot\alpha\right)$$

$$H_s/\Delta D_{n50} = a_3 \xi_m^{0.5} \qquad \text{with} \qquad a_3 = f\left(\frac{S}{\sqrt{N}}, P, cot\alpha\right)$$

$$H_s/\Delta D_{n50} = a_4 \xi_m^{0.6} \qquad \text{with} \qquad a_4 = f\left(\frac{S}{\sqrt{N}}, P, cot\alpha\right)$$

Note 2.3: *Impermeable is a relative notion, wave penetration into clay or even sand is almost negligible, so, in these stability relations the slope is considered impermeable.*

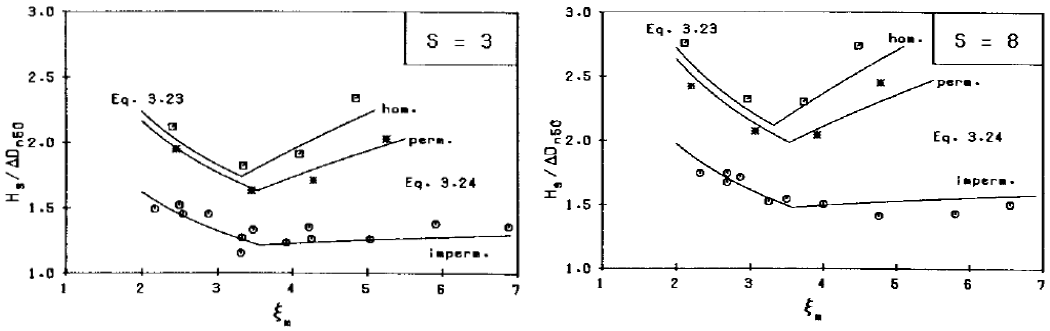

Figure 2.5 - Influence of the core permeability with cot α=2

The other variables ($S/\sqrt{N}$, P, $cot\alpha$) are fitted in the same way. The equations for the three structure types become:

Impermeable core: $$H_s/\Delta D_{n50} = 1.35 \cdot \xi_m^{0.1} \cdot \left(\frac{S}{\sqrt{N}}\right)^{0.2} \sqrt{cot\alpha} \qquad (2.1)$$

Permeable core: $$H_s/\Delta D_{n50} = 1.07 \cdot \xi_m^{0.5} \cdot \left(\frac{S}{\sqrt{N}}\right)^{0.2} \sqrt{cot\alpha} \qquad (2.2)$$

Homogeneous structure: $$H_s/\Delta D_{n50} = 1.10 \cdot \xi_m^{0.6} \cdot \left(\frac{S}{\sqrt{N}}\right)^{0.2} \sqrt{cot\alpha} \qquad (2.3)$$

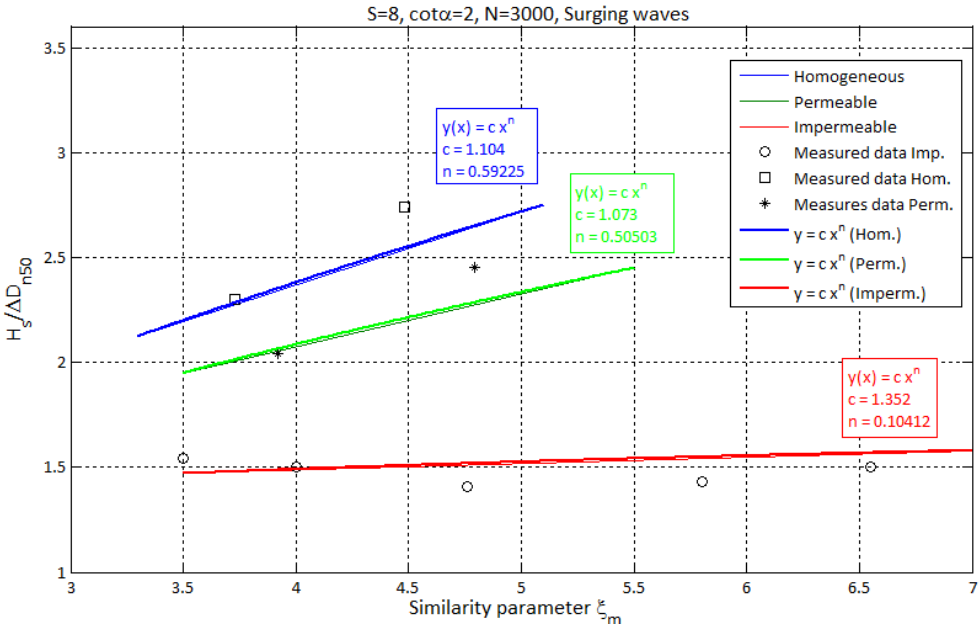

Figure 2.6 - Example of curve fitting for different permeability's.

Introduction of the permeability coefficient, P

VAN DER MEER [1988] suggested that for surging waves the power coefficient of the similarity parameter ξ_m has a value, depending on the permeability of the structure, of 0.1, 0.5 and 0.6 respectively. Therefore, P is defined by P is 0.1 for impermeable core, 0.5 for the permeable core, and 0.6 for the homogeneous structure. Now the power coefficient of the similarity parameter ξ_m can be replaced by this P. Hence, the permeability coefficient has no physical meaning, but was introduced to ensure that the permeability of the structure is taken into account. Below the values for the notional permeability factor P for various structures are shown. The value 0.4 is an assumed value and is based on practical experience and not on test results of VAN DER MEER [1988].

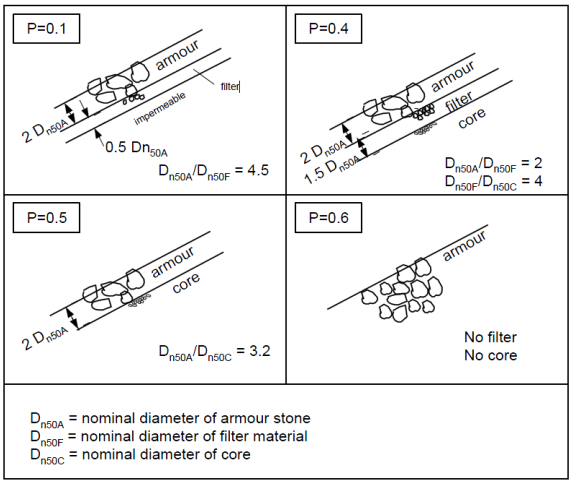

Figure 2.7 - Notional permeability P according VAN DER MEER [1988]

Final formulae

With the introduction of the permeability coefficient, P, the factors 1.35, 1.07 and 1.10 can now be described as a function of this coefficient. The permeability coefficient can be included in the formula as follows:

$$\frac{H_s}{\Delta D_{n50}} = a_1 P^{b_1} \left(\frac{S}{\sqrt{N}}\right)^{0.2} \xi_m^P \sqrt{cot\alpha}$$

Curve fitting of $a_1 P^{b_1}$ gives the final formula for surging waves:

$$\frac{H_s}{\Delta D_{n50}} = 1.0 P^{-0.13} \left(\frac{S}{\sqrt{N}}\right)^{0.2} \xi_m^P \sqrt{cot\alpha} \tag{2.4}$$

The derivation for the plunging waves is similar, the final formula for plunging waves can be described as:

$$\frac{H_s}{\Delta D_{n50}} = 6.2 P^{0.18} \left(\frac{S}{\sqrt{N}}\right)^{0.2} {\xi_m}^{-0.5} \tag{2.5}$$

Collapsing waves are presented at the intersection of both curves. This intersection is derived from the two final equations from above and is given by:

$$\xi_m = (6.2 P^{0.31} \sqrt{tan\alpha})^{1/(P+0.5)} \tag{2.6}$$

Depending on the slope angle and the permeability this transition lays between ξ_m= 2.5 to 4.

The findings on these results are described as follows by VAN DER MEER [1988]:

Plunging ($\xi_m < 3$)

1. The influence of the wave period for plunging waves shows the same trend for all three structures, although a more permeable structure is more stable.
2. In the plunging region the fast wave run-up after breaking of the wave is decisive for stability. The forces during run-down are relatively small.

Surging (ξ_m>3.5)

3. A more permeable structure is also more stable for surging waves (ξ_m>3.5), but the stability increases with larger wave periods. The curves are steeper for larger permeability.
4. In the surging region the wave does not break and forces during run-up are small. Instability in this region is caused by run-down.

The phenomenon of steeper curves for larger permeability can be explained in physical terms by the difference in water motion on the slope: For a slope with an impermeable core the flow is concentrated in the armour layer causing large forces on the stones during run-down. For a slope with a permeable core the water penetrates into the core and the flow becomes less violent. With longer waves periods (larges ξ_m) more water can percolate and flow down through the core. This reduces the forces and stabilizes the slope. It can be seen in the Figure (2.5) that there is a clear difference between plunging and surging waves. The smallest difference is showed for the transition from surging to plunging waves, referred as collapsing waves.

2.2.4 Discussion (or a detailed problem description)

In Chapter 1 a brief description of the problem is formulated. Based on the additional background information, presented earlier in Chapter 2, the problem is described in more detail hereafter. This description takes into account following key elements of the problem:

- The notional permeability factor is the only expression that describes the influence of the core permeability on the armour layer stability.
- The introduction of this permeability factor follows from a derivation of the stability formula. This derivation is based on curve fitting of test results and is therefore not directly based on a physical process. A stability relation based on sequencing curve fittings of all variables can serve as a good tool for the design of the armour layer, but due to the rounding errors of each curve fitting the exact influence of each variable is no longer realistic. In other words, a rounding error in one curve fitting provides an inaccuracy in the following curve fitting.
- The 'notional' permeability coefficient has no physical meaning, but was introduced to ensure that the permeability of the structure is taken into account.
- The extra term 'notional' in the definition indicates explicitly it cannot be assumed that this permeability coefficient describes exactly the permeability.
- The accuracy of the curve fittings for mainly the permeable and homogeneous structures is questionable. The curve fittings for both structures are based on only four data points, see Figure 2.5. In addition, also the direction, i.e. the power coefficient is in both cases questionable.
- The permeability is only defined the basis of three different structures compositions

These observations show that the description of the permeability is a sensitive point in the stability formulas of VAN DER MEER [1988]. With this background a hypothesis is formulated for the remaining part of this research.

2.2.5 Hypothesis

This study attempts to improve the insight in the physical process related to the core permeability influence on the armour layer stability. While the stability relationship includes the notional permeability coefficient P, the focus of this study lies especially on the research of concretization of this permeability coefficient in the formulae of VAN DER MEER [1988]. The ultimate aim is to determine values for this permeability coefficient P for other than the three tested structures. Moreover it can also aid in better understanding the implications of the permeability on the stability.

In the past VAN DER MEER [1988] has tried to give the notional permeability coefficient P a physical background using the model HADEER. This model can calculate the discharge dissipation in the core. With the use of the ODIFLOCS-model of VAN GENT [1995] the same principle predictions are also tried by DE HEIJ [2001]. He considered the discharge, extreme velocities and $U_{2\%}$. However, these methods are not very accurate and due to the numerical approach they are not easy to use in practice. In addition, these studies assumed that the P-factor is a description of the permeability

Caused by the disappointing results of the models listed above, this research will not elaborate further on these methods. At the contrary, other methods are looked at in order to gain a better understanding of the notional permeability coefficient or in general the influence of the core permeability on the armour layer stability. Several methods are available, the most obvious methods are: (1) get more test results, (2) define a physical description of the wave-structure-interaction and (3) a full computational modelling of the wave-structure-interaction. For this study the second method seems to be the most appropriate. With a physical description it is possible to determine for each individual structure the influence of the core permeability. It may also lead to a simple practical method in contrast to the above mentioned numerical models. The first method has the disadvantage that the designer is still limited to the tested structures. The last method is still in a research stage and will therefore not be used in this study. However, it is expected that computer modelling is increasingly making access in the design of a structure. This study is trying to give a physical description of the wave interaction process, the associated hypothesis is as follows:

> *Using an independent description of both the external and internal motion it should be possible to link these two processes with the use of a 'transfer function'. Together with this, a description of the wave-structure-interaction process is realized and can lead to a better insight of the influence of core permeability on the armour layer stability. With this description an analytical model can be developed for calculating the core influence on the external process. This model can be used to determine the notional permeability coefficient for structures other than the tested ones.*

Chapter 3

Wave-structure-interaction processes

3.1 Introduction

For a good physical description of the influence of core permeability on armour layer stability it is necessary to understand the physical processes of the wave-structure-interaction. For non-breaking waves, such as the surging waves considered in this study, the physical processes are primarily affected by the permeability of the structure.

Previous studies have shown that a detailed description of the full wave-structure-interaction is complex. For that reason, the full wave-structure-interaction is divided into two separate processes. The first process can be described as the external water motion in and on the armour layer that is influenced by the presence of the structure. The second process is defined as the internal water motion. The internal water movement, in this study, is defined as the water movement that takes place within the construction (filter and core) for a certain imposed external water movement. In the next two paragraphs these two processes will be discussed. At first both processes are considered to be independent of each other, meaning an impermeable structure slope has been assumed. The last paragraph of this chapter describes some methods to link both processes. Chapter 4 continues taking the coupling approaches to the application of a working model. Analytic feasibility of the model will then mainly determine which model is eventually chosen for further development.

3.2 External water motion

The interaction of a wave with a rubble mound breakwater results in a complex flow of non-linear and turbulent effects, in particular within the region close to the surface of the structure. In the previous chapter the influence of the structural and hydraulic parameters on the run-up process has been described. The run-up is one of the most important factors affecting the design of coastal structures, but this it is just a single part of the entire interaction process. Besides, the destabilization of the armour units is mostly a result of the rush-down process. Therefore, a more specific description of the total external flow is needed. Below, the most common descriptions of the external flow are given. With this, a briefly analysis of the methods is given. It aims to provide a clear overview of the possibilities of each method.

The descriptions of the external water motion are arranged into three general approaches:

1. *Paramaterized analytical descriptions;* These approaches give an analytical method to determine the slope velocity. The methods are based on an energy approach in front of the structure.
2. *Description based on the momentum balance;* These approaches require a discrete solution and can be seen as numerical methods.
3. *Descriptions based on a volume approach;* These approaches describe water level changes in front of the slope and can be seen as volume change approaches on the slope. These approaches assume conservation of mass.

3.2.1 Parameterized analytical descriptions

In this section two parameterized analytical methods are described that determine the slope velocity. An expression of the slope velocity can be seen as a description of the external water motion.

Reflection method by HUGHES ET AL. [1995]

The first method is presented in HUGHES ET AL. [1995]. It provides a realistic estimate of irregular wave kinematics near coastal structures. These velocity estimates are particularly suited for estimations near the seabed. This method uses the linear wave theory approximation. An effect for the reflected wave is added, based on the reflection coefficient Kr. Physical processes in the vicinity of coastal structures are influenced by flow hydrodynamics resulting from the combination of incident and partially reflected wave trains. When reflection is less than perfect, the reflected wave amplitude is reduced by a factor known as the reflection coefficient. For irregular waves, the root-mean-squared (RMS) velocity is calculated by adding all components of the individual waves. For a single wave component the RMS velocities can be written as:

$$u_{rms}^2 = \left[\left(\frac{gk}{\sigma}\right)^2 \frac{cosh^2 k(h+z)}{cosh^2 kh}\frac{a^2}{2}\right] \cdot (1 - K_r \cos(2kx + \theta) + K_r^2) \tag{3.1}$$

These velocity estimates are as said particularly suitable for estimations near the seabed. The Hughes-reflection method also has the advantage that it is based on adding wave components in an irregular wave field. However the theory is based on the linear wave theory, and since surging waves are non-linear processes uncertainties can be expected

Energy balance by VAN DER MEER [1990]

This conservative method for the estimation of the slope velocity is introduced by VAN DER MEER [1990]. The method assumes that energy conservation occurs. The energy dissipation by wave breaking and friction on the slope in this method is considered negligible. The water velocity on a slope due to breaking waves depends largely on the process of wave run-up, run-down and wave impact. With respect to the run-down velocity, v_d, the theory is based on the fall velocity of a particle, falling without friction.

$$E_{kin} = \frac{1}{2} m v_d^2 = mg(R_u - z) = E_{pot} \tag{3.2}$$

Elaboration of the energy balance gives the following equations for run-down and run-up velocity (respectively) given by VAN DER MEER [1990]:

$$\frac{v_{Rd}}{\sqrt{gH}} = \sqrt{2\frac{R_u}{H}}\sqrt{(1 - \frac{z}{R_u})} \tag{3.3}$$

$$\frac{v_{Ru}}{\sqrt{gH}} = \sqrt{\frac{1}{2\pi s}}\sqrt{(1 - \frac{z}{R_u})} \tag{3.4}$$

This method gives a good indication for the upper bound velocities, since it neglects energy dissipation. However, the real acting slope velocities cannot be calculated accurately with this method.

Conclusion

Both methods can also be seen as energy approaches. An energy approach has in theory the advantage that it contains (or can be rewritten in) a measurable initial and final condition (respectively the incoming and reflective wave). However, neither the Hughes reflection method nor the energy balance by Van der Meer can give an accurate description of the full external water movement. Since the Hughes reflection method is based on the linear wave theory and the energy approach of van de Meer assumes a conservation of energy.

3.2.2 Descriptions based on the momentum balance

In this section some descriptions of the water motion using a momentum balance equation are given. Momentum balance equations require in this particularly case discrete solutions. And therefore call for numerical methods. For practical purposes a numerical method is not the most obvious choice. However, since computer modelling is more and more used in the design of structures as well, these methods are also described for the sake of completeness.

Navier-Stokes equations

The motion of an incompressibe Newtonian fluid can be described accurately by the Navier-Stokes equations. For flow condition in which air-entrainment or wave impacts occur, compressibility has to be taken into account, although, in most wave motions the effects of compressibility can be neglected. This non-linear process can be computed with the two-dimensional (vertical) Navier-Stokes equations. For conditions in which the non-linear convective term is important, e.g., for relatively high waves in coastal areas, no analytical solutions exist and discrete solutions are required. Such solutions are also required because of non-linearity caused by free-surface boundary conditions.

Shallow water equations

Another obvious choice for the calculation of the water velocity around the slope might be a long wave momentum equation, adapted for use on a slope. These equations are based on the Navier-Stokes equations and can be used where vertical accelerations in the water can be ignored (the waves are called long waves). This means that the shallow water equations are based on a constant vertical velocity. This implies however the use of a momentum balance, with of course accompanying boundaries, imposed conditions and the use of one control volume area, with too many simplifications. Therefore, analytical solutions for the shallow water equations are limited to non-breaking waves on uniform slopes without any energy dissipation. For wide application these analytical solutions are too restrictive and lack versatility and therefore a numerical approach should be used again.

Although the equations are not strictly valid for steeper slopes nor for describing the breaking process, several numerical models have been developed that use these equations to simulate wave motion on steep coastal structures, including breaking waves. For the finite-amplitude shallow-water wave equations the absence of frequency dispersion prevents adequate counteracting of amplitude dispersion, which results in overestimation of non-linear effects. This leads to a steepening of the wave front which is too fast.

Non-linear dispersive Boussinesq equations

In the shallow-water wave equations non-linear effects are overestimated. This is related to the omission of the effect of vertical flow accelerations on the pressure, resulting from the absence of frequency dispersion. Boussinesq-like equations contain additional terms to improve these characteristics. For waves with small amplitudes in relation to the water depth and travelling over long distances, for instance on beaches and mildly sloping structures, this effect cannot be neglected. Although their applicability may be wide for spilling breakers on beaches, their field of application is smaller for wave motion on structures. The standard Boussinesq equations have three major limitations that make then only applicable to relative shallow water depth. (1) It is a depth-averaged model and it described therefore poorly the frequency dispersion of wave propagation in intermediated depths. (2) Weekly non-linear equations like the Boussinesq equation are preferable to describe waves before they start to break. (3) Disadvantage of this model is the time it takes to develop an useful and accurate operational model.

Conclusion

The most obvious choice for the calculation of the water motion around the slope are the Navier-Stokes equations. The shallow water equations and the Boussinesq equations use a constant vertical velocity (or a depth average velocity), while the Navier-Stokes waves have a more realistic variable vertical velocity. This is one of the reasons that the finite-amplitude shallow-water wave equations or Boussinesq-like equation cannot easily model the wave front in detail. With the use of the two-dimensional Navier-Stokes equations this can be overcome. However, also a Navier-Stokes-model has the disadvantage that it takes time to develop an useful and accurate operational model.

3.2.3 Descriptions based on a volume approach

This section presents some approaches for the water level changes. These approaches can also be seen as a volume displacement on the slope and describes the external water by using a volume (or mass) approach.

Triangular shaped wave run-up wedge

ARCHETTI AND BROCCHINI [2002] (reference: HUGHES [2004]) gives the following simple physical argument; the weight of the fluid contained in the hatched wedge area ABD ($W_{(ABC)}$) (Figure 3.1) is proportional to the maximum depth integrated wave momentum flux of the wave before it reached the toe of the structure slope.

$$K_p(M_F)_{MAX} = K_M W_{(ABD)} \tag{3.5}$$

Refer to Hughes [2004] or Appendix C.3 for the expression of the depth integrated wave momentum flux. In HUGHES [2004] the area of water per unit width contained in triangle ABD (Figure 3.1) is given by:

$$\text{Area ABD} = \frac{1}{2} \cdot \frac{{R_u}^2}{\tan\alpha} \cdot \left[\frac{\tan\alpha}{\tan\theta} - 1\right] \tag{3.6}$$

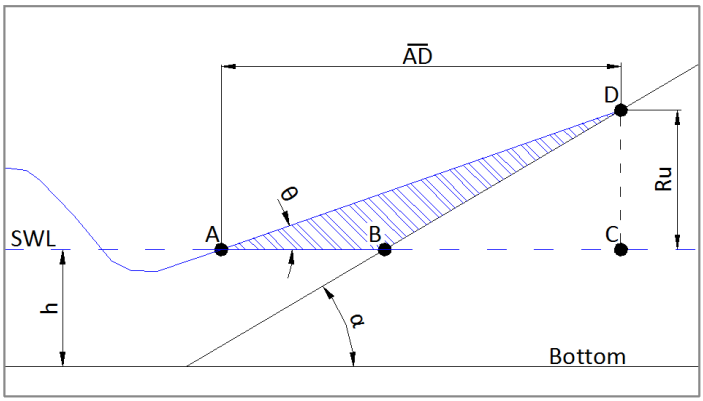

Figure 3.1 - Triangular wedge approach based on HUGHES [2004]

The only unknown variable in Eq. (3.6) is the angle θ. When using an existing run-up height approach, this angle can be calculated. The angle is then a function of the proportionality factor and the maximum depth-integrated wave momentum flux in the wave at or near the toe of the slope. Although, this proportionality factor is also not known.

Representing the run-up sea surface slope as a straight line is an approximation, this might be a reasonable assumption for gentle slopes where wave breaking occurs, but, on steeper slopes where waves behave more like surging breakers, the sea surface elevation will have a more concave shape. Other points of attention are: the method considers only the wave run-up process and slope friction is not included.

Parabola shaped wave run-up wedge

In JUANG AND JIUN-YAN YOU [2009] a parabola wave run-up wedge is used to replace the linear wave run-up wedge's hypothesis. They used the parabola wave run-up wedge theory of CROSS AND SOLLITT [1972]. CROSS AND SOLLITT [1972] proposed that at maximum run-up, the shape of the run-up wedge is assumed to be a parabola with it is vertex at the bottom of the first wave trough (Figure. 3.2). The corresponding equation is:

$$Y = MX^N - A \tag{3.7}$$

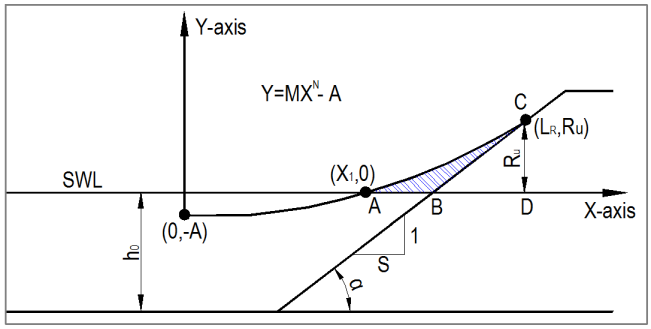

Figure 3.2 - Wave run-up wedge according CROSS AND SOLLITT [1972]
(reference: JUANG AND JIUN-YAN YOU [2009]

JUANG AND JIUN-YAN YOU [2009] compared the parabola wave run-up wedge model with the linear wave run-up wedge approach and concluded that the parabola approach obtained a little bit higher accuracy. Moreover, this method considers only the wave run-up process and due to the concave shape of the run-up wedge, the run-up area is difficult to determine.

Wave run-up wedge according to analytical approaches of the SWE

Analytical approaches based on the solution of the classical shallow water equations are given in CARRIER AND GREENSPAN [1958]. A non-linear solution to the classical shallow water equations, which describe the wave characteristics on a slope, is obtained by LI [2000]. A comparable solution is obtained by SYNOLAKIS [1986], the maximum run-up predicted with that solution is smaller than the solution of Li [2000]. A big disadvantage of these solutions is the complicated character for practical use.

Conclusion

A disadvantage of the above volume approaches is that they only describe a volume during maximum wave run-up. This is because the run-up is an important process in the wave-structure-interaction and therefore the process has been extensively studied and described in the past. In contrast, the run-down can only be calculated by a few rules of thumb based on curve fitting.

3.2.4 Conclusion: *Descriptions of the external water motion*

From above descriptions follows that no complete description exists of the external water motion. This is because of the complexity of water motion during this wave-structure-interaction process. In general, it can be concluded that a description by means of a momentum balance needs a discrete solution, so a numerical model is required. Considering the practical design formulae by VAN DER MEER [1988] a numerical approach should be avoided. In contrast, for a description of the water motion considering a volume or 'energy' approach analytical solutions are available. However, whether these descriptions are suitable for a description of a full wave-structure-interaction should be reflected in the ways in which the internal water movement can be determined. In other words, it should be possible to link the analytical descriptions of the external water motion with a description of the internal water motion. In addition it must be said that the analytical volume and energy methods presented here are not directly applicable without modifications.

3.3 Internal water motion

In this section a description of the internal water motion is given. The internal water motion can be seen as a water flow through a porous medium. Since there is time dependence in the flow resistance in a porous medium, also the variation in time of the internal process is described (see Paragraph 3.3.2).

3.3.1 Forchheimer

The internal water flow can be described as a water flow through a porous medium. For the structures studied in this research, it can be assumed that the flow in the porous part of the structure, is a 'fully' turbulent flow or a Forchheimer flow, therefore Darcy's Law is not valid. The resistance of this water flow through a porous medium of coarse granular material can be reasonable well expressed by a term

that is linear with the flow velocity ($a \cdot u$) and a term that is quadratic with the flow velocity ($b \cdot |u|u$). Such a relation was proposed by FORCHHEIMER [1901] (reference VAN GENT [1995]).

$$I = au + bu|u| \tag{3.8}$$

Where *a* and *b* are both dimensional coefficients. The first term can be seen as the laminar contribution and the second term can be seen as the contribution of turbulence, although the influence of large-scale convective transport is also included in this second term (small-scale convective transport occurs on the scale of the pores). This equation is applicable for turbulent porous media flow as well as in the transitional region between laminar and turbulent flow. The friction coefficients *a* (s/m) and *b* (s^2/m^2) are dimensional and contain several parameters.

Laminar term: $$a = \alpha \frac{(1-n)^2}{n^3} \frac{\upsilon}{gD^2} \tag{3.9}$$

Turbulent term: $$b = \beta \frac{1-n}{n^3} \frac{1}{gD} \tag{3.10}$$

The Forchheimer equation (Eq. 3.8) is valid for stationary flow. However, usually the porous flow in the core of a rubble breakwater is not permanent due to the dynamic effect of the wave. This dynamic effect can be seen in the water flow speeding up and slowing down in alternating directions within a full wave period. In case of a non-continuous flow in a porous medium, the inertia effect should be included. POLUBARINOVA KOCHINA [1952] (reference VAN GENT ET AL. [1994]) therefore added a time-dependent term. This type of formula for unsteady porous flow is referred to as the extended Forchheimer equation:

$$I = au + bu|u| + c\frac{\partial u}{\partial t} \tag{3.11}$$

Where *c* is the inertia term (m^2/s) which take the added mass into account. The expression for the inertia term is:

Inertia term: $$c = \frac{1+\gamma\frac{1-n}{n}}{ng} \tag{3.12}$$

Note 3.1: *In this report the assumption is made that the flow in the porous medium is a Forchheimer flow. However, in case of larger 'grain' diameters, the flow is fully turbulent. In that case other friction terms must be used to determine the water level gradient (see section 5.4.3).*

VAN GENT [1995] performed experiments to find out what the contributions are of the three abovementioned terms of the Forchheimer equation to the pressure gradient. He found that the turbulent term was the first and the inertia term was second in influence. The results are given in Figure 3.3.

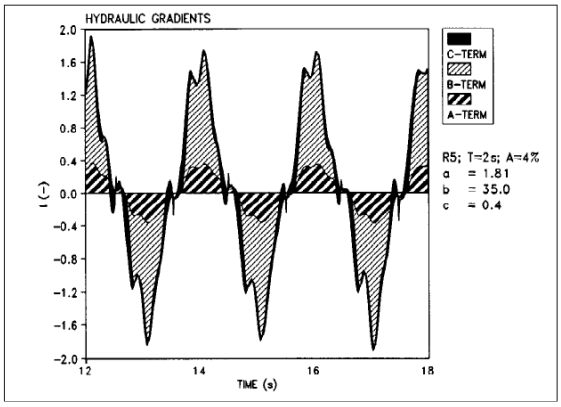

Figure 3.3 - Contributions of the friction terms to the hydraulic gradient (VAN GENT [1995]).

MUTTRAY [2001] describes also the proportions of the laminar, turbulent resistance and the inertia forces on the total hydraulic resistance, results of which are shown in Figure 3.4. The forces of resistance have been shown for a averaged wave period $T = 5\ s$, the determined specified magnitude corresponds to a variation of $T = 3 - 10\ s$.

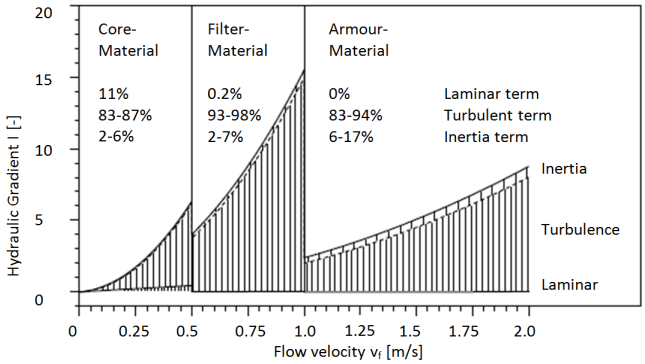

Figure 3.4 - Contributions of the friction terms in the different layers (MUTTRAY [2001]).

Note 3.2: *Simplifications are used for this plot (Figure 3.4), the filter velocity is multiplied by the velocity amplitude ($v_f = \Delta u$) and the velocity curve is assumed sinusoidal ($\delta u/\delta t = \omega \Delta u$).*

Influence of the permeability for surging waves and plunging waves

According to BATTJES [1988] (taken from WITTEMAN [1999]), inertia can be linked to the permeability of the structure. A structure that is permeable according to definition of VAN DER MEER [1988] (Figure 2.7), will have an influence on the run-up. Water is present inside the structure and when waves attack on the structure, the inertia of the water inside the structure will reduce the run-up capacity of the waves. It is likely that this will happen in case of non-breaking waves. This type of waves usually has large periods and therefore, the water inside the structure is able to 'follow' the waves. Breaking waves usually move faster and it is likely that the energy dissipation of those waves will mainly not take place by inertia of the water inside the structure; these waves will lose energy by breaking and dissipating

their energy inside the armour layer. The formation of a large-scale vortex takes place so quickly that viscosity can have no significant effects except at micro scales. Vortex formation as such therefore causes no immediate decrease of the total kinetic energy of the large-scale motion, although it does imply a loss of energy that can be ascribed to the wave. A decay of the wave height can take place so rapidly that it is not accompanied by an induced mean horizontal pressure gradient. Due to the quick motion of swash and back swash, the phreatic surface inside the slope will not be able to keep up. Because of this, the water can infiltrate into the unsaturated zone and thereby dissipate energy due to turbulent friction. So, breaking waves dissipate energy due the breaking phenomenon itself and due to turbulent friction on and in the slope. Permeability of the structure therefore will have the largest influence on the run-up when surging waves are considered. Its influence on breaking waves probably can be neglected.

3.3.2 Friction influence in time

A description of a wave distribution in time provides insight for establishing a simple coupling model and corresponding assumptions. For that reason the observation of the wave motion by MUTTRAY [2001] are mentioned. The wave lines are based on pressure observations in the structure for a given wave period, wave height and water depth. The wave motion is divided in a run-down period (Figure 3.5) and a run-up period (Figure 3.6).

(The following observation are based or taken from MUTTRAY [2001])

Run-down period
Time step T_0: An important feature is that at a highest wave run-up the pressure gradients in the surface region of the top and filter layer (above the SWL) are high. This causes a strong inflow, which is directed nearly normal to the slope surface. Beneath SWL slope parallel downward flow predominates in the surface layer. In the filter layer slope parallel and slope normal currents mix. Over almost the entire depth, an inflow takes place in the breakwater core.

Time step T_1: During the wave run-down the flows are predominantly downwards and slope parallel in the surface layer. In the filter layer slope normal and slope parallel flow components mix continuesly. The water level in the core has risen considerably. For this reason the pressure gradients in the transition from the filter layer to the core have been reduced. However, water continues flowing from the filter layer into the core.

Time step T_2: During the advanced wave process the currents in the armour and filter layer are predominantly slope parallel. The inflow into the core ends at the toe of the slope and creates a distinct, horizontally directed outflow. During the entire wave run-down of the surface layer there is a water level set-up in the core of the breakwater. This raises the transition from inflow to outflow in the core, whereby is never passes "a state of relative calm water" as the wave rushes down (T_1).

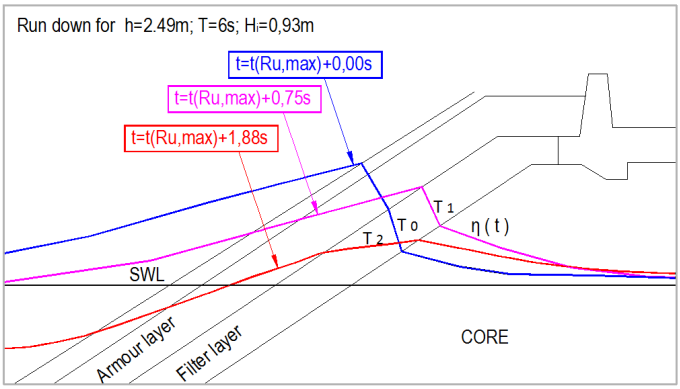

Figure 3.5 - Pressure observations during the run-down period (MUTTRAY [2001]).

Run-up period

The water elevations during run-up are shown in Figure 3.6. Starting from the lowest run-down (T_3), the pressure distribution at the onset (T_4) and the advanced wave run-up (T_5):

Time step T_3: At the lowest wave response the flow in the surface region of the top and filter layer remains more or less parallel to the layer's boundaries. The inflow to the core is stopped and the water level in the core starts to fall. At the toe of the slope there is a significant predominantly horizontal outflow from the core and in the armour and filter layer the outflow is normally aligned with the slope surface.

Time step T_4: At the onset of wave run-up an alternation occurs between the end of the outflow and the start of the inflow leading to an approximate standstill of the flow processes within the structure. The water level and the pressure gradients in and on the structure are very low at this moment in time. In the armour and filter layer already a slope parallel upward flow is starting, which initiates the wave run-up process.

Time step T_5: With increasing wave run-up the water gradients, in the armour and filter layer, are formed. In the entire slope area (surface layer, filter layer and the core area near the slope) outweighing slope normal flow occurs, leading to a strong inflow.

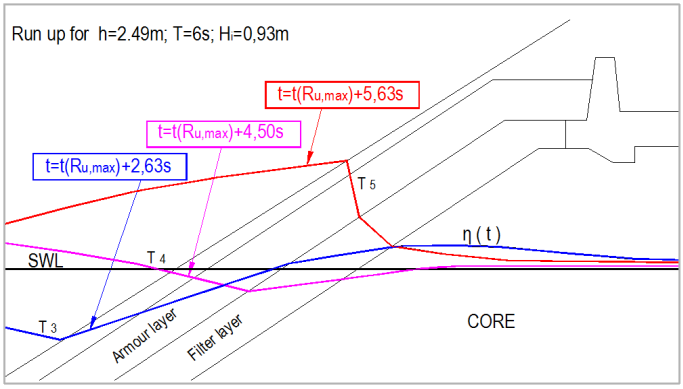

Figure 3.6 - Pressure observation during the run-up period (MUTTRAY [2001]).

Remarks:

- The surface elevation at T_0 and T_5 are located almost on the same position, from this it can be concluded that the wave period of the internal flow is the same as the period of the external flow.
- It is clearly visible that the internal water movement cannot follow the external water movement. This can easily be explained by the flow resistance that occurs in the armour and filter layer.
- When the wave period and the wave height are fixed, the delay is determined by the degree of permeability. In other words, the permeability determines the phase difference between the external and internal flow.
- The largest changes in water levels occur between the time step T_2 and T_3 and between time step T_5 and T_0. From this it can be assumed that in these periods the slope velocities are the highest.
- The volume flow into the structure will create a positive impact on the stability of the armour units, this is caused by the drag force in the direction of the construction. In contrast, the outflow will create a negative impact, this is again a consequence of a drag force which now introduces a 'weight reduction' of the armour unit.

MUTTRAY [2001] observes in his study also the phase difference between layers. The graph in Figure 3.7 is an example of the elevation of the water level on the surface of the armour layer, in the filter layer and in the core for a periodic wave with $T = 6\ s$, $H_i = 1{,}09\ m$ and $h = 2.495m$. In addition, the graph shows that the run-up period in the armour layer is larger than the run-down period, with the result that the run-down velocity is higher than the run-up velocity. Probably it can be assumed that with an increasing permeability the difference between the run-down and run-up period is also increasing, caused by the less amount of water that flows into the armour layer. Besides, the run-up period from the lowest run-down level till the SWL is almost equal to the run-up from the SWL till the highest run-up level. The motion of the water level on the armour layer surface shows a distinct asymmetry (steeper crest, a longer flat trough), which is less pronounced in the filter layer and the core. The average water level in the filter layer and the core is substantially higher than in the armour layer. The lowest run-down achieved in the core reaches only the SWL.

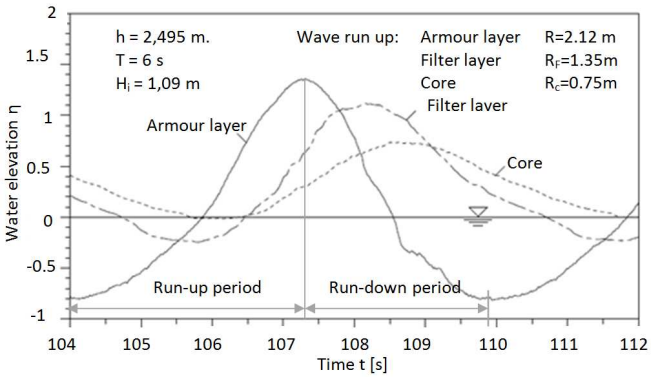

Figure 3.7 - Water elevation in the armour/filter layer and the core (MUTTRAY [2001]).

3.3.3 Conclusion: *Description of the Internal water movement*

The internal water movement can be described by the Forchheimer relation. For a description of the external water movement, a distinction is made between three different approaches: energy approach, momentum approach and a volume approach. For the internal water movement these three approaches can also be describes. A volume or energy approach can be realized if an instantaneous description of the internal water motion is considered. BURCHARTH AND ANDERSEN [1995] shows that, for steady flow in a porous medium, also the Navier-Stokes equations (momentum approach) can be converted to the Forchheimer model. However, due to the time dependence of the internal flow, an analytical method of the above approaches is limited.

3.4 Coupling of the internal and external flow

In this section some possible coupling options will be discussed. In developing this coupling function the previous descriptions of the internal and external motion are used. An analytical way to couple the external and internal water motion is however not available. The existing couple models are based on numerical methods. But, considering the practical design formulae by VAN DER MEER [1988] a numerical modification is not the ideal solution. Also a few recently published articles show that it takes time to develop an useful and accurate operational model. Therefore the objective of this research is to try and find an analytical description of the coupling of the internal and external water movement. Refer to the paper of HALL AND HETTIARACHCHI [1992] for a review of numerical modeling. The most recent review is given by LIN [2008]. In this book ,a reference is made to numerous widely used packages.

In this study three different coupling options are discussed. The first one is to link the internal and external water movement by means of an energy approach. The second one is a coupling by using a momentum balance. The last one is to describe the full interactional process by using a volume exchange principle. Below for each coupling option a brief description is given. With this description, insight is obtained to assess which transfer function is best suited for further development. The choice of which model will further be analyzed will depend on the usability and accuracy of the model. For example, when the model requires a lot of simplifications to realize a model for practical use. In which the simplifications can lead to somewhat distorted results then it might not be the best choice. Besides that it must also be feasible to develop the model based on new findings.

Coupling method 1: Energy approach

From internal and external descriptions follow that a description of the wave-structure-interaction process with an energy approach is a plausible option. However, with the methods mentioned in this study an accurate coupling between the external and internal flow is not possible. A not previously mentioned, but certainly interesting alternative is the method where the energy is expressed in local wave heights. The incoming wave height is the initial condition and the reflective wave the final condition. The dissipation of the energy (or wave height decrease between the incoming and reflective wave) is due to the wave-structure-interaction. The energy dissipation on the slope can be determined by using the method of VAN DER MEER [1990]. For the energy dissipation in the structure some theories are known that could possibly be used ((BURCHARTH ET AL. [1999] and MUTTRAY & OUMERACI [2005]). At this stage of the research it is not clear whether the energy approach can be elaborated in an analytical way.

It should be said that this method offers much potential, because it is based on a measureable initial and final condition (respectively the incoming and reflected wave).

Coupling method 2: Momentum approach

A coupling by means of a momentum balance is an alternative. In that case both the external and internal water movement should be described by the Navier-Stokes equations. The review of in this report shows that both internal and external description requires a discrete solution. This type of linking will therefore lead to a numerical coupling method.

Coupling method 3: Volume approach

In this case a volume exchange is supposed. This can be achieved by linking the internal and external water level. In this chapter, descriptions for both the external and internal water levels are given. For the external part, the linear water level description of HUGHES [2004] can be used. The Forchheimer equation can be used to determine the internal water level by calculating the internal water level gradient. The volume approach is relatively simple to validate, since volume changes can be properly measured. However, the phase difference between the different layers in the structure is a difficult feature. The influence of this effect should therefore be looked after properly.

Conclusion

From the foregoing coupling options it can be concluded that a momentum approach is the least obvious way. Since numerical calculation methods are unavoidable for this option. For the remaining two methods no direct choice can be made without further research. In addition, these two methods have the advantage that they contains many components that are measurable and observable, think of the reflective wave height, the incoming wave height and the run-up. The final choice between the two models should be reflected in the elaboration of the couplings options in the next chapter.

Chapter 4
Detailed description of the energy and volume model

The previous chapter proposed two possible coupling approaches for describing the wave-structure-interaction process, namely the energy and volume approach. With help of these approaches it is assumed that the effect of core permeability on the armour layer stability can be described. With the detailed descriptions a found choice is made for one of the two models. This model will be subjected to further development in the remainder of this study.

4.1 The Energy model

4.1.1 General

The methodology of this model is based on the energy balance. In order to give insight into the processes that may affect the energy balance, a description is given of the energy transformations that take place at different slopes and for different processes. At first a description of the energy transformation for the most simple case is given; an energy transformation on a smooth impermeable slope not influenced by energy dissipation. After that there is a description of the energy transformation for a rough slope and finally the energy transformation for a rough permeable slope will be described.

For non-breaking wave run-up on a 'frictionless' slope, the wave shape and velocities are continuous for the run-up and run-down process. Therefore, the total energy of the wave should be conserved. Any energy loss due to the viscous effects on the free surface and the foreshore bottom which are generally small will be neglected here. As the wave moves towards the slope, the wave shape deforms as the depth decreases (non-linear effects), hereby transforming a part of the waves' kinetic energy into potential energy. During the run-up process the kinetic energy decreases and transforms to potential energy. For non-breaking wave run-up on a frictionless slope, the potential energy reaches a maximum when the wave reaches the maximum run-up position, The kinetic energy at this position is very small. This small amount of energy may be associated with the mild reflected wave from the slope or the small and negligible water particle velocity associated with the run-up tongue. When the wave has reached its maximum run-up, the potential energy decreases again and now the kinetic energy increases as the water begins to rush down on the slope. During the entire process (when energy dissipation is neglected), both the total energy and total volume are constant which means that the mass and the energy are conserved.

With this theory as background, the next step will be made by describing the energy distribution in a wave-structure-interaction where the friction effect is included. The left part in Figure 4-1 shows a schematization (FÜRHBÖTER [1993]) of the energy distribution for the run-up period on a impermeable rough slope, where the roughness of the armour layer determines the rate of reflection. FÜRHBÖTER [1993] described that at the breaking point of a surging breaker the water mass forms a nearly vertical front which flattens out producing a strong up-rush swell with a high reflection rate of the wave energy. This high rate of reflection will decrease again during the run-down even before the actual reflection

wave has developed (the right part of Figure 4.1). The high up-rush and down-rush velocities on the slope, causes high tangential forces (shear stresses) over the large run-up height R_u and run-down height R_d, being the main contributors to energy dissipation during run-up and run-down.

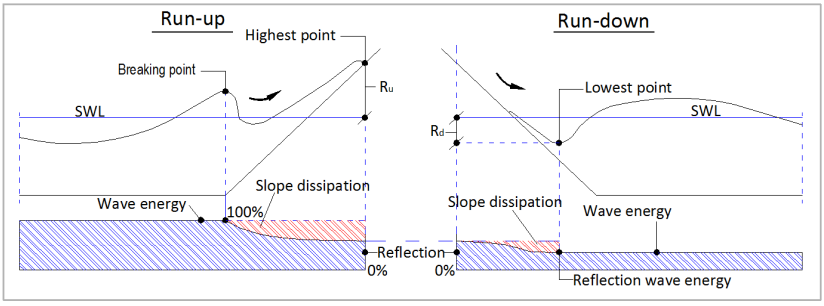

Figure 4.1 - Energy distribution for a rough impermeable structure (FÜRHBÖTER [1993]).

The last but most difficult step is the description of the energy distribution for a wave-structure-interaction, where both the body and slope have a permeable and rough character. The left part of Figure 4.2 shows a schematization of the energy distribution for the run-up period on a permeable rough slope. In this case, mostly the roughness and permeability determine the rate of reflection. During the run-up period, a part of the water mass flows into the structure body and the other portion will cause a run-up on the slope. If wave run-up exceeds the crest level, overtopping takes place. In such cases, the wave energy reaching the lee side originates from transmission and overtopping. The last two processes (overtopping and transmission) will not be considered in this model. The dissipated energy can now be expressed as: $E_d = E_{d,s} + E_{d,b}$; where $E_{d,s}$ is the energy dissipated on the slope of the structure; and $E_{d,b}$ the energy dissipated in the body of the structure. Simply adding an extra dissipation term (on behalf of the dissipation in the body) to the energy loss of the run-up for a rough impermeable slope (example Figure 4.1) is not possible. This is due the fact that the energy loss on the slope will be less in case of a permeable slope, for the reason that the amount of water on the slope will be reduced by the inflow of water into the structure's body. The same process holds for the run-down period (right part of Figure 4.2).

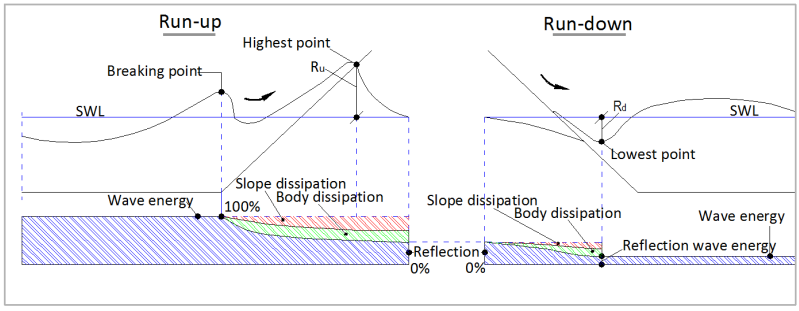

Figure 4.2 - Energy distribution for a rough permeable structure

With this example in mind the following conclusion can be made:

The energy distribution for a wave-structure-interaction, where both the body and slope have a permeable and rough character, can be separated into four different components: (1) dissipation in the structure's body, (2) dissipation on the slope, (3) the reflective wave from the structure's body, and (4) the reflective wave from the slope. Where the components (3) and (4) together form the total reflective wave. In mathematical notation this basic concept can be summarized dimensionless as follows:

$$1 = \frac{H_{body}}{H_i} + \frac{H_{slope}}{H_i} + \frac{\Delta H_{slope}}{H_i} + \frac{\Delta H_{body}}{H_i} = \frac{H_r}{H_i} + \frac{\Delta H_{body}}{H_i} + \frac{\Delta H_{body}}{H_i} \quad (4.1)$$

This model assumes that there is conservation of energy, if $\mathrm{E_i}$ represents the free wave energy of an incident wave, then conservation of energy yields:

$$E_i - \Delta E_{slope} - \Delta E_{body} = E_{slope} + E_{body} = E_r \quad (4.2)$$

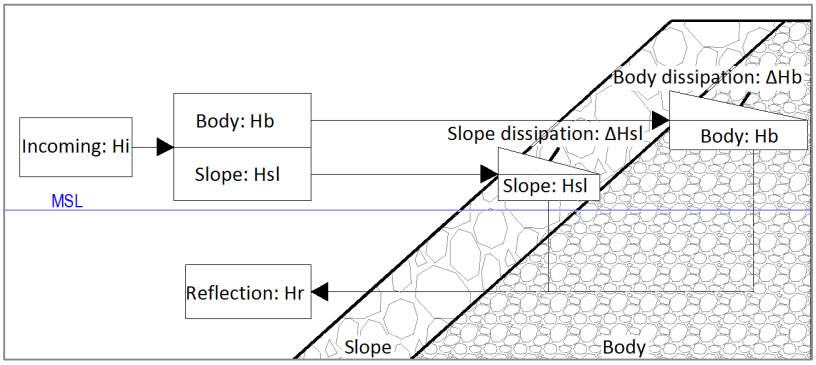

Figure 4.3 - Schema of the wave components on the foreshore and in /on the structure

The principle of this model is to characterize the aforesaid components, with the incident wave as the initial condition and the reflective wave as the final condition. Below first a brief description of the initial condition and the components (1) and (2) is given. After that follows a detailed description of the reflective wave. Finally there is tried to link the components (3) and (4) with these reflection terms.

4.1.2 Initial condition: incoming wave

This term can be seen as the incident wave height. As mentioned before, a passing wave has a potential and a kinetic term. Below a description of both terms and the total energy for a free incident wave is given.

Potential energy

As the fluid is assumed incompressible and surface tension is neglected all the potential energy originates from the gravitational forces. Furthermore, only the energy caused by displacement of the water surface from the mean water level is included. With these assumptions the value of the potential energy E_p can be written as:

$$E_p = \frac{1}{2}\rho g\overline{\eta^2} = \frac{1}{2}\rho g\frac{H^2}{4}\overline{cos^2\theta} = \frac{1}{4}\rho g a^2 \quad (4.3)$$

Kinetic energy

When an ideal fluid is considered no turbulent kinetic energy present. Therefore, only the particle velocities caused by the wave itself are considered. The corresponding time-averaged (over one period) kinematic energy in the entire column, from bottom to surface, is, per unit surface area:

$$E_{kin} = \overline{\int_{-d}^{\eta} 1/2\rho u^2 dz} = \frac{1}{4}\rho g a^2 \tag{4.4}$$

Total energy

In general, the total wave energy density per unit area in the horizontal plane for a free incident wave, $\mathrm{E_i}$ (kinetic and potential energy), can be expressed as the sum of the kinetic energy density E_k and the potential energy density E_p:

$$E_{\ i} = E_p + E_k = \frac{1}{2}\ \rho g a^2 \tag{4.5}$$

4.1.3 Dissipation in the body of the structure

Component (1): The first component is the wave dissipation or energy dissipation in the body of the structure. This process can be considered as the energy dissipation during the infiltration and seepage of the wave in the body of the structure. The main sources of energy dissipation are friction and turbulence in the pores. For determining the energy dissipation in the structure body the energy flux should be determined. A correct verification of this flux needs a time-varying flow model, and this requires a numerical approach. The use of a simplified Forchheimer model, which takes only the laminar and turbulent terms into account, is a possible solution for this problem. However, in the filter and the armour layer the inertia term is relative high. In determining the energy flux, the absence of this term could lead to unrealistic results.

Note4.1: *The damping approaches of the wave oscillation by BURCHARTH ET AL. [1999] and MUTTRAY & OUMERACI [2005] cannot directly be used in this case, because these approaches describes a wave envelop instead of one single wave.*

4.1.4 Dissipation in and on the structure slope

Component (2): The second component is the wave dissipation or energy dissipation in or on the structure slope. In this study the non-breaking (surging) waves are taken into consideration, therefore the energy dissipation is mostly a result of the slope dissipation (instead of dissipation due to wave breaking). As said before, any energy loss due to the viscous effects on the free surface and the foreshore bottom which are generally small will be neglected here. With these assumptions the energy dissipation can be expressed in the following term.

$$\Delta E_{slope} = E_i - E_r - \Delta E_{body} \tag{4.6}$$

Since the slope dissipation is only a result of the slope velocity it can be said that the velocity on the slope is equal to the velocity that must occur with a given slope velocity. In other words, if the incident wave, reflection wave, and the 'body' dissipation are known, the slope velocity can be determined on the basis of the slope dissipation. In formula form this is:

$$\Delta E_{slope} = f(u_{slope}) \tag{4.7}$$

It is necessary to have an energy 'dissipation' approach for flows in which the rough elements of the structure are in the same order of magnitude as the water depth. For the determination of E_{slope} the shear stress of moving water layers above the boundary layer for a given flow velocity is considered as follows:

$$E_{slope} = \frac{1}{T}\int_0^T \tau_0 U_\delta dt \tag{4.9}$$

This is a theoretical formulation for the time integrated power dissipation by friction near the bottom. With the use of the Chezy equation, the hydraulic radius, and the expression of Airy, the shear stress τ_0 can be calculated. LE ROUX [2003]: "However, in case of waves, the form of the velocity distribution is uncertain (TELEKI, 1972) and τ_0 cannot be measured directly on a moving bed (SOULSBY AND WHITEHOUSE, 1997). It is, therefore, usually derived from the peak near-bed wave orbital velocity U_δ using the quadratic friction law".

$$\tau_{sl} = \frac{1}{2}\rho_w f_w {U_\delta}^2 \tag{4.10}$$

The peak near-bed wave orbital velocity can be written as:

$$U_\delta = \widehat{U}_\delta \sin(\omega t) \tag{4.11}$$

With this expression Equation 4.10 becomes:

$$\tau_{sl} = \frac{1}{2}\rho_w f_w {\widehat{U}_\delta}^2 sin^2(\omega t) \tag{4.12}$$

The following equation for slope induced dissipation can be described:

$$E_{slope} = \frac{\rho f_w {\widehat{U}_\delta}^3}{2T}\frac{1}{T}\int_0^T sin^3(\omega t)dt = \frac{4}{3\pi}\rho f_w {\widehat{U}_\delta}^3 \tag{4.13}$$

For turbulent boundary layers, several methods have been proposed to calculate f_w. The most widely used equations are those of JONSSON [1963], SWART [1974] and SOULSBY [1997] (see LE ROUX [2003]).

Note 4.2: *In Eq. 4.9-4.13 different notation is used as in the referred literature.*

4.1.5 Final condition: reflective wave

This is term can be seen as the reflective wave height. The wave reflection coefficient used in this study is a bulk parameter for the hydraulic processes at a rubble mound structure, i.e. for wave run-up, wave run-down and wave penetration into the structure. As mentioned before the wave reflection at a non-overtopped rubble mound structure is for non-breaking waves determined by two processes:

- Wave energy dissipation on the slope;
- Wave energy dissipation in the body of the structure.

In contrast to the expressions described in literature, MUTTRAY ET AL. [2006] included the effect of porosity and slope roughness in the reflection coefficient. Because in the approach OF MUTTRAY ET AL. [2006] the wave penetration is not seen as a second order effect, this approach is better suited for this study. However the wave penetration term should be looked after in more detail since it consists of

components that differ in time, i.e., the reflection component of the armour layer will have a phase difference with the reflection component of the filter layer. The influences of both effects should therefore be investigated more thoroughly (see also Figure 3.9).

The reflective wave can be divided into two wave parts. The first wave part is the part that is reflected from the body of the structure (Component 3). The second part is the wave that reflects from the structure slope (Component 4). Below a description for both components of the wave height is given.

Component (3) - *wave from the structure body*

The flow from the structure body is defined as the "body wave". When the dissipated energy in the body of the structure is calculated, then the reflecting energy from the body is the remaining term of the advanced body wave. The complicated part of determine the body wave is to make a distinction between the water outflow (“body wave”) and the water on the interface (“slope wave”). To make this distinction a numerical method is inevitable. The numerical model ODIFLOCS developed by VAN GENT [1994] describes a model that simulates the wave action both on, and within coastal structures. This numerical model couples a hydraulic model with a porous flow model. With given hydraulic model conditions (run-up and run-down), this numerical model is a good tool to describe the flow through the interface (armour and filter layer).

Component (4) - *wave from the structure slope:*

If the total dissipation is determined by the reflective wave term, then the slope wave is the total reflection wave reduced by the body wave (component). The slope wave says something about the amount of energy of the water flow on the slope at the time that the water flow is no longer affected by the environmental impact (no energy dissipation). This term is a useful tool to indicate the ratios in the reflective term between the 'body wave' and 'slope wave’.

4.1.6 Remarks regarding the energy model

Component (3) and (4) are both a function of the slope velocity and therefore related to the destabilization process of the armour layer. For this reason, the external and internal process can be coupled. Furthermore, the water outflow from the structure body has also a considerable impact on the armour layer stability. Other points of attentions are:

- Separation of the volume flow on the slope (i.e. in and on the armour layer) and the volume outflow from filter layer to the armour layer.
- In present time an accurate analytical description of the volume flow in the body as a function of time and space is not available. It can be concluded that a numerical approach is inevitable for a description of the wave dissipation in the body of the structure. A possible solution for this problem is the use of a simplified form of the Forchheimer equation, with only the laminar and turbulent term. The reliability of this solution needs further research.
- Energy of the reflection wave: there are several approaches to determine the reflection factor, however there is no approach available with a porosity or permeability coefficient explicitly included.

- Energy dissipation on the slope of the structure: with the use of an analytical wave curve solution (for example Carrier and Greenspan [1958]), an approach for the dissipation on the slope is possible. However, the thicknesses of the water layer of down-rush and up-rush flow are unknown.

4.2 The volume-exchange-model

4.2.1 General

This model assumes that the volume change of the external water volume is equal to the volume change of the internal water volume ($V_{2\_out}=V_{2\_in}$), see Figure 4.4. If the water volume in front of a rough impermeable sloped structure is known and also the change of the internal water volume, the water surface elevation in front of a rough permeable sloped structure can be determined. In this model only the run-up process is included, because it is assumed that this process mostly described the influence of the permeability.

With the use of existing run-up approaches it is possible to determine the run-up for an impermeable rough slope, the run-up is then a function of the incoming wave height, the wave period, the slope angle and the slope roughness (expressed in the D_{n50}). The assumption for this concept is that the total external run-up volume is reduced by the volume that flows into the structure (V_2). Further, it is assumed that the reduction of the external volume is equal to the volume that flows into the structure ($V_{2\_in}=V_{2\_out}$). With this assumption the run-up is then also a function of the permeability. Besides this, it is assumed that this volume can be determined with the inflow that would prevail for a run-up on a rough impermeable slope. Figure 4.4 shows a schematization of this process.

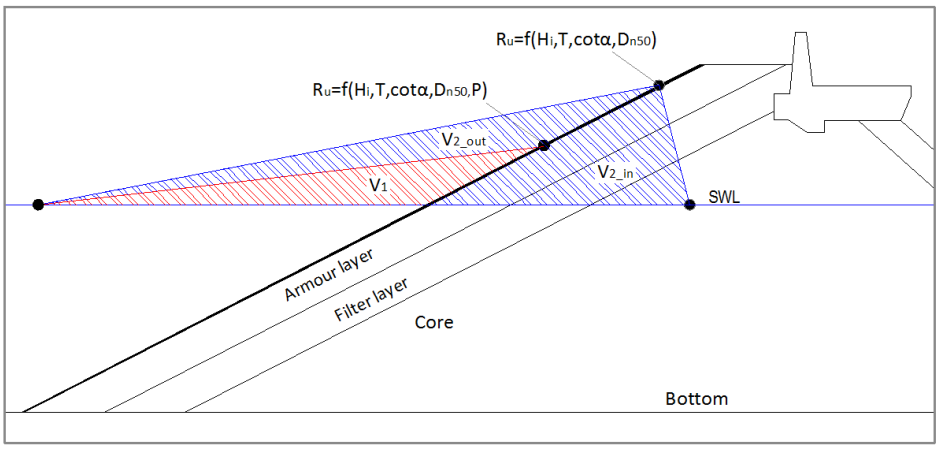

Figure 4.4 - Schema of external volume change and volume inflow during maximum wave run-up

4.2.2 External water volume

The volume-exchange-model requires a description of the water-surface elevation, when the wave interacts with the rough slope of the structure. Section 3.2 gives a description of these methods. For a triangular wave run-up, as illustrated in Figure 4.4, the method of HUGHES [2004] can be used.

4.2.3 Internal water volume

Since this model assumes a maximum imposed external water level, it is not necessary to use a time varying model. The model should only be able to determine the volume that flows into the structure during a run-up from SWL till the maximum run-up level. A simplified Forchheimer model therefore can be used in this case.

4.2.4 Remarks regarding the volume-exchange-model

- For the reason that only the maximum run-up water surface level is used, a time varying model is not necessarily for the external and internal movement.
- Research in the past showed that the influence of the permeability on the run-up for high Iribarren numbers (surging waves) is very large. This indicates that for the wave conditions, which are examined in this study, the volume exchange model is a good model to apply.

4.3 General conclusion

The energy approach is based on an energy flux. A correct verification implies a time-varying flow model, which again requires a numerical approach. However, the basic principle is to realize an analytic model. Therefore the numerical approach should be followed by a time averaged approach, which then can give an analytical description of the waves on the slope, inside the structure and a coupling of both models. For practical use the time-varying flow model requires a lot of simplifications. There is a risk that all the simplifications will lead to somewhat distorted results. Therefore ultimately the energy balance approach will be a long and tedious exercise to get useful results.

In contrast, the volume-exchange-model appears more straightforward. By linking an approach for the run-up wedge to the wave kinematics in front of the structure a simply theoretical model of the run-up process can be draw. With the use of a similar internal water level fluctuations model, the internal and external waterline can be coupled. This will probably require some iteration. Due to the simple principle of the model, the model can easily be further developed on basis of new findings. This process can be linked almost directly to the armour layer stability, because it is more focused on the run-up/run-down process.

By reason of the analytical and transparent principle, the volume-exchange-model shall be further developed in this study. However, the obtained knowledge of the energy approach will also be used.

Chapter 5

The volume-exchange-model

5.1 Introduction

In this chapter, the volume-exchange-model, discussed in the previous chapter, will be elaborated. This model has the advantage that the basics of the method are simple and straight forward. Therefore it could lead easily be developed on the basis of new findings. To determine the permeability of the structure only the run-up process is included, because it is assumed that this process mostly describes the influence of the permeability. In addition, the assumption is made that the incoming wave is a regular sinus wave, which can be refined in a later stage.

For the determination of the external water volume the triangular wave run-up wedge according to HUGHES [2004]] is used. Because this theory includes an unknown angle between still water level and surface water run-up, a simplification is necessary to apply it directly. A more complete description is achieved by linking the run-up wedge approach of HUGHES [2004] to the wave kinematics in front of the structure. This description of the external run-up volume can be used as an imposed external condition in the volume-exchange-model. The volume inflow can be determined according to this external water volume. This leads to a reduced external water volume and a corresponding external wave run-up reduction. The influence of the permeability on the external process can now be calculated. At the end of the chapter several options are mentioned to further develop the model. These options will be discussed briefly and will not be implemented in the model.

5.2 Deriving a 'new' run-up volume approach

In preparation for drafting a volume-exchange-model, first a run-up approach for a non breaking sinus wave on a smooth impermeable structure slope will be elaborated. This model contains the principle of a triangular wave run-up shape introduced by HUGHES [2004]. As mentioned before, in the theory of HUGHES [2004] an unknown variable (angle between still water level and run-up water surface) is included, thus this description is not directly applicable.

The basic principle behind the 'new' run-up volume description is that the incoming 'sinusoidal' wave crest has the same volume as the run-up volume. If the incoming wave is assumed to be a sinusoidal wave, the crest volume (half of the wave length) can be described as follows (see Figure 5.1):

$$V_i = \frac{H_s L_0}{2\pi} \tag{5.1}$$

Considering the triangular wedge approach the total wave run-up volume can be expressed as:

$$V_{Ru} = \frac{1}{2} d R_u \tag{5.2}$$

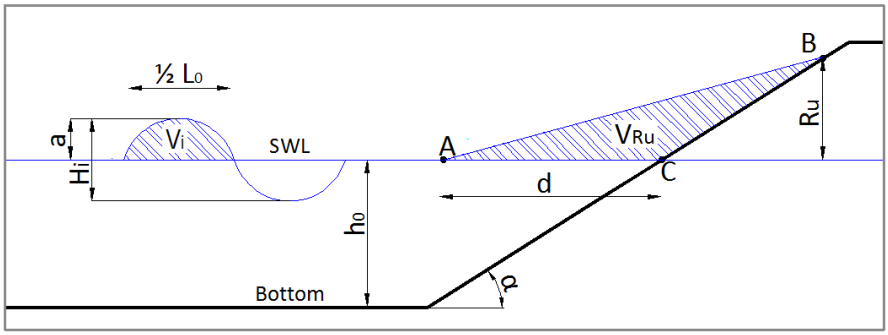

Figure 5.1 - Schematization of the wave run-up model for a 'frictionless' slope

This approach assumes no energy losses due to bottom friction (foreshore and structure slope) and viscous effects on the free surface. With this assumption it can be stated that the energy of the incoming wave crest is equal to the total energy of the run-up volume. In the previous chapter is given that the total wave energy density of an incident wave can be expressed as the sum of the kinetic energy density $\mathrm{E_k}$ and the potential energy density $\mathrm{E_p}$. The expression of the total energy of half a wave length is:

$$E_i = \frac{1}{8}\rho g {H_s}^2 \cdot L_0 \tag{5.3}$$

When the wave reaches the maximum run-up position, the potential energy reaches a maximum. The kinetic energy at this position is very small. This small amount of energy could be associated with the mild reflected wave from the slope or the small negligible water particle velocity associated with the run-up tongue. The small amount of kinetic energy will be neglected here. The energy of the wave run-up triangle can be described as:

$$E_{pot} = E_{tot} = \frac{1}{6}\rho g {R_u}^2 d \tag{5.4}$$

It is assumed that the volume of the crest of the incoming wave is equal to the 'triangular' run-up volume and that no energy dissipation occurs. In formulae this can be expressed as:

$$E_i = E_r \tag{5.5}$$
$$V_i = V_{Ru} \tag{5.6}$$

Using the equations and assumption from above the unknown R_u and d can be calculated, which leads to the following expressions:

$$R_u = \frac{3}{4}\pi H_s \tag{5.7}$$
$$d = \frac{4L_0}{3\pi^2} \tag{5.8}$$

With the use of these equations the 'new' run-up wedge volume description (Eq. 5.2) can now be expressed as:

$$V_{Ru} = \frac{2}{3}\frac{L_0}{\pi^2} R_u \tag{5.9}$$

According to this theory the run-up for non-breaking waves is only related to the wave height. This theory is confirmed by the following quote of HUGHES [2004]: "*run-up data for non-breaking waves that surge up steeper slopes does not correlate as well to the Iribarren number, and instead run-up appears in this case to be directly related to wave height.*"

Reliability test

The assumption that the run-up volume has a triangular shape will lead to an underestimation of the actual run-up in case of non-breaking waves, because these waves will have a more concave shaped sea surface elevation (see also HUGHES [2004]). However, it is expected that the simplifications used in the 'new' run-up wedge approach are not very unrealistic. By testing the reliability an indication of the inaccuracy can be given. This is done by comparing this approach with the run-up approach described in the CUR/CIRIA [2007] However, it should be remembered that also this approach is based on a simplification of the reality. This approach can be expressed as:

$$\frac{R_{u_{2\%}}}{H_s} = A\xi + B \tag{5.10}$$

ALLSOP ET AL. [1985], described in the CUR / CIRIA [2007], suggested the following coefficients (which do not include safety margins): $A = -0.21$ and $B = 3.39$. The method of ALLSOP ET AL. [1985] describes the run-up of smooth slopes (frictionless). For this model it should be taken into consideration that it is also a simplification of the realitiy. This run-up estimation is not only a representation of the wave run-up on smooth slopes, but it takes also a certain degree of energy dissipation into account, for the foreshore and viscous effects on the free surface. In this comparison the Iribarren breaker parameter is between 3.5 and 6 and the significante wave height H_s is 5. This leads to the following results:

Run-up according to ALLSOP ET AL. [1985]:

$$R_u = H_s \cdot (A\xi + B) = 5 \cdot (-0.21 \cdot (3.5 \; or \; 6) + 3.39) = 13.3 - 10.7 \; m$$

Run-up according to the 'new' run-up wedge approach:

$$R_u = \frac{6}{8}\pi H_s = \frac{6}{8} \cdot \pi \cdot 5 = 11.7 \; m$$

Without drawing conclusions, this comparison does show that the run-up using the method of energy and volume conservation is a realistic value. It can be concluded that this external volume approach is a realistic basis for the volume-exchange-model, described in the next section.

In the run-up determination according to the 'new' run-up volume approach a correction for the roughness of the structure slope is not yet included. However, to have a reliable imposed external wave run-up a roughness reduction must be included. A problem is that the reduction factors for the roughness described in literature, for example in the CUR / CIRIA 2007, have the disadvantage that they also express a degree of permeability of the layers. Appendix A contains a table where a more specific composition of the armour layer is given. The composition of the armour layer considered in this study is between code 7 and 9. Here a reduction value (γ_f) of 0.75 is used. The reduced run-up due to slope roughness can be described as follows:

$$R_{u,f} = \gamma_f \cdot R_u = 0.75 \cdot R_u \quad (5.11)$$

Also for determination of the run-up volume (Eq. 5.9) this friction factor should be included. This leads to the following equation:

$$V_{Ru,f} = \frac{2}{3} \cdot \frac{L_0}{\pi^2} \cdot R_{u,f} \quad (5.12)$$

Note 5.1: *Further research is necessary to be able to express the porosity and roughness separately.*

5.3 Volume exchange approach

5.3.1 Basic principle

In this study the permeability of the structure is expressed as a reduction of the external wave run-up volume. This reduction is caused by the inflowing water volume V_b that prevails during the maximum wave run-up process (run-up from SWL till maximum run-up). The volumes of water in and on the structure can be divided into three elements: the run-up volume with friction ($V_{Ru,f}$), the volume in the body of the structure (V_b) and the reduced run-up volume ($V_{Ru,r}$). In formulae this is:

$$V_{Ru,r} = V_{Ru,f} - V_b \quad (5.13)$$

By using the run-up volume approach (friction included) from the previous section including the assumption that the internal water volume has a triangular shape, the total internal water volume can be calculated. This is realized with the following formula (see also Figure 5.2), in which *n* is the porosity of the granular material and *I* the internal water level gradient:

$$V_{b1} = \frac{1}{2} \cdot n \cdot \left(\frac{1}{I}\right) \cdot R_{u,f}^2 \quad (5.14)$$

Assuming that the wave run-up triangle for permeable structure is equal to the wave run-up triangle for impermeable slopes, the reduced run-up is then the volume ratio of the two run-up wedges multiplied by the run-up for a rough impermeable slope:

$$R_{u,r} = \frac{(V_{Ru,f} - V_b)}{V_{Ru,f}} \cdot R_{u,f} \quad (5.15)$$

The only unknown variable in the volume exchange method (Eq. 5.13) is the internal water level gradient (I), required for calculating the body volume. The determination of this gradient will be described in the next section.

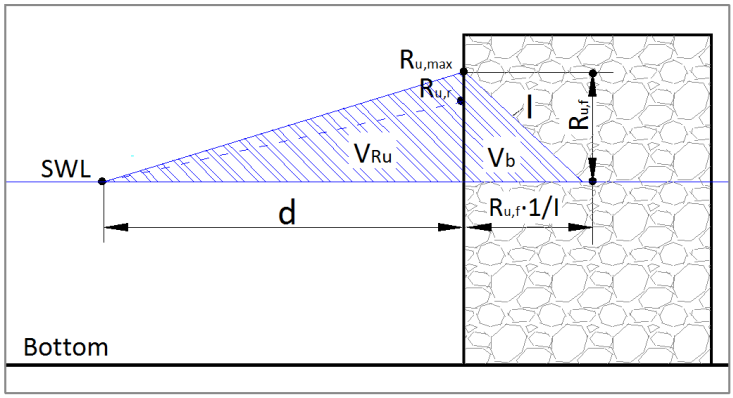

Figure 5.2 - Volume-exchange-model for a homogeneous structure with a vertical transition

5.3.2 Determination of the water flow into the body of the structure

In chapter 3 is described that the resistance of the water flow through a porous medium of course granular material can be reasonable well expressed by a term that is linear with the flow velocity $(a \cdot u)$, a term that is quadratic with the flow velocity $(b \cdot |u|u)$ and a time-dependent term, which takes the added mass into account $(c \cdot \partial u/\partial t)$. This type of formula for unsteady porous flow refers to the extended Forchheimer equation:

$$I = au + bu|u| + c\frac{\partial u}{\partial t} \tag{3.8}$$

In this study, the internal water volume is determined, for a given maximum wave run-up, on the basis of a previously estimated internal water gradient. With a previously estimated gradient the (internal) velocity in a porous medium can be determined. Initially, only the turbulent term $(b \cdot |u|u)$ is taken into account. The reason behind this is that according to the results in study of VAN GENT [1995], mentioned in chapter 3, the influence of this term is the highest and is in the order of 90%. It is also assumed that the porous grain material is homogeneous (non-layered structure type), which can still be refined in a later stage. The volume inflow (in the same period) should be equal to the water volume that the gradient 'prescribed'. If this is not the case, the gradient should be modified until both volumes are the same (iteration). In the simplest case, the flow velocity in the porous medium can be expressed as the relation between the water level gradient and turbulent term:

$$u = \sqrt{\frac{I}{b}} \tag{5.16}$$

Assuming a 'Forchheimer flow' (see Chapter 3.3) the turbulent term can be expressed as:

$$b = \beta \frac{1-n}{n^3}\frac{1}{gD} \tag{3.10}$$

From this relationship follows when using the Forchheimer model it is important to accurately determine the porosity of the porous material, since b is very sensitive to variations of n. In practice it is very difficult to estimate the value of the porosity correctly, especially when it concerns the porosity of a core of a rubble breakwater in situ. This will always require special attention in further practical

applications of the model. Another point of attention is the rate of grading of the granules. In case of a high D_{85}/D_{15}-value (wide grading) the porosity is low, because small grains will fill the pores between the large grains.

Using formula 5.16, the volume inflow in the body of the structure can be determined. Initially a vertical transition is considered.

Vertical transition

The coupling between the external flow and the internal flow is mainly determined by the pressures, caused by the variations in the free surface elevations. In case of a horizontal transition this results in a horizontal flow in the porous region. To determine the volume inflow a sinusoidal wave run-up is considered with a maximum wave run-up height in a time span of one quarter of the wave period. This time span is based on test results of MUTTRAY [2001], see Figure 3.5-3.7 in Section 3.2.2. The period represents the up-rush period from SWL till the maximum wave run-up height. In reality, this period is longer, because the run-down period is not the same as the run-up period. See Figure 5.3 for a simplified illustration of this process (the direction of the flow is landwards). The volume inflow for a rough vertical transition can be expressed as:

$$V_{b2} = \int_0^{0.25T_0} \sqrt{I/b}\ R_{u,f} \cdot \sin(\omega t)\ dt = \frac{1}{\omega}\sqrt{I/b} \cdot R_{u,f} \cdot \left(1 - \cos\left(\omega \cdot \frac{T_0}{4}\right)\right) \tag{5.17}$$

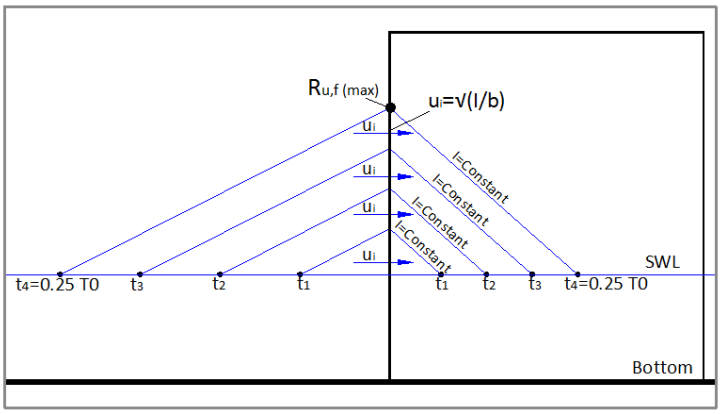

Figure 5.3 - Schematization of the wave run-up model for a permeable vertical transition

To determine the occurring water level gradient (I), the following equation must be satisfied:

$$V_{b1} = V_{b2}$$

$$\frac{1}{2} \cdot n \cdot \left(\frac{1}{I}\right) \cdot R_{u,f}^2 = \frac{1}{\omega}\sqrt{I/b} \cdot R_{u,f} \cdot \left(1 - \cos\left(\omega \cdot \frac{T_0}{4}\right)\right) \tag{5.18}$$

The waterlevel gradient can be determined iteratively

Sloped transition

For a sloped transition, the volume inflow is not the same as for a vertical transition. In reality, for a sloped transition, the waterline hangs under the sloped transition, wherefore the water inflow is limited. In such case it is difficult to determine the water inflow, because the water flow is not exactly horizontal

(landwards) but mainly downwards. VAN GENT [1994]: “The downward vertical velocity of the phreatic surface has a maximum. This is the result of the equilibrium of gravity and friction. If this maximum would be exceeded, the gradient in the pressures would be larger than one. This means that the water would flow quicker than the "free seepage velocity" which is not possible. The upward velocity has a maximum as well. This velocity is in the same order of magnitude as the maximum downward velocity. The maximum vertical velocity is taken the same in both directions.” In formula:

$$I_y = a \cdot w + b \cdot w|w| \ \leq 1 \tag{5.19}$$

This means that the flow velocities cannot be calculated using the same principle as for a vertical transition (Eq. 5.18). However, the exact maximum differs from this value because the real flow does not have to be completely vertical at the phreatic surface. A solution for this unknown maximum gradient is to determine a predefined maximum gradient, corresponding to the geometric properties of the structure (slope angle, porosity and D_{n50}) and a non-horizontal flow. If the gradient from the water level iteration surpass this maximum predefined gradient, the predefined gradient should be used in the calculation of the volume inflow. If the predefined maximum water level gradient is not considered, the gradient iteration for a rough sloped transition can be expressed similarly as for a vertical transition with a different distance of inflow:

$$V_{b1} = V_{b2\_\mathrm{slope}}$$

$$\frac{1}{2} \cdot n \cdot \left(\frac{1}{I}\right) \cdot R_{u,f}^2 = \frac{1}{\omega}\sqrt{\mathrm{I/b}}\,\frac{\mathrm{R_{u,f}}}{\sin(\alpha)}\left(1 - \cos\left(\omega \cdot \frac{\mathrm{T_0}}{4}\right)\right) \tag{5.20}$$

An indication of the water level gradient iteration for a sloped transition is shown in Figure 5.4.

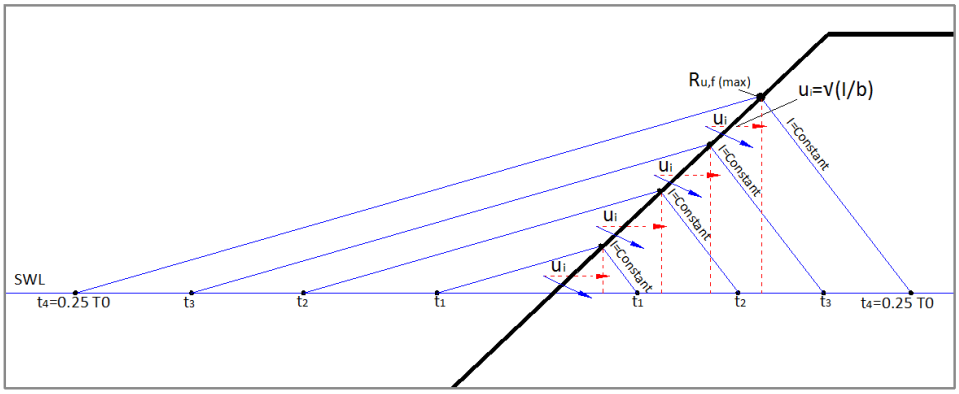

Figure 5.4 - Schematization of the wave run-up model for a permeable sloped transition

The dotted red line and red arrows show the gradient and volume inflow in case of a vertical transition. The only difference in the gradient iteration for a sloped transition is the inflow length. However, the volume inflow in reality is better described by the blue arrows. This iteration error is limited by the predefined maximum water level gradient. Nevertheless, an exact description of this process needs more research. Therefore, in section 5.3.3 only the volume exchange method for a vertical transition will be explained. In Chapter 6 the gradient iteration for a sloped transition will be further discussed.

5.3.3 Run-up reduction for a permeable structure

With the use of Equation 5.18 it is now possible to determine the reduced run-up volume and the reduced run-up for an imposed maximum run-up (friction included):

$$V_{Ru,r} = V_{Ru,f} - V_b \tag{5.13}$$

$$V_{Ru,f} = \frac{2}{3} \cdot \frac{L_0}{\pi^2} \cdot R_{u,f} \tag{5.12}$$

$$R_{u,r} = \frac{(V_{Ru,f} - V_b)}{V_{Ru,f}} \cdot R_{u,f} \tag{5.15}$$

Since inflow will only take place over a run-up height that is reduced by friction **and permeability,** the reduced volume ($V_{Ru,r}$) will be smaller in reality. This is caused by the determination of the incoming volume for a run-up height with only a reduction for friction. By iterating a new value for the water level gradient (Eq. 5.18) using the corrected $R_{u,r}$ (Eq. 5.15) instead of the original $R_{u,f}$, the inflowing volume is determined for a reduced run-up including slope friction and permeability:

$$V_{b\_1} = \frac{1}{\omega}\sqrt{\mathrm{I_1/b}} \cdot \mathrm{R_{u,f}} \cdot \left(1 - \cos\left(\omega \cdot \frac{\mathrm{T_0}}{4}\right)\right) \tag{5.21}$$

This new body volume V_{b_1} results in a new reduced run-up volume $\mathrm{V_{Ru,r\_1}}$ and can be determined by the expression for the volume reduction (Eq. 5.22) with the corresponding run-up reduction (Eq. 5.23):

$$V_{Ru,r\_1} = V_{Ru,,f} - V_{b\_1} \tag{5.22}$$

$$R_{u,r\_1} = \frac{V_{Ru,r\_1}}{V_{Ru,f}} \cdot R_{u,f} \tag{5.23}$$

Equations 5.21-5.23 imply that an iteration is performed to determine the actual volume of water that flows into the structure. This iteration should continue until there is no significant difference between the inflowing water volumes. The equations for the last iteration can be described as follows.

$$V_{b\_x} = \frac{1}{\omega}\sqrt{I_x/b}\, R_{u,r\_(x-1)} \left(1 - cos\left(\omega \cdot \frac{T_0}{4}\right)\right) \tag{5.24}$$

$$V_{Ru,r\_x} = V_{Ru,f} - V_{b\_x} \tag{5.25}$$

$$R_{u,r\_x} = \frac{V_{Ru,r\_x}}{V_{Ru,f}} \cdot R_{u,f} \tag{5.26}$$

Where x indicates the number of iterations for which there is no significant difference in the inflow volume. In Figure 5.5 a schematization is given of the exchange model for different external run-up heights. The blue line indicates the volume inflow without a correction of the run-up height. The red line shows the adjusted volume-exchange-model, from which a new volume-exchange-model can be drawn. The green line represents the volume-exchange-model after a number of iterations and shows a more realistic approach.

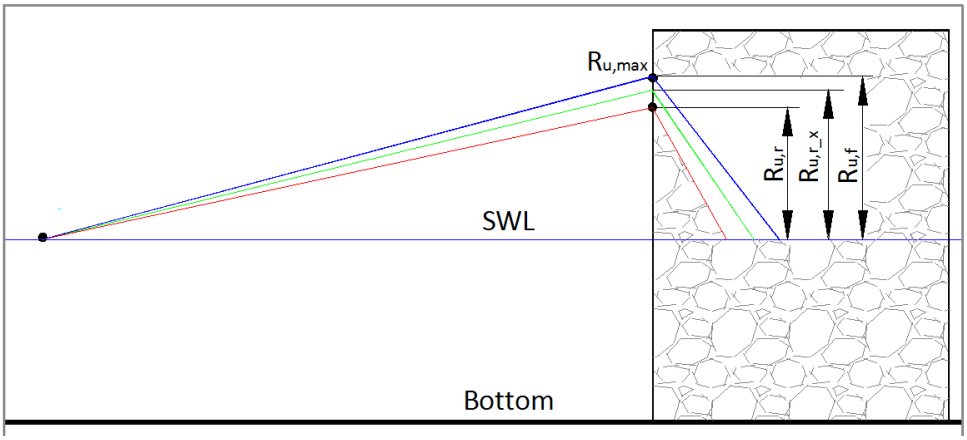

Figure 5.5 - Illustration of the volume-exchange-model with corrected run-up heights

The run-up reduction factor

Using the above formulas it is now possible to determine a run-up reduction factor for any type of structure with a vertical transition. The advantage of describing a run-up reduction instead of a volume reduction is that the run-up process can be visually related to the destabilization process of the armour layer units. This relationship is described in more detail in the next chapter. The run-up reduction factor represents the relationship between the run-up according to the 'new' run-up wedge approach (with a reduction of the roughness) and reduced run-up according to the exchange volume approach.

Run-up reduction factor: $$c_r = \frac{Ru,r,x}{Ru,f} \quad (5.27)$$

In practice, the structures are often composed of different layers. In this case the determination of the internal volume is done similar, only now each layer (with a different porosity and grain diameter) has a different water level gradient (for examples, see Chapter 6).

5.4 Improving the principle of the exchange model

The basic principle of the exchange volume model, described in the previous paragraphs, is based on quite some simplifications. This section describes a number of important modifications to improve this model in the future. However, to keep the model practical, these points are only recommendations which are not implemented in this study. The main points for modifications are:

- Distance d calculated according to the linear wave theory
- Internal water set-up
- Distinction between a Forchheimer flow (scale model) and a fully turbulent flow (prototype)
- Gradient calculation for a scale model including the laminar and inertia term
- Instantaneous values of the turbulent friction term
- Distribution of the external waterline by a concave line description
- Irregular waves instead of a regular waves
- Water flow below SWL
- Maximum internal water level gradient for a sloped transition

Below the topics mentioned above are further discussed. For a more detailed description of some of these points is referred to Appendix C.

5.4.1 Distance d calculated according to the linear wave theory

In determining distance d in section 5.2, a not varying bottom profile is assumed. However, in case of wave-structure-interaction the wave is influenced by the shallower water. According to the linear wave theory a wave has a lower propagation speed in shallow water $\left(\sqrt{gh(x)}\right)$. In that case the intersection of wave profile and SWL (P2) will propagate towards the slope with a somewhat larger velocity than the wave crest (P1). The assumption that is made in section 5.2, for determining the length d, is therefore not completely conclusive. For the calculation of the length d according to the linear wave theory is referred to Appendix C1.

5.4.2 Internal water set-up

Another phenomenon that is not included in the model is the internal set-up in case of a low permeability. "According to BURCHARTH [1993] the internal set-up is due to higher water level being attained during wave up-rush than the water surface reached during down-rush". The large friction limits the internal water velocities much more than the external velocities. As the water surface cannot move quicker than the water, also the motion of the internal phreatic surface is more limited than the motion of the external free surface. Thus, the friction causes a limited upward speed of the internal phreatic surface during up-rush and a limited downward speed during down-rush. This yields the phenomenon of "disconnection" of the water surfaces: the point (highest run-up), where the external water surface meets the slope, is higher than the point (highest core run-up) where the internal phreatic surface meets the slope during wave up-rush and the other way around during down-rush. This means that the incoming wave trough cannot penetrate in the same proportion as the wave crest. This penetration depends strongly on the permeability of the structure (Figure 5.6).

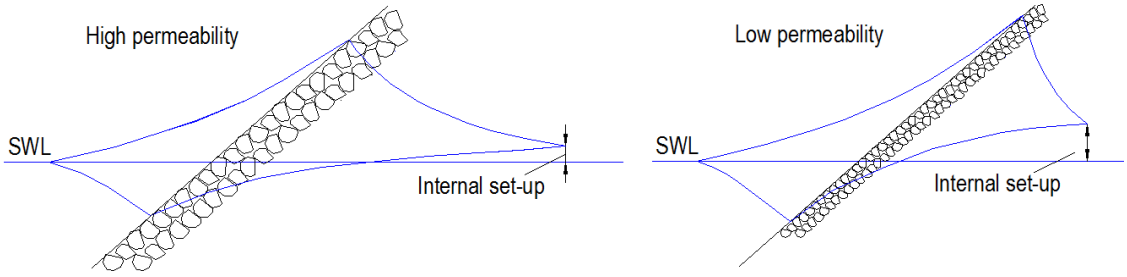

Figure 5.6 - Illustration of variation in the internal water table

Note 5.2: *The illustration in Figure 5.6 differs from the illustration in Chapter 2 (Figure 2.3). The gradient of the water level is supposed to be better reflected in this figure.*

In TROCH [2000] the practical formulae, for the calculation of the maximum average set-up, of BARENDS [1988] and BÜRGER ET AL. [1988] are described. BÜRGER ET AL. [1988] suggests as a rule of thumb for the

average increase of phreatic water table compared to the SWL. The rule consist of a "set up" range between 10% and 20% of the incident wave height H_i:

$$0.10H_i \leq su \leq 0.20H_i \tag{5.28}$$

BARENDS [1988] suggested for the set-up values:

$$0.10h_0 \leq su \leq 0.20h_0 \tag{5.29}$$

In experiments of TROCH [2000] the values of su_{max} are for all tests below the predicted set-up values. The prototype set-up values are not in the range proposed by Barends, but are considerably smaller. The set-up values of the prototype are in the range according to the set-up of BÜRGER ET AL. [1988]. For more information about the critical analysis of the internal set-up calculations of the "Barends formula", see TROCH ET AL. [1996-b] (reference TROCH [2000]). Due to the results in TROCH [2000] the rule of thumb suggested by BÜRGER ET AL. [1988] is recommend. Nevertheless, additional research is needed on this topic.

5.4.3 The real acting flow

Initially, in this research physical descriptions are used that are based on test results from scale models. For these type of models it is assumed that the porous medium is a Forchheimer flow. However, in Figure 5.7 is shown that for high filter velocities, so in the case of larger 'grain' diameters, the flow is fully turbulent.

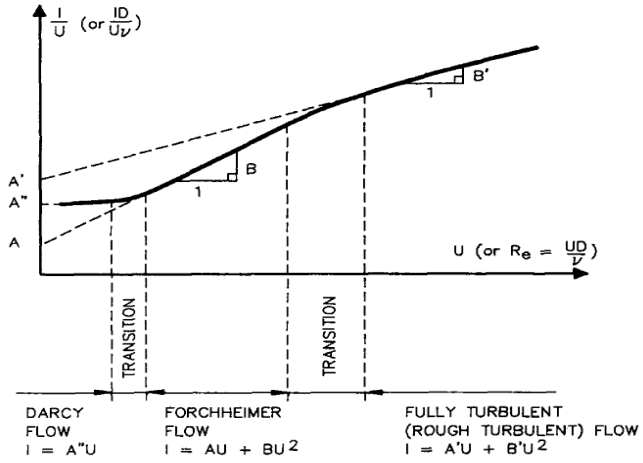

Figure 5.7 - Conventional representation of flow regimes for porous flow based on a Forchheimer equation analysis, from BURCHARTH AND CHRISTENSEN [1995].

For the determination of the internal water level gradient it is important to know which type of flow occurs in the porous medium. This report assumes a Forchheimer flow, because in most literature the results of scale models are based on a Forchheimer flow. However, for high Re_p-values the porous flow is a fully turbulent flow and for low Re_p-values the porous flow is a Darcy flow. The following table displays this relationship with the corresponding expression of the water level gradient. From TROCH [2000] follows a mutual relation: $Re \approx 1.5Re_p$

Table 5.2 - Classification of flow types in a porous medium according to Forchheimer model and limits of the Reynolds number Re_p. [TROCH 2000]

Type	Flow	Re_p Boundaries	Relation	
(I)	Darcy flow	Re_p < 1-10	I = a''V	(5.30)
(II)	Laminar Forchheimer flow	1-10<Re_p < 150	$I = aV + bV^2$	(3.8)
(IV)	Fully turbulent flow	300 < Re_p	$I = a'V + b'V^2$	(5.31)

To determine the water level gradient, where another flow type occurs, a different equation must be used. For a prototype model Equation 5.31 should be used. In Appendix C.2 a detailed description of a fully turbulent flow is given. For scale models, where the core grading is very small, a common problem is that due to scaling a laminar Darcy flow occurs. However, this problem is usually circumvented by applying the Froude scaling law. Therefore it is assumed that in the models, used in this study, Darcy flows do not occur.

Note 5.2: *The values of a/b-term or a'/b'-term in equation 3.8 and 5.31 have the same expression, although the expression has a different shape factor of respectively of α/β or α'/β' (see Appendix B and C.2).*

5.4.4 Water level gradient iteration including the laminar and inertia friction term

In determining the internal water level gradient only the turbulent friction term is taken into consideration. A more accurate approach for the existing water level gradient can be obtained if the laminar and the inertia friction term are also included. Especially in case of scale models involving relatively small diameters, where the influence of the laminar term is not completely negligible (see Figure 3.4). Including the laminar term is easily to realize because the term has a linear character. In the determination of the water level gradient a continuous flow is assumed, but in practice this is not the case. Therefore the effect of the inertia must also be taken into account. For the volume-exchange-model in the present form it is not possible to take this inertia term into account.

Note 5.3: *The values of the friction factors a and b, in case of continuous flow are assumed to be also valid for non-continuous flow, described by ANDERSEN [1994] (taken from TROCH [2000]).*

5.4.5 Instantaneous values of the turbulent friction term

For the sake of simplicity, in this report, a fixed value for the form factor is assumed. This value depends on the type of flow and the material properties. However, these coefficients are not constant and should in principle be treated as instantaneous values, even for oscillatory flow conditions. Since this is an important topic a more detailed description is given in Appendix D.

5.4.6 Distribution of the external waterline by a concave line description

The external volume approach, based on the triangular wave run-up wedge approach of HUGHES [2004], used in this study, might be a reasonable assumption for gentle slopes where wave breaking occurs. However, on steeper slopes where waves behave more like surging waves, the sea surface

elevation will have more of a concave shape (stated by HUGHES [2004]). In JUANG AND JIUN-YAN YOU [2009] an alternative wedge approach of CROSS AND SOLLITT [1972] is described. In CROSS AND SOLLITT [1972] is proposed that, at maximum run-up, the shape of the run-up wedge is a parabola with its vertex at the bottom of the first wave trough. The corresponding equation is:

$$Y = MX^N - A \tag{5.32}$$

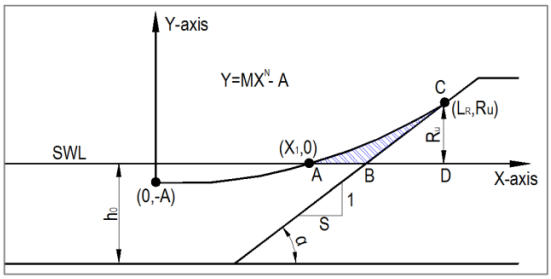

Figure 5.8 - Parabola wave run-up wedge (CROSS AND SOLLITT [1972])

In which Y = the water surface elevation above the sea water level; X = the distance from the trough shoreward; A = the amplitude at the trough; M= the constant coefficient in parabola equation; N= the exponent in parabola equation. For a more detailed description of this topic is referred to Appendix C.3

5.4.7 Irregular wave instead of a regular wave

In this study the waves are assumed to be regular, whereas in reality the waves are irregular. In order to take into account the effect of the changed wave distribution, the run-up and the wave height in these depth-limited conditions would be better described by using the 2 per cent of the wave run-up and wave height, respectively $R_{u2\%}$ and $H_{2\%}$. To apply this modification in the volume-exchange-model the run-up reduction coefficient should be calculated for a full wave spectrum. However, this will take a lot of time. Below a simplified method is given to make the model applicable for irregular waves:

- An existing approach for the $R_{u2\%}$ can be used to determine the volume inflow (V_b), E.g. approach in CUR/CIRIA [2007].
- For a sea state situation the $R_{u2\%}$ is determined by the H_s. This run-up will mainly occur for $H_{2\%}$. In deep water, this $H_{2\%}$ can be calculated by multiplying the H_s with 1.4. For shallow water the method of BATTJES AND GROENENDIJK [2000] (taken from CUR/CIRIA [2007]) can be used. The CUR/CIRIA [2007] notes that in shallow water $H_{2\%}<1.4H_s$. Therefore under the assumption that high waves leads to instability it is supposed that the use of $H_{2\%}$ is reliable.
- With these estimations for the $R_{u2\%}$ and the $H_{2\%}$, the run-up reduction coefficient for irregular waves can easily be calculated.

5.4.8 Water flow below SWL

The water level gradients inside and outside the structure will not only generate a flow above SWL, but also below SWL. The flow between seabed and SWL has been neglected in the model. The internal water volume would probably be larger if this flow (below SWL) would be included. Further research is needed to describe the influence of this water flow on the external process.

Chapter 6

Application of the volume exchange method

6.1 The relation of the volume-exchange-model with the destabilization process

With the volume-exchange-model a description of the influence of the permeability on the run-up process can be given. The run-up process is used because it is strongly correlated to the destabilization process of the armour units. The relation between the stability and the permeability can be explained by changes in the up-rush velocity in case of varying core permeability. Due to the water volume flowing into the structure, the run-up height reduces while the period of wave run-up process does not change. Consequently the up-rush velocity decreases. The same applies to the rush-down velocity, the distance is also smaller in case of a reduced run-up height. The relation between velocity on the slope and the wave induced forces on individual armour units is described by the Morison–type equations. The tangential and normal force components are calculated from the following formulas.

$$F_s = \frac{1}{2} C_{Ds} \rho A_s u \cdot s |u \cdot s| + C_{Ms} \rho \forall \frac{\partial u}{\partial t} \cdot s \pm \frac{1}{2} C_{Ln} \rho A_n (u \cdot n)^2 \quad (6.1)$$

$$F_n = \frac{1}{2} C_{Dn} \rho A_n u \cdot n |u \cdot n| + C_{Mn} \rho \forall \frac{\partial u}{\partial t} \cdot n \pm \frac{1}{2} C_{Ls} \rho A_n (u \cdot s)^2 \quad (6.2)$$

Where s and n are tangential and normal unit vectors with respect to the slope. Positive directions are up along the slope and down into the structure.

Another description (but the same principle) of the effect of core permeability on armour layer stability is given by BURCHARTH ET AL. [1998]. He accounted the smaller stability of the armour units in case of fine core material to the small penetration depth of the waves in the core: fine core material is relatively impermeable and hinders the water to flow into the voids of the structure. Consequently, all waves will cause damage but long waves will be more damaging than short waves, since long waves carry more water into the structure than short waves. On the other hand, in the case of coarse core material, the long waves have sufficient time to penetrate deep into the structure, and thereby reducing the flow in the armour layer. Damage due to these long waves is minimal. However, short waves have less time to penetrate into the core, and hence a large amount of the flow due to these short waves is situated in the armour layer thereby reducing its stabilility. This latter phenomenom is also visible in the volume-exchange-model because the run-up volume is much more dependend on the wave period then the volume inflow.

With these descriptions it is clear that the volume-exchange-model is directly related to the stability relation of VAN DER MEER [1988]. Before the volume exchange method is coupled with the stability relations of VAN DER MEER [1988], first the sensitivities of volume exchange method is investigated. This sensitivity analysis is done by determining the volume exchange for a homogeneous vertical structure type, where the variables independently will be changed. Thereafter the volume-exchange-model is coupled with the notional permeability coefficient.

6.2 Sensitivity analysis of the volume-exchange-model for a vertical transition

In this section the sensitivity of the volume exchange method is investigated. With this analysis insight is obtained into the influence of the hydraulic and structural parameter in the model. This has the aim to make better assumptions in the remaining part of the research.

6.2.1 The basic equations in the volume exchange method

Below a short overview of the complete exchange model is given. The general equation of the volume-exchange-model can be expressed as follows:

Volume-exchange-model $$V_{Ru,r} = V_{Ru,f} - V_b \quad (5.13)$$

In which the run-up volume ($V_{Ru,f}$) can be expressed as:

Run-up volume: $$V_{Ru,f} = \frac{1}{2} \cdot d \cdot R_{u,f} \quad (5.\ 2)$$

The run-up for a frictionless and the run-up for a rough transition can be given with the following equations, were the roughness reduction coefficient is assumed to be 0.75 (see appendix A):

Run-up without friction $$R_u = \frac{3}{4}\pi H_s \quad (5.7)$$

Run-up with friction $$R_{u,f} = \gamma_f \cdot R_u \quad (5.11)$$

From the 'new' run-up volume approach, given in Chapter 5, follows that the base of the run-up triangle can be expressed as:

Base of the run-up triangle $$d = \frac{4L_0}{3\pi^2} \quad (5.8)$$

Initially it is assumed that the type of flow in the structure is a Forchheimer flow. Dependent on the actual flow this can be changed in a fully turbulent flow. In this later case, the turbulent b is the required to determine the water level gradient:

Water level gradient $$I = bu^2 \quad (3.8)$$

Turbulent friction term $$b = \beta \frac{1-n}{n^3} \frac{1}{gD} \quad (3.10)$$

For a reliable value of the turbulent friction term b, the value of porosity associated with the D_{n50} should be determined. However, in practice these values are in most cases not known as the grading of the D_{n50} largely determines the porosity. In general, the following classification (Table 6.3) is used for the grading of rubble mound material.

Table 6.3 - Classification of grading of rubble mound material and the functional use (reference: CUR/CIRIA 2007)

Grading	D_{85}/D_{15}	Functional use
Small	≤ 1.5	Armour layer, berm
Average	1.5-2.5	Filter layer, sublayer (armour layer)
Wide, various (quarry run of rip-rap)	2.5-5 (or larger)	Core

An indication of the influence of the grading of the rubble mound material on the porosity is given in Table 6.3. The given rock classes in Table 6.4 correspond to those mentioned in Table 6.3. These values are taken from a breakwater built in Zeebrugge, described in TROCH [2000].

Table 6.4 - Class of rock with corresponding grading and porosity

Class of rock	D_{85}/D_{15}	Porosity n
2-300kg	2.9	0.33
300-1000kg	1.3	0.4
1-3 ton	1.3	0.4
3-6 ton	1.2	0.4

This table explicitly shows the influence of rock grading on the porosity. Tables 6.3 and 6.4 indicate the large variation of the grading of the core material and its influence on the porosity. Consequently, determination of the porosity of the core material, without taking the grading into consideration can lead to large inaccuracies

The value of the shape factor β is based on Table B.7 in Appendix B. In this study a value of 3.6 is chosen, corresponding with test results of BURCHARTH AND CHRISTENSEN [1991] for irregular / angular grains. This shape factor is generally used in practice for rubble mound structures. Using realistic values of the porosity and shape factor for a given D_{n50}, the turbulent friction term b can be calculated. The water volume flowing into the body of the structure can then be determined using the equations below which take into account the iteratively determined water level gradient.

$$V_{b1} = V_{b2}$$

$$\frac{1}{2} \cdot n \cdot \left(\frac{1}{l}\right) \cdot R_{u,f}^2 = \frac{1}{\omega}\sqrt{\mathrm{I/b}} \cdot \mathrm{R_{u,f}} \cdot \left(1 - \cos\left(\omega \cdot \frac{\mathrm{T0}}{4}\right)\right) \quad (5.18)$$

By coupling the volume inflow to the run-up process, the influence of the core (and filter) permeability on the external process becomes clear. The reduced run-up and the related run-up reduction coefficient can then be expressed as:

Reduced run-up: $$R_{u,r} = \frac{(V_{Ru,f} - V_b)}{V_{Ru,f}} \cdot R_{u,f} \quad (5.15)$$

As mentioned in chapter 5, the actual reduced run-up will be smaller, because the initial incoming volume is determined for a run-up height with only reduced for slope friction. In reality, inflow can only take place over a run-up height that is reduced by friction **and permeability.** By using the volume iteration, described in Chapter 5 (Eq. 5.21-5.26), a more correct volume inflow and reduced run-up can be calculated. Subsequently, the run-up actual reduction coefficient can be determined with:

Run-up reduction factor: $$c_r = \frac{Ru,r\_x}{Ru,f} \quad (5.27)$$

With the use of these equations it is possible to determine the influence of each variable in the volume-exchange-model. It should be taken into account that the value of the hydraulic parameters (wave height and wave period) should correspond with a surging wave ($3.5 \leq \xi \leq 6$). In Appendix E follows an overview of the values of the applied parameters and the corresponding test results. In this sensitivity analysis the volume-exchange-model is elaborated for a homogeneous vertical structure varing the wave height, wave period, D_{n50} and porosity. The values of the hydraulic and structural parameters used in this example are related to a test model of the Zeebrugge breakwater (reference BURCHARTH ET AL. [1999]). Below follows a discussion of the calculation results of the individual variables.

6.2.2 Wave period

Internal water level gradient: When the wave period increases, the internal water level gradient decreases. The water has more time to flow into the structure in case of longer wave. This results in a water line in the structure on the same level as the reduced run-up and consequently in a smaller gradient. For a short wave period there is hardly time for the water to flow into the structure. The waterline in the breakwater will almost be vertical because the volume of water that flows into structure is small (see left graph in Figure 6.1).

Run-up reduction coefficient: For increasing wave period, the water level gradient reduces and the volume inflow increases. Therefore the run-up reduction coefficient could be expected to reduce as the wave period increases. However, in the right graph in Figure 6.1 this is not observed. This can be explained by the different influence of the wave period on the wave crest volume and the water volume inflow: as the wave period increases, the incoming wave crest volume will increase significantly while the water volume inflow will increase only marginally. Therefore the run-up reduction coefficient increases as the wave period increases.

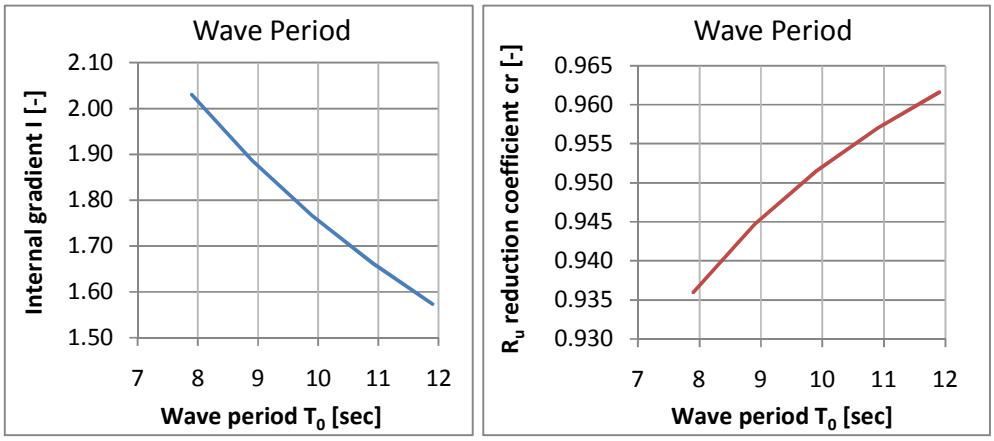

Figure 6.1 - Calculation results of the internal gradient and the run-up reduction coefficient for a varying wave period

6.2.3 Wave height

Internal water level gradient: For increasing wave height, the internal water level gradient is also increasing. A physical explanation is that for a constant wave period run-up velocity decreases as the wave height decreases. In case of a low run-up velocity the water inflow is large and the water level gradient becomes small. Consequently, the water level gradient increases for increasing wave height.

Run-up reduction coefficient: The run-up reduction increases for increasing wave height. In case of an increasing wave height, with a constant wave period, the wave becomes steeper. This results in a greater interface with the structure slope. The volume inflow for steeper waves is larger than for long waves. As a result, the run-up reduction for steeper (non-breaking) waves is higher than for less steep waves. Or the run-up reduction coefficient decreases as the wave height increases at constant wave period.

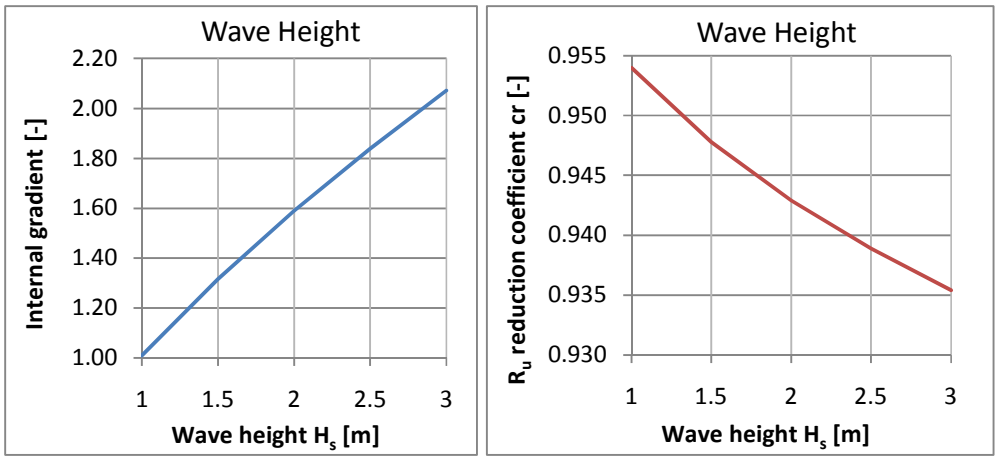

Figure 6.2 - Calculation results of the internal gradient and the run-up reduction coefficient for a varying wave height

6.2.4 Porosity and D_{n50}

Internal water level gradient: The left graphs in Figures 6.3 and 6.4 clearly indicate that smaller stones or lower porosity increases the gradient. Physically this can be explained by the higher hydraulic resistance in case of a small stone diameter or low porosity. This higher resistance results in a smaller water inflow and a larger gradient. This is because the water in the breakwater is lifted at the point $R_{u,r}$ and fixed on another point at SWL. The higher the hydraulic resistance, the less water flows in, the closer are the two points together and the larger is the gradient.

The run-up reduction coefficient: In this case only the geometrical properties are changing, so the external run-up volume remains the same. Therefore the run-up reduction can be directly related to the porosity and D_{n50}. The run-up reduction decreases in case of a decreasing porosity or D_{n50}. The reason for this is that in a relatively impermeable core the water cannot percolate into the voids of the core and the wave will run-up higher.

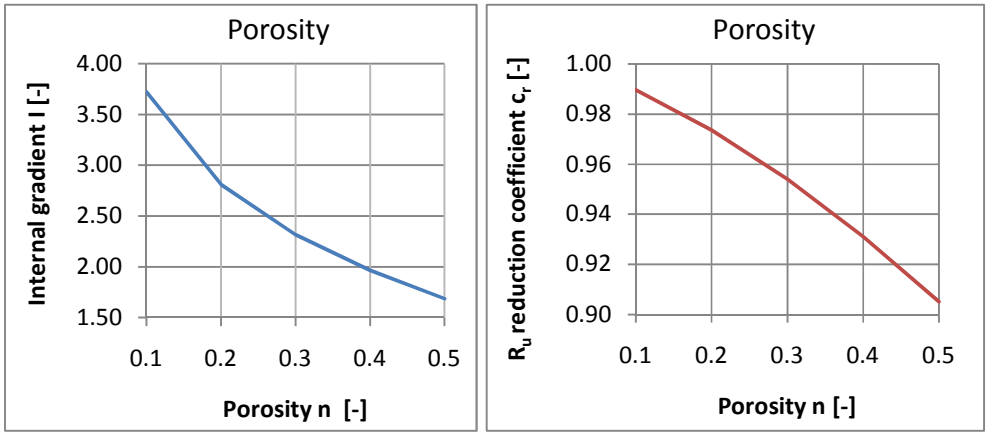

Figure 6.3 - Calculation results of the internal gradient and the run-up reduction coefficient for a varying porosity

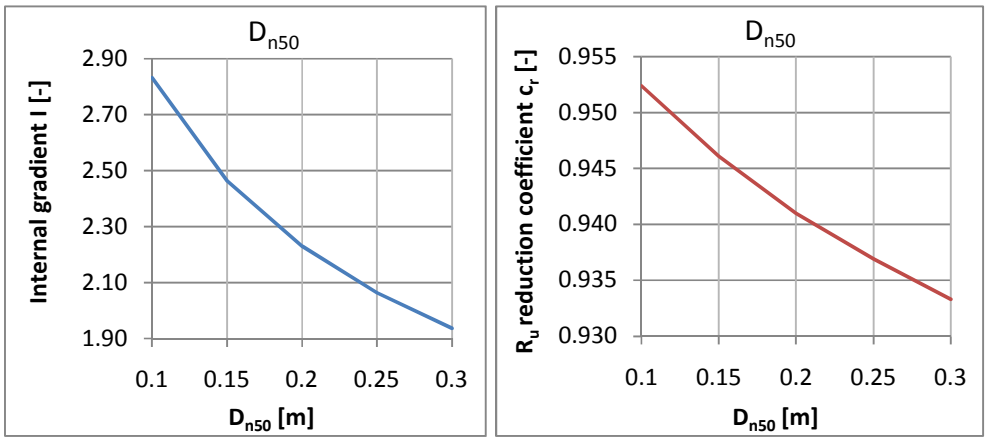

Figure 6.4 - Calculation results of the internal gradient and the run-up reduction coefficient for a varying D_{n50}

6.2.5 Final remarks

The results of VAN DER MEER [1988] suggest that the stability of armour units is higher in case of long waves (higher ξ values). At first sight, this is not directly corresponding to the results of the volume-exchange-model. The run-up reduction reduces in case of higher ξ-values. However, as mentioned before, the destabilization process is not directly linked to the run-up reduction but to the slope velocity. In general, the stability decreases as the slope velocity increases. The sensitivity analysis indicates that the slope velocity is lower for longer waves (higher ξ values) than for steep non-breaking waves (lower ξ values), in other words the volume-exchange-model is not a contradiction with the VAN DER MEER [1988] results.

With these results insight has been gained into the influence of hydraulic and structural parameters on the volume-exchange-model. Once again the importance of a careful determination of the influential parameters is emphasized. In the next section, the volume-exchange-model is coupled with the notional permeability coefficient of VAN DER MEER [1988]. In contrast to the elaboration in this section only the environmental parameters are varying since the geometric properties of the tested structures by VAN DER MEER [1988] are fixed.

6.3 Volume-exchange-model coupled with the notional permeability

As already mentioned VAN DER MEER [1988] introduced the notional permeability coefficient P to ensure that the permeability of the structure is taken into account. The correctness of this permeability description is questionable, but since the stability relationship includes the notional permeability, this value should be determined. For this reason the notional permeability is coupled with the volume-exchange-model. This is done by determining the run-up reduction coefficient for each structure for which a notional permeability value is defined. In the previous chapter is described that in case of a sloped transition, and especially when the core material is fine, more research is needed to determine the internal water level gradient. Therefore, initially a vertical transition is assumed.

6.3.1 Structural and environmental properties

In the sensitivity analysis in the previous section the volume-exchange-model is elaborated for a homogeneous structure. This is because the notional permeability coefficient P reflects the influence of the core (and filter) permeability and not the permeability of the complete structure. On behalf of a proper comparison between the ‘Van der Meer structures’, the homogeneous structure should be included an 'imaginary' armour layer in the elaboration.

Moreover, an accurate coupling of the volume-exchange-model to the notional permeability coefficient P requires the use of the normative variables on basis of the tested variables by VAN DER MEER [1988]:

- The ratios between the layers for the different structures are given in Figure 1.2.
- The porosity of the concerned layers is based on Tables 6.3 and 6.4 from the previous section.
- The grading values are given in the illustrations of the tested structures (see Appendix E). For the non-tested structure type (P= 0.4) an assumption is made for the grading values. Since this structure type is a typical practical example, with a core mostly built of quarry run, a large

grading is selected. This results in a low porosity. Table 6.5 shows an overview of the concerning values.

Table 6.5 - Filter laws, grading values and porosity values of the four 'P-structures' by Van der Meer [1988].

		Notional permeability			
		P=0.6	**P=0.5**	**P=0.4**	**P=0.1**
Armour layer	D_{85}/D_{15}	1.25	1.25	1.25	1.25
	Porosity n	0.4	0.4	0.4	0.4
Filyer layer	D_{n50a}/D_{n50f}			2	4.5
	D_{85}/D_{15}			2.25	2.25
	Porosity n			0.38	0.38
Core	D_{n50a}/D_{n50c}		3.2	8	
	D_{85}/D_{15}		1.5	4	
	Porosity n		0.4	0.3	

Note 6.1: *The porosity values (blue) are based on Table 6.3 & 6.4, the grading values (red) are assumed values and the other values (black) are taken from the tested structures by VAN DER MEER [1988] (see appendix E).*

By assuming a shape factor β of 3.6 it is possible to determine the turbulent friction term b by using Eq. 3.10. The internal water level gradient can now be determined iteratively and with this gradient the volume inflow can be calculated. In Appendix E a determination of the volume inflow is given for each structure type. As a result of the fixed geometry of the structures the only varying parameters are the wave height and the wave period. It should be taken into account that the value of the environmental parameters should correspond to a surging wave ($3.5 \leq \xi \leq 6$). The values of the hydraulic parameters used in this example are related to a test model of the Zeebrugge breakwater (reference BURCHARTH ET AL. [1999]).

6.3.2 Vertical transition

In appendix E.4 the results of the volume-exchange-model for each structure type are given. Below follows a discussion of these calculation results. At first the influence of the wave height and wave period are described separately. Thereafter, the combined influence of both parameters is looked at by using the wave steepness. Finally some conclusions are drawn and an expression for the notional permeability is derived.

Varying wave period

In the first case, the wave period is varying with a fixed wave height of 2.91 m. The following graph shows for all 4 notional permeability factors (with varying wave period) the volume inflow.

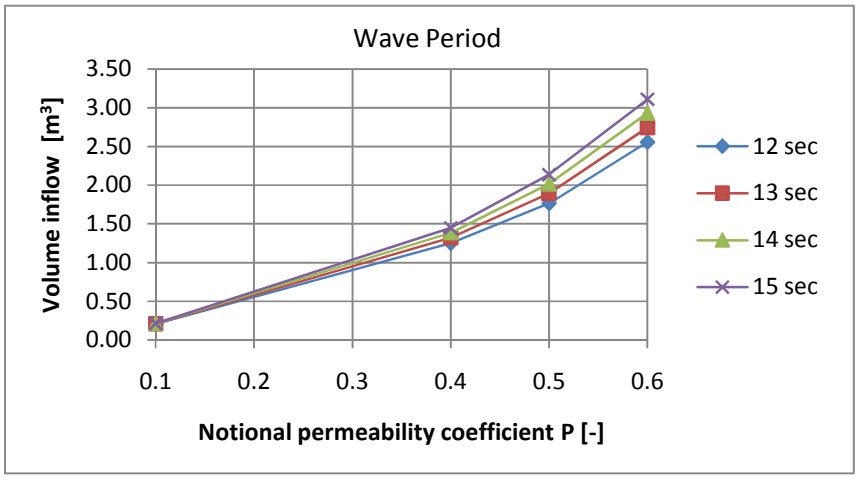

Figure 6.5 - Calculation results for the volume inflow with varying wave period for the defined 'P-structures' (vertical transition)

Figure 6.5 indicates that for a larger wave period (wave height = constant) the volume intake increases. Physically this can be explained as follows: when the wave period is larger, more time is available for the external water volume to flow into the structure (see also Section 6.2.2).

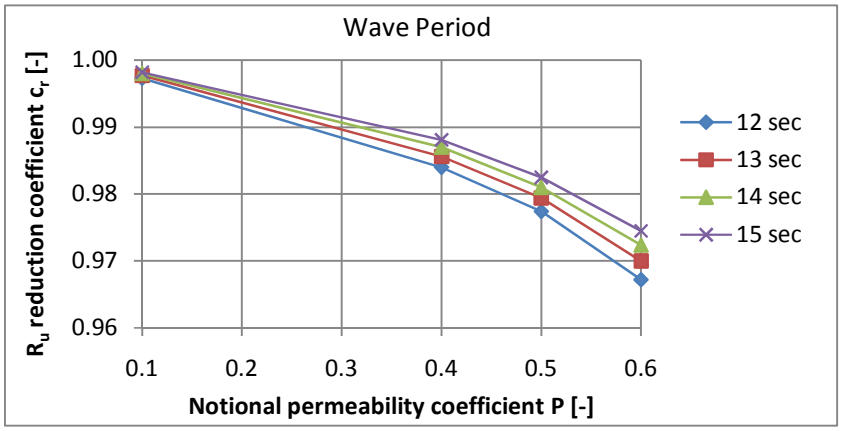

Figure 6.6 – Calculation results of the c_r-coefficient with varying wave period for the defined 'P-structures' (vertical transition)

Figure 6.6 indicates that for a larger wave period the run-up reduction factor increases. This can be explained by the fact that the volume inflow is less dependent on the wave period then the run-up volume (see also Section 6.2.2.).

Varying wave height

In case of a varying wave height the wave period is fixed on 14 sec. The following graph shows for all 4 notional permeability factors (with variable wave height) the volume inflow.

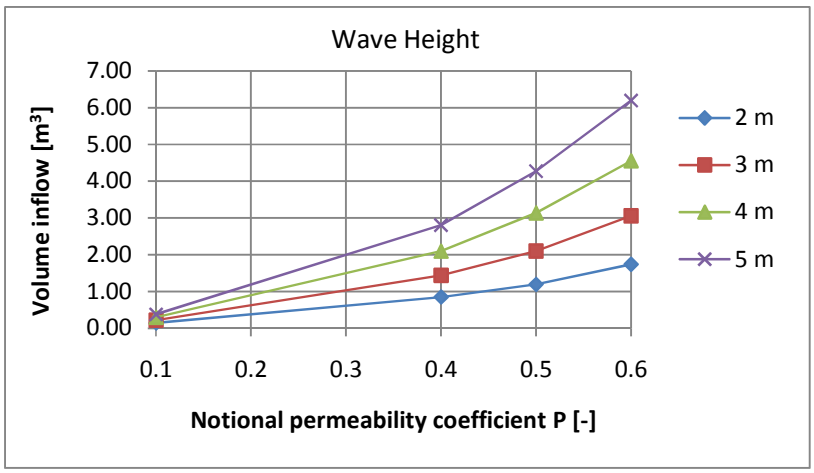

Figure 6.7 - Calculation results of the volume inflow with varying wave height for the defined 'P-structures' (vertical transition)

Figure 6.7 shows that the volume inflow is larger when the wave height increases. This is a logical consequence of a larger run-up interface, because the run-up increases with a higher incoming wave ($R_u = 3/4 \cdot \pi H_s$), see also Section 6.2.3.

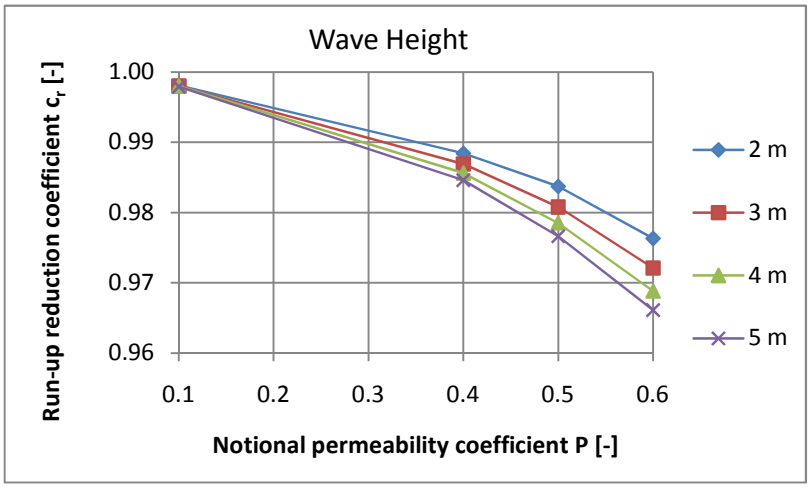

Figure 6.8 – Calculation results of the c_r-coefficient with varying wave height for the defined 'P-structures' (vertical transition)

By increasing the wave height the run-up reduction factor decreases or the run-up reduction is larger, see Figure 6.8. This can be explained by the fact that the waves becomes steeper in case of an increase of the wave height with a constant wave period. This results in a greater interface with the structure slope. The volume inflow for steeper wave is larger than for long waves. As a result, the run-up

reduction for steeper, shorter (non-breaking) waves is higher than for less steep waves (see also section 6.2.3).

Varying wave steepness

In this section, above calculation results are expressed as a function of wave steepness. In literature, often the Iribarren number is used, but in case of a vertical transition this is not possible. Figure 6.9 shows the notional permeability coefficient P versus the run-up reduction coefficient for varying wave steepness.

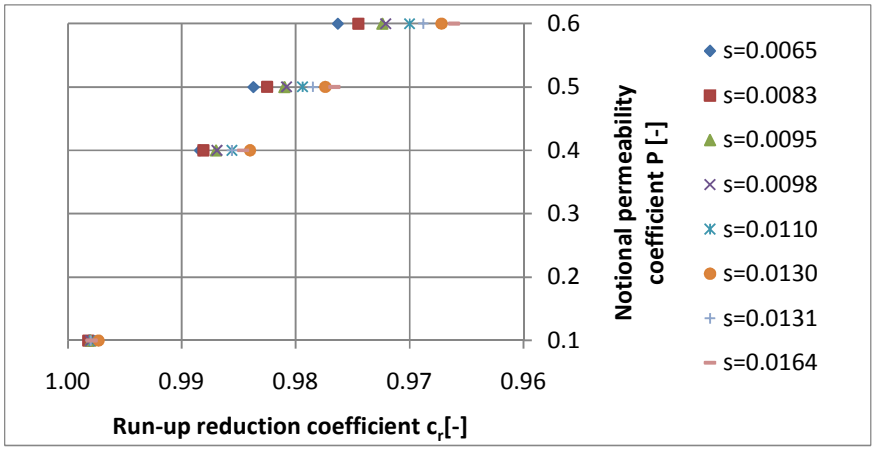

Figure 6.9 -Calculation results of the c_r-coefficient versus the 'notional permeability' for a varying wave steepness and vertical transition

Below a summary of the observations that can be made about the relation between the run-up reduction coefficient and the notional permeability coefficient P are given. These observations are closely linked to the observations described in the sensitivity analysis in Paragraphs 6.2. Remember that a large notional permeability coefficient P indicates a more permeability structure.

- The influence of the wave steepness increases when the permeability of the structure increases. Physically this can be explained as follows: when the steepness is small, the wave period is long with respect to the wave height. Therefore, more time is available for the external water volume to flow into the structure. The rate of volume inflow is limited due to the flow resistance in the pores. The associated limited pore velocity is higher in case of a larger permeability. Consequently, the influence of the wave steepness is higher in case of increasing permeability, because in that case the internal flow can easier follow the external flow.
- The run-up reduction increases for increasing wave steepness. Physically this can be explained by the fact that for a long wave (low steepness) the incoming wave crest volume is more significant than in case of a short wave.
- A clear trend is visible between the notional permeability factor and the run-up reduction coefficient. This may indicate that the volume-exchange-model is a good method to determine the notional permeability for non-standard structure types. However, the correctness of the permeability description P is questionable.

- It is remarkable that the run-up reduction coefficients are very low. One reason is that the run-up period from SWL to maximum run-up is in reality higher than assumed (a quarter of a wave period). This is also visible in Figure 3.7, wherein the run-up and run-down period for one wave period are shown.

Notional permeability formula for a vertical transition

In Appendix F.5 above calculation results are used to give a relationship between the run-up reduction coefficient and the notional permeability coefficient P. A curve fitting of the calculation results lead to the following equation for the notional permeability in case of a vertical transition:

$$\mathrm{P} = 1.7 \cdot \mathrm{s}^{-0.25} \cdot (1 - \mathrm{c_r})^{0.6} \tag{6.3}$$

This equation indicates that the notional permeability coefficient *P* is related to wave steepness (*s*) and geometric properties of the structure material ($c_r = f(D_{n50}, n\ etc)$), so also the permeability of the structure. This is contradictory to the notional permeability coefficient *P*, described by VAN DER MEER [1988], since this factor is only related to the structure geometry. This equation is not useful in practice, but gives a good idea about the influential parameters.

6.3.3 Sloped transition

As already mentioned in the case of a sloped transition the volume exchange method differs from a vertical transition. For a sloped transition the waterline hangs under the structure slope, wherefore the water inflow is limited. In such case it is difficult to determine the water inflow, because the water flow is not exactly horizontal (landwards), but mainly downwards. Flow velocities cannot be calculated by the 'horizontal flow iteration' anymore. Therefore a maximum water level gradient should be applied in the calculation (i.e. a gradient which corresponds to a downward flow). For this maximum water level gradient is referred to VAN GENT [1994], he suggest a maximum gradient that is related to the maximum gradient of the vertical velocity. This gradient has maximum value of one and when only the turbulent friction term is included the equation becomes:

$$I = bU^2 \leq 1 \tag{6.4}$$

If the gradient from the water level iteration surpasses this maximum predefined gradient value, then this maximum value should be used in the calculation of the volume inflow. The gradient iteration for a rough sloped transition can be expressed similarly as for a vertical transition but with a different distance:

$$\tfrac{1}{2} \cdot n \cdot \left(\tfrac{1}{I}\right) \cdot R_{u,f}^2 = \tfrac{1}{\omega}\sqrt{\mathrm{I/b}}\,\tfrac{\mathrm{R_{u,f}}}{\sin(\alpha)}\left(1 - \cos\left(\omega \cdot \tfrac{\mathrm{T0}}{4}\right)\right) \tag{5.20}$$

The sensitivity analysis in Section 6.2 shows an increase of the gradient when porosity or D_{n50} decrease. This indicates that the above iteration stops working at low porosity or small stone diameter and the maximum gradient should be used. In this case the determination of the volume inflow is less accurate.

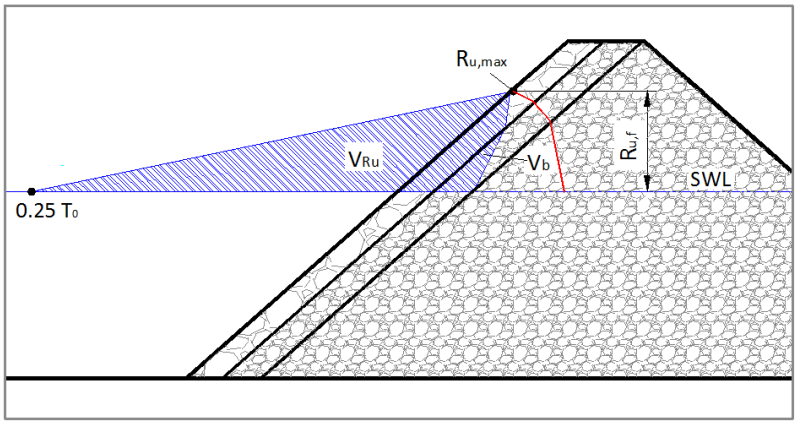

Figure 6.10 - The iterated gradient (red line) and the instantaneous water level (blue line)

For a homogeneous structure it is assumed that the above method works well. However, in case of a layered structure, this method is no longer applicable as at the moment of maximum wave run-up, the gradient no longer describes the water level in the individual layers (see the red line in Figure 6.10). This is because the water levels in the different layers will be subject to phase differences, as discussed in Section 3.3.2. Therefore it is difficult to determine the volume in the individual layer in an analytical way. A solution is found by limiting the number of layers to two (core and armour). An assumption still to be made is the elevation of the imposed internal run-up in the armour layer for the initial run-up height in the core ($R_{u,c}$), see Figure 6.11.

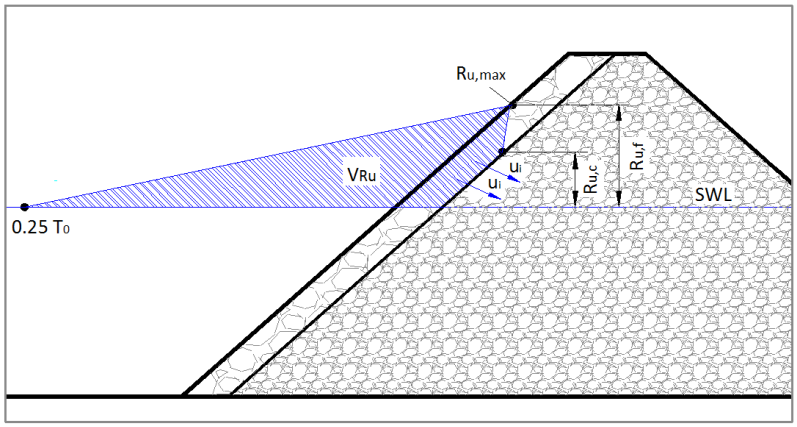

Figure 6.11 - The volume-exchange-model for a sloped structure type with two layers

For the initial water level in the core the ratio between the maximum wave run-up level (above SWL) in the armour layer ($R_{u,f}$) and filter layer ($R_{u,c}$) is used, see Figure 6.12. This ratio should be calculated when the external wave run-up is at his maximum level. In this study the measurements of MUTTRAY [2001] are taken for this ratio. In reality, this ratio is closely related to the geometric properties of the armour layer (D_{n50}, porosity, etc), but here it is assumed that this ratio is constant. However, under the assumption that the seawards gradient is not affected by the landward side of the breakwater, this consideration seems to be reliable. The graph shows a ratio between the run-up in the armour and a

run-up in the filter of approximately 0.5. The imposed run-up in the core is therefore 50% of the maximum external run-up ($R_{u,c} = 0.5 \cdot R_{u,f}$). In this notation the index f stands for 'friction reduction' instead of 'filter'.

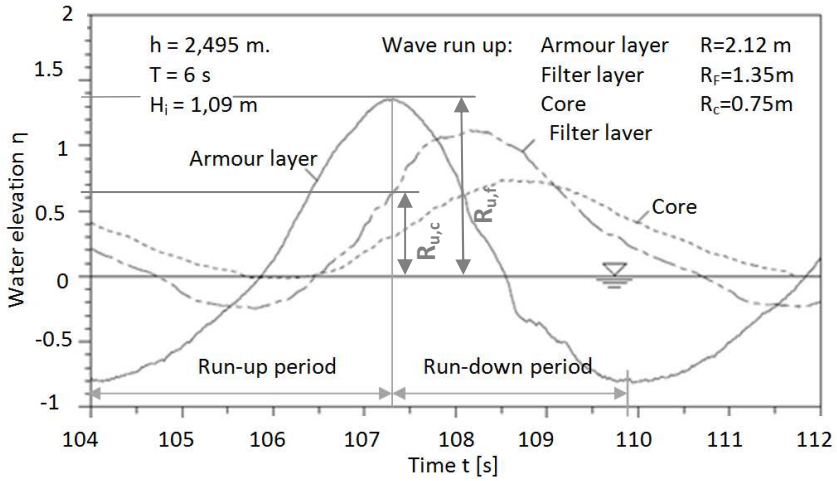

Figure 6.12 - Ratio between the armour layer and core, MUTTRAY [2001]

Note 6.2: *For a better support of above assumptions, further research is needed. However, for this moment the assumptions seem to be acceptable.*

With this assumption equation 5.20 becomes:

$$\frac{1}{2} \cdot n \cdot \left(\frac{1}{I}\right) \cdot \left(0.5 \cdot R_{u,f}\right)^2 = \frac{1}{\omega}\sqrt{\frac{I}{b}} \cdot \frac{0.5 \cdot R_{u,f}}{\sin(\alpha)}\left(1 - \cos\left(\omega \cdot \frac{T0}{4}\right)\right) \tag{6.5}$$

If the iteration(Eq. 6.5) results in $I \leq 1$ the following equation should be used to determine the body volume:

$$V_b = \frac{1}{\omega}\sqrt{\frac{I}{b}} \cdot \frac{0.5 \cdot R_{u,f}}{\sin(\alpha)}\left(1 - \cos\left(\omega \cdot \frac{T0}{4}\right)\right) \tag{6.6}$$

If the iteration gives $I > 1$, then the following equation should be used:

$$V_b = \frac{1}{\omega}\sqrt{\frac{1}{b}} \cdot \frac{0.5 \cdot R_{u,f}}{\sin(\alpha)}\left(1 - \cos\left(\omega \cdot \frac{T0}{4}\right)\right) \tag{6.7}$$

With these assumptions and the formulas given in Section 6.2.1 it is possible to determine, for a homogeneous structure type (P is 0.6) and a permeable structure type (P is 0.5), the run-up reduction coefficient. In case of a layered structure type (P is 0.4) this is not possible and therefore this structure type is excluded. For an impermeable structure type (P is 0.1) it is assumed that due to the small layer thickness the filter layer is fully saturated. The geometric properties and hydraulic parameters are described in section 6.3.1.

In Appendix G.1 the calculation results of the volume-exchange-model for each structure type are given. In this Appendix also an overview of the formulae used for a double layered sloped transition are

given. Below the calculation results are plotted, where the run-up reduction coefficient is plotted versus the notional permeability coefficient for a varying wave steepness (s).

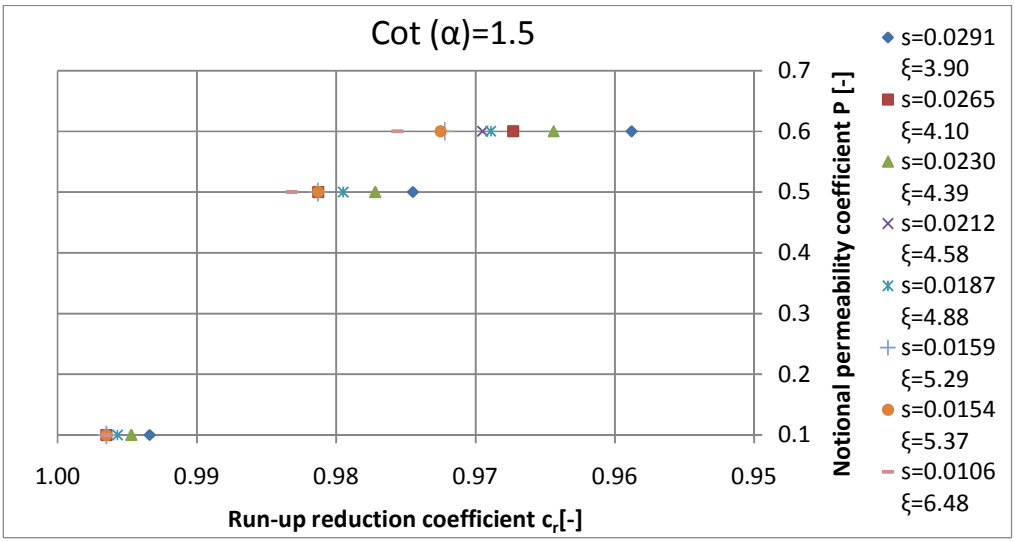

Figure 6.13 - Calculation results of the P-factor versus the c_r-coefficient for a transition with cot(α) is 1.5 and varying *s*

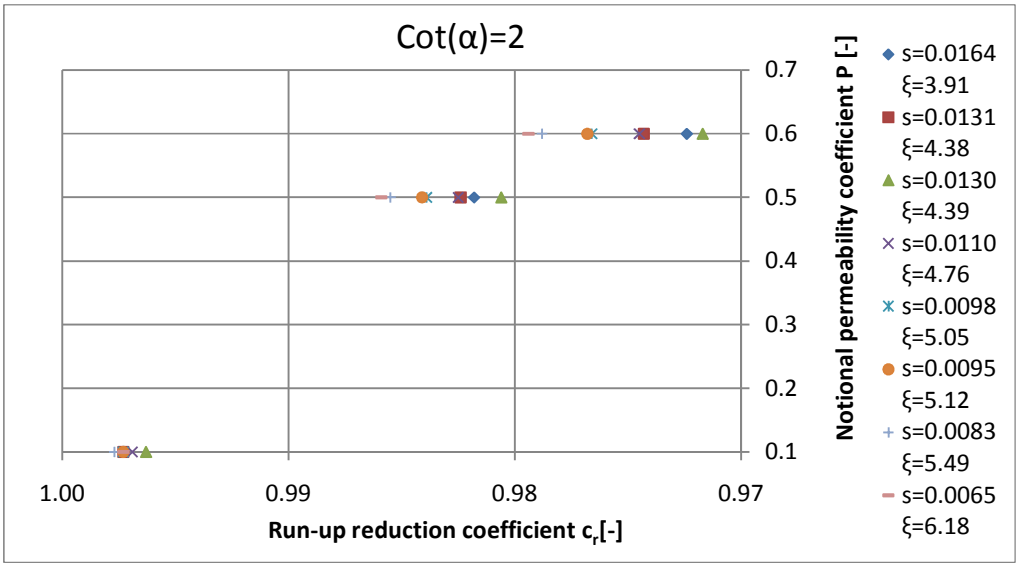

Figure 6.14 - Calculation results of the P-factor versus the c_r-coefficient for a transition with cot(α) is 2 and varying *s*

From these plots (Fig. 6.13 and 6.14) the following observations can be made:

- For long waves (low wave steepness) the wave steepness is related to the run-up reduction coefficient. When the waves become shorter this relationship is not longer visible. This difference is probably due to the fact that the inflow volume is dependent on both the wave height as the wave period, but both do not have the same effect.

- The other trends are quite similar as in case of a vertical transition, therefore is referred to the observation in Section 6.3.2.

In the last two graphs the results are plotted as a function of wave steepness. These results can be combined by replacing the wave steepness into the similarity parameter (Iribarren number). In Figure 6.15 the results from Figure 6.13 and 6.14 are combined.

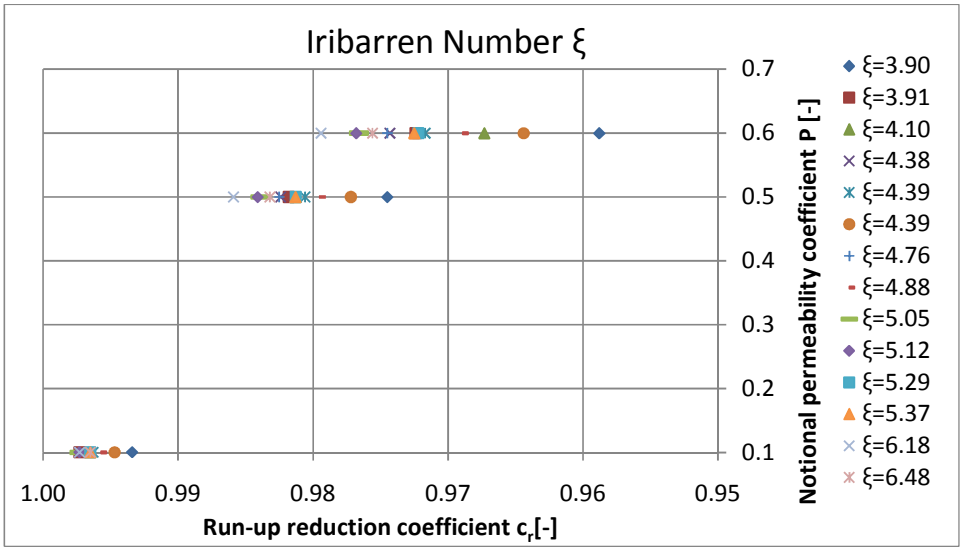

Figure 6.15 - Calculation results of the P-factor versus the c_r-coefficient with varying Iribarren number

In this plot there is no general trend for a varying similarity parameter. This is clearly visible in differences of the run-up reduction value for the Iribarren number of 4.39. A possible explanation of this follows below.

Notional permeability formula for a sloped transition

In Appendix G.2 and G.3 the calculation results from above are used to give a relationship between the run-up reduction coefficient and the notional permeability coefficient. A curve fitting of the calculation results leads to the following equation for the notional permeability in case of a sloped transition:

$$\mathrm{P} = 3.1 \cdot \mathrm{s}^{-0.3} \cdot (1 - \mathrm{c_r})^{0.8} \tag{6.8}$$

This equation indicates that the notional permeability coefficient P is related to wave steepness (s) and geometric properties of the structure material ($c_r = f(D_{n50}, n\ etc)$). This is contradictory to the notional permeability coefficient P, described by VAN DER MEER [1988], since this factor is only related to the structure geometry.

Moreover, this equation also indicates that the notional permeability coefficient P is not related to angle of the structure slope. In reality this is questionable. A possible reason for this independence is that in the case of a gentle slope the run-up velocity is large compared to a steep slope, on the other hand for a gentle slope the inflow length is large compared to a steep slope. A combination of effects results in a negligible influence of the slope steepness on the notional permeability coefficient P. Doubts

about the correctness of this independence are also strengthened by the difference in the correlation value of the curve fitting.

Notes 6.3-6.5:

- Equation 6.8 is only shown with the purpose to indicate the relation between the hydraulic parameters and the notional permeability coefficient P. Hence, this curve fitting is only valid for this specific case and cannot be considered as a general formula.
- This formula cannot be used in the stability formula of VAN DER MEER [1988], because the stability relation of VAN DER MEER [1988] is fitted by using fixed P-coefficients. Moreover, the value of these fixed coefficients is doubtful, see Chapter 2.2.4. Consequently, the stability relation of VAN DER MEER [1988] gives only reasonable results when the fixed P-values (0.1, 0.5 and 0.6) are used. However, Eq. 6.8 gives varying P-values.
- Eq. 6.8 is fitted on basis of varying hydraulic parameter, but without considering varying structural parameters (*n* and D_{n50a}). A more realistic curve fitting can be provided when also these parameters are considered in the fitting.

6.4 Using the run-up reduction factor in the 'Van der Meer'-Formulae

In the previous two paragraphs the notional permeability coefficient P is expressed as a function of the run-up reduction coefficient and the wave steepness. Given the realization of the P-factor, it cannot be automatically assumed that this factor actually described the influence of the permeability on the armour layer stability. Therefore, this section gives an proposal to exclude the P-factor from the stability formulae by VAN DER MEER [1988]. Before this is done first a brief overview is given of the introduction of the notional permeability coefficient P.

In Chapter 2 has already been described that the P-factor is introduced by means of curve fitting. Before the introduction of the P-factor, the stability formulae for the three tested structures were written by:

Impermeable core: $$\frac{H_s}{\Delta D_{n50}} = \mathbf{1.35} \cdot \boldsymbol{\xi_m^{0.1}} \cdot \sqrt{cot\alpha} \cdot \left(\frac{S}{\sqrt{N}}\right)^{0.2} \quad (2.1)$$

Permeable core: $$\frac{H_s}{\Delta D_{n50}} = \mathbf{1.07} \cdot \boldsymbol{\xi_m^{0.5}} \cdot \sqrt{cot\alpha} \cdot \left(\frac{S}{\sqrt{N}}\right)^{0.2} \quad (2.2)$$

Homogeneous structure: $$\frac{H_s}{\Delta D_{n50}} = \mathbf{1.10} \cdot \boldsymbol{\xi_m^{0.6}} \cdot \sqrt{cot\alpha} \cdot \left(\frac{S}{\sqrt{N}}\right)^{0.2} \quad (2.3)$$

Since the power coefficient of the Iribarren number has three different values, VAN DER MEER [1988] assumed that this coefficient describes the permeability of structures. However, if the curve fitting of mainly the permeable and homogeneous structure is looked at more critically, the accuracy of this curve fitting is questionable. The curve fitting of each of these two structures is based on only four data points, see Figure 2.5. In addition, the direction (i.e. the power coefficient), are in both cases doubtful. The fitting of the structure with an impermeable core is based on more data points and can be seen as a more precise curve fitting. In Appendix H a value of 0.2, instead of 0.1, is calculated and seems to be more reliable. Therefore, in this study the value 0.2 is selected as the power coefficient of the Iribarren number for impermeable structures.

These points show that the description of the permeability is a sensitive point in the stability formulas of VAN DER MEER [1988]. In this report the so-called run-up reduction coefficient c_r is introduced. Since this coefficient is based on physics, in contrast to the P-value, it is assumed that the influence of the permeability on the armour layer stability can be better described by the run-up reduction coefficient. As mentioned before, the influence of the core permeability on the armour layer stability depends on hydraulic parameters and structural parameters. This is contradictory to the permeability description P given by VAN DER MEER [1988], since the notional permeability coefficient P only depends on the structural parameters, see Figure 1.2. This also explains the dual permeability notation in the stability formula for surging waves. By using the run-up reduction coefficient, which depends also on the wave steepness, the dual permeability notation in the stability formula can be replaced by one permeability notation only. Knowing this, the aforementioned description of the impermeable structure (with a power coefficient of 0.2 for the Iribarren number) can be used as initial form for the stability formula. Resulting in the following general formula for all structure types:

$$\frac{H_S}{\Delta D_{n50}} = \boldsymbol{a_1} \cdot \boldsymbol{\xi_m^{0.2}} \cdot (\boldsymbol{c_r})^{\boldsymbol{n_1}} \cdot \sqrt{cot\alpha} \cdot \left(\frac{S}{\sqrt{N}}\right)^{0.2} \tag{6.9}$$

In Appendix H, the run-up reduction coefficients are calculated for the tests of VAN DER MEER [1988]. Trough curve fitting the calculation results the coefficient a_1 and n_1 are determined. However, the range of the fitting coefficient a_1 and n_1 indicates that a general stability relation (for all structures types) cannot be derived by using the current expression for c_r. The reason of the wide range is that the calculated run-up reduction coefficients are not sufficiently dependent on the Iribarren number, see note H.3 in Appendix H.2. This is contradictory to the test results of VAN DER MEER [1988] and the Van-der-Meer-formula, which clearly shows a more dependent relation between the Iribarren number and the influence of the permeability (P is 0.1, 0.5 and 0.6). Since the run-up reduction coefficient is less dependent on the Iribarren number, the stability relation for permeable and homogeneous structure types should be described separately:

Homogeneous structure: $$\frac{H_S}{\Delta D_{n50}} = \boldsymbol{3.1} \cdot \boldsymbol{\xi_m^{0.2}} \cdot \sqrt{cot\alpha} \cdot \left(\frac{S}{\sqrt{N}}\right)^{0.2} (c_r)^{11} \tag{6.10}$$

Permeable structure: $$\frac{H_S}{\Delta D_{n50}} = \boldsymbol{2.7} \cdot \boldsymbol{\xi_m^{0.2}} \cdot \sqrt{cot\alpha} \cdot \left(\frac{S}{\sqrt{N}}\right)^{0.2} (c_r)^{15} \tag{6.11}$$

However, the calculation results are promising when some assumptions are changed, because the stability relations for homogeneous and permeable structures show an increasing similarity. Therefore, it is assumed that refinement of the c_r calculation and expansion of the data set of VAN DER MEER [1988] should lead to a general stability relation in the proposed form (Eq. 6.9). Further research should also determine whether the suggested form (Eq. 6.9) is the best proposal. Nevertheless, the ultimate aim of applying the volume-exchange-model should be; replacing the non-physical notional permeability coefficient P in a physical permeability description arising from the volume-exchange-model.

This literature research can be seen as a good basis to modify the stability relation in terms of permeability. However, practical application of the volume-exchange-model requires further research. Therefore, the following section describes some experiments that should be executed to specify the variables n_1 and a_1 in Equation 6.9.

6.5 Formulating a hypothesis for further research with an associated test program

In this study a conceptual method is introduced to describe the influence of the core permeability on the armour layer stability. Since the introduced method is a theoretical research, additional tests are needed to make the method practically applicable. In the previous section a proposal is given to replace the notional permeability coefficient in the run-up reduction coefficient. The underlying hypothesis of this relation between the volume-exchange-model and the armour layer stability can be formulated as follows:

By using the permeability description c_r, introduced in this research, it is possible to replace the non physical notional permeability description P in the stability formulae of VAN DER MEER [1988]. Since the run-up reduction coefficient is dependent on the wave steepness and presumably also on the similarity parameter, the dual permeability notation can be replaced by one notation only.

However, due to the lack of significant number of meaningful test results, further research must be executed to refine the permeability description c_r. Below a list of tests that can contribute to solve the main issues within the exchange volume model is shown. Their results may help to refine the model and integrate the c_r-coefficient in the Van-der-Meer-formulae. In all tests, a surging wave should occur.

Test series 1 -3: separation of the permeability and roughness

Based on table A.1 in appendix A, the volume exchange method uses a roughness run-up reduction of 0.75. Due to the significant influence of this value, a more precise determination is required. Test series 1-3 (see Figure 6.16) give a test program to separate the roughness and permeability reduction. The laboratory tests can be divided into three different tests:

- Test 1: Measuring the run-up height for a smooth slope,
- Test 2: Measuring the run-up height for a rough impermeable slope,
- Test 3: Measuring the run-up height for a rough permeable slope, wherein the roughness of the permeable slope should have the roughness as the impermeable rough slope (Test 2).

With these laboratory tests it is possible to describe the influence of the roughness and the permeability separately.

In addition, with this test program the run-up volume (V_r, $V_{r,f}$ and $V_{r,f,p}$) and the base of the run-up triangle (d_s, d_f and $d_{f,p}$) can also be measured. In the current description of the volume-exchange-model it is assumed that the run-up wedge has a triangle shape, but in practice, the waves will have a more concave shaped sea surface elevation. Besides this, there is no difference between the triangle bases calculations (d_s, d_f and $d_{f,p}$) when the permeability is taken into account.

Test series 3-8: Influence of the structure geometry on the volume-exchange-model

A significant part of the volume-exchange-model is the water level gradient iteration for a sloped transition. In this study a predefined maximum gradient based on the vertical velocity is used. In this study a predefined maximum gradient based on the vertical velocity is used. However, the exact maximum differs from this value because the flow does not have to be completely vertical at the phreatic surface. Due to the essential role of the internal gradient, it is necessary to gain more insight in the value of this gradient. It is therefore proposed to measure the instantaneous internal pressures for

an x number of homogeneous structures. The test models should have a varying permeability (n, D_{n50}) and slope angle, see Figure 6.16 (in which the ratios are based on the tested structures of VAN DER MEER [1988]). For a detailed description of this kind of measurements please refer to MUTTRAY [2001].

With these measurements more insight is obtained in the local and instantaneous gradient for varying hydraulic and structural parameters. With this it is possible to determine a predefined maximum gradient that is based on a real acting gradient. In addition, these measurements can be investigated to see if it is possible to derive an expression of the real acting gradient.

When choosing homogeneous test models, the influence of the material remains perspicuous. This insight can help when the volume in layered structure types should be determined. For example, the individual test results of the homogeneous structure types can be combined. Assuming however, that the seaward internal gradient is not influenced by the landward gradient.

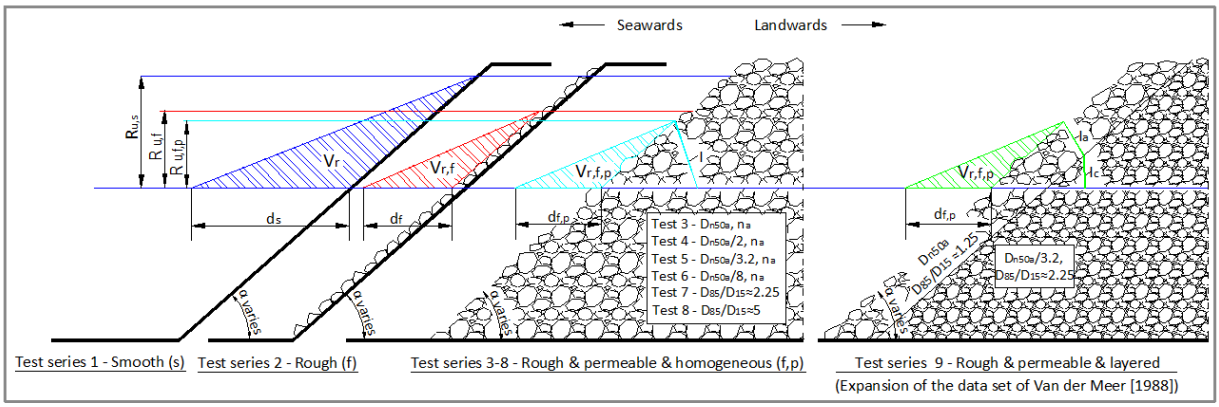

Figure 6.16 - A test program to refine the volume-exchange-model

Test series 9: Expansion of the data set of VAN DER MEER [1988]

If it is assumed that above tests lead to a reliable approach of the run-up reduction coefficient c_r, it is expected that the notional permeability coefficent P can be replaced by this coefficient. This can only be achieved by expanding the data set of VAN DER MEER [1988]. The main problem of the current data set is that the permeability of the structure cannot be fitted separately. This is because the other values (*S*, *N*, *ξ*, *α* and *Δ*) should be fixed in a curve fitting when only the permeability is considered. However, with the current data set it is not possible to have a fixed Iribarren number and also have other variables fixed. An expansion of the data set, where the Iribarren number can be fixed, can help to include the permeability separately. By using the c_r-coefficient it's possible to have a physical basis of this 'permeability fitting'. With these test series also the aforementioned tests (test series 1-8) can be executed.

Additional observations or tests

In the test series mentioned above the influence of the following elements can probably also be investigated:

- Flow below SWL
- Internal water set-up
- Irregular and regular waves

Chapter 7

Conclusions and recommendations

Chapter 7.1 contains recommendations and conclusions which are based on the problem and the objective of this research. Additional conclusions can be found in section 7.2 where as final recommendations for further research can be found in the final section of this chapter.

7.1 Conclusions regarding the problem and objective

In this section, feedback is presented concerning the problem and the objective which are further defined in chapter 1

> *The influence of the core permeability on armour layer stability is not completely described in literature. In the widely used stability formulas of VAN DER MEER [1988] the influence of the core permeability is described by a coefficient (notional permeability coefficient P) that has no physical basis. Since the permeability has large influence on the stability relation, a more precise description of the core permeability influence is important.*

In this study, a so-called run-up reduction coefficient is introduced to describe the influence of the core permeability on the external run-up process. Since the external run-up process is directly related to the armour layer stability, a physical description is given of the influence of the core permeability on the armour layer stability. Up until now, such an analytical description of the influence of the core permeability has not been realized. The only description of this influence is the so-called notional permeability coefficient, introduced by VAN DER MEER [1988]. This description has no physical basis, it is introduced by a curve fitting of test results only to ensure that the permeability is taken into account. Therefore, the permeability description, introduced in this report, can be seen as a step forward with respect to describing the influence of core permeability on the armour layer stability.

However, the present form of the stability relation of VAN DER MEER [1988] includes the non-physical notional permeability coefficient P. The correctness of this permeability description is questionable, but since the stability relationship includes the notional permeability coefficient, this value should be determined. The notional permeability coefficient P is defined for 4 structure types. The non-physical basis of P, makes it impossible to determine a notional permeability value for a different structure type. In practice this often leads to the use of values that do not correspond to the actual value, which results in overdesigned sizes of the D_{n50}. With the here developed volume-exchange-model it is now possible to determine a value for different 'notional permeability structures'. Because of this, the influence of the core permeability is better included in the determination of the armour layer stability. Consequently, a more realistic value of the stone diameter can be obtained.

As mentioned before, the influence of the core permeability on the armour layer stability depends on hydraulic parameters and structural parameters. This is contradictory to the permeability description P given by VAN DER MEER [1988], since the notional permeability coefficient P only depends on the structural parameters, see Figure 1.2. This also explains the dual permeability notation in the stability

formula for surging waves. By using the run-up reduction coefficient, which also depends on the wave steepness, the dual permeability notation in the stability formula can be replaced by single permeability notation only. In Chapter 6.4 and Appendix H a proposal is given to replace the notional permeability coefficient with the run-up reduction coefficient. This is the proposed formula:

$$\frac{H_s}{\Delta D_{n50}} = \boldsymbol{a_1} \cdot (\boldsymbol{c_r})^{\boldsymbol{n_1}} \cdot \boldsymbol{\xi_m^{0.2}} \cdot \sqrt{cot\alpha} \cdot \left(\frac{S}{\sqrt{N}}\right)^{0.2} \qquad \text{Where } c_r = f(\alpha, H_s, T_0, b) \tag{6.9}$$

Note 7.1: *A more detailed description of this c_r-function is given on page 55-57 of this report. The afore-mentioned physical basis of the c_r coefficient is highlighted again in this 'c_r-function'.*

To determine the fitting coefficients a_1 and n_1 the volume exchange model is elaborated for the test program of VAN DER MEER [1988]. This elaboration shows that with the calculated c_r-values no general stability relation for all structure types can be derived. Through curve fitting the calculation results give the following relations:

Homogeneous structures:
$$\frac{H_s}{\Delta D_{n50}} = 3.1 \cdot \boldsymbol{\xi_m^{0.2}} \cdot \sqrt{cot\alpha} \cdot \left(\frac{S}{\sqrt{N}}\right)^{0.2} \cdot (c_r)^{11} \tag{H.7}$$

Permeable structures:
$$\frac{H_s}{\Delta D_{n50}} = 2.7 \cdot \boldsymbol{\xi_m^{0.2}} \cdot \sqrt{cot\alpha} \cdot \left(\frac{S}{\sqrt{N}}\right)^{0.2} \cdot (c_r)^{15} \tag{H.8}$$

However, the calculation results are even more promising when some assumptions are changed. The stability relations for homogeneous and permeable structures show an increasing similarity. Therefore, it is assumed that refinement of the c_r calculation and expansion of the data set of VAN DER MEER [1988] should lead to a general stability relation in the proposed form (Eq. 6.9). Recommendation for refining the calculation of the c_r-value will be described in Chapter 7.3. Further research should also determine whether the suggested form (Eq. 6.9) is the best proposal. Nevertheless, the ultimate aim of applying the volume-exchange-model should be; replacing the non-physical notional permeability coefficient P in a physical permeability description arising from the volume-exchange-model.

The objective of the research was defined as follows:

> *Improving the insight in the physical process related to the core permeability influence on the armour layer stability. Particularly focusing on the research of concretization of the 'notional' permeability coefficient P in the formulae of VAN DER MEER [1988]. Aim is to investigate whether more physical background can be given to the 'notional' permeability coefficient, which ultimately should lead to more adequate guidance for breakwater design practice.*

As previously stated, the volume-exchange-model gives a better insight into the physical process of the armour layer stability on a permeable core. This research shows that this method can be used to provide a physical basis of the notional permeability coefficient, contributing to a more accurate value determination of this coefficient. The current use of the volume-exchange-model, as worked out in this study, is of practical significance since the actual used values for the notional permeability coefficient are questionable. As already mentioned, eventually the volume-exchange-model must lead to a separate permeability description. By using this new permeability description, the notional permeability coefficient in the stability formula, can be replaced by the run-up reduction coefficient.

7.2 Discussion and additional conclusions

In this section some additional conclusions are mentioned. These additional conclusions are described for the following subjects:

Analytical model

The third and fourth chapter describes various methods to couple the internal and external motion. In these Chapters is shown that the methods for preparing an analytical coupling model are limited. With an energy and momentum approach a numerical model was unavoidable. The volume-exchange-model described in this report can be used in an analytical way when the approach remains simple. However, for a detailed estimation of the run-up reduction a better determination of the inflow volume is needed. It is therefore strongly suggested to execute further additional research to keep the model analytical.

The dependency of the hydraulic parameters

The description of the notional permeability values currently implies that the permeability of the structure depends solely on the geometric properties of the breakwater. However, this study clearly shows that the permeability of the structure also depends on the hydraulic parameters (H_s and T_0). As mentioned before, this explains the dual permeability notation in the stability formulae. To indicate the dependency between the notional permeability coefficient and the hydraulic parameters, a formula is derived by curve fitting the calculation results of the volume-exchange-model. The formula for a sloped transition is described by:

$$P = 3.1 \cdot s^{-0.3} \cdot (1 - c_r)^{0.8} \tag{6.8}$$

However, this formula is not directly applicable in practice. This is because the derivation of the stability formula by VAN DER MEER [1988] is fitted with fixed permeability values. Consequently, the stability relation that is fitted, on basis of fixed P-values, is not the same as the stability relation for varying notional permeability's. To make Eq. 6.8 applicable in the stability relation, a modified curve fitting of the test results should be executed. In this modified curve fitting varying P-values should be considered. In addition, Eq. 6.8 only valid for the structure geometry considered in this report and can therefore not be considered as a general formula.

The independency of the slope angle

From the calculation results in Chapter 6 and the curve fitting in Appendix G follows that the structure permeability is not depending on the structure slope. A reason for this independence is that in the case of a gentle slope the run-up velocity is large compared to a steep slope, on the other hand for gentle slope the inflow length is large compared to a steep slope. This has the effect that the influence of the steepness of the slope is negligible. More research is needed to verify this conclusion. Doubts about the correctness of this independence are also strengthened by the difference in the correlation value of the curve fittings.

7.3 Recommendations

In this section some recommendations are summarized to stimulate for further research. In the volume-exchange-model many assumptions were made to determine the run-up volume and the associated inflowing body volume. However, not every assumption has a significant influence on the model. Partly, for this reason only the items are described which are expected to have a decisive influence on the eventual outcome. Refer to Section 6.5 for recommended additional laboratory tests.

Literature study

In this report assumptions are made not only because related test data were not available, but also to keep the model analytical and simple. However, a more detailed literature research could lead to more complete and comprehensive assumptions. Below two examples of such studies are listed.

Friction terms

In this research, the hydraulic resistance for non-stationary flow in coarse porous media is approximated by the Forchheimer equation. Accepting only the turbulent friction term in the exchange method seems to be acceptable since the influence of this term is approximately 90%. The possibilities to include the laminar and inertia term in the exchange model should be investigated. In addition to that a more precise approach of the turbulent friction term is preferred. Mainly the value of the shape factor β should have special attention. In this research a fixed value of 3.6 is considered. However, VAN GENT [1993] determined empirically that the value of this factor depends on the Keulegan-Carpenter number ($KC = \tilde{v}_f T/(nd)$). This Keulegan-Carpenter number characterizes the flow pattern and the porous medium. This dependency implies that the turbulent friction term cannot be described by a fixed shape factor β. Therefore, a more detailed study of this effect should be executed. Appendix D briefly discusses this non-fixed shape factor.

Modified curve fitting of Eq. 6.8

In this report a relationship between the run-up reduction coefficient and the notional permeability coefficient (Eq. 6.8) is derived by fitting calculation results. However, this curve fitting uses calculation results where only the hydraulic parameters are varying. A more realistic curve fitting can be provided when also the structural parameters are considered in the curve fitting, see also note 6.4 in Chapter 6.3.3.

Laboratory tests: Imposed external conditions

In the volume-exchange-model some imposed conditions are assumed arising from the external wave process. These assumptions are based on related test results. An improvement of these test results may lead to a more precise determination of the run-up reduction coefficient. Below some of these influential assumptions for the imposed external conditions are described.

Roughness reduction factor

In the volume-exchange-model an assumption is made for the roughness reduction factor. This assumption is based on an interpolation of slope roughness between two armour layer types, described in Table A.6. Because the roughness reduction factor has a significant influence on inflowing body volume it is necessary to determine this coefficient as accurately as possible.

Run-up period

For the run-up period one quarter of the wave period was adopted. This period is based on test results of MUTTRAY [2001], see Figure 3.5-3.7 in Section 3.2.2. The run-up period represents the period of up-rush from SWL till the maximum wave run-up height. In reality, this period is longer, since the run-down period is not the same as the run-up period. Additional tests, as performed by MUTTRAY [2001], could result in a more precise determination of the run-up period.

Run-up volume estimation

Energy and volume conservation is used for determining the run-up volume. From this consideration follows that the run-up height is only dependent on the wave height and the base of the run-up triangle is only dependent on the wave period. In literature the run-up height is mainly described as a function of the similarity parameter, consequently the run-up height is not only dependent on the wave height but also on the wave period and slope angle. Additional tests are required to determine the most realistic approach. In this study, the base of the run-up triangle depends only on the wave period. This implies that the base is not affected by the run-up height and this also implies that the base of the run-up traingle is independent of the permeability, the wave height, gradient, etc. The accuracy and influence of these assumptions should be examined in test models. For possible scale tests about this topic, see Section 6.5.

Laboratory tests: Internal conditions

This study was conducted to give an analytical description of the influence of the internal flow process on the external flow process. No such description has been elaborated previously partly due to the fact that the internal process is difficult to describe. This problem also existed when considering the volume-exchange-model. Consequently, some assumptions in the exchange volume model have been made about the internal process. As previously indicated, a more extensive literature review can lead to a more accurate determination of internal friction whereas tests are recommended for the following topics.

Internal water set-up

This phenomenon is neglected in the current volume-exchange-model. The internal water set-up is due to a "disconnection" between the external and the internal water level, as a result from a limited internal velocity. This disconnection results in an internal water setup, see Section 5.4.2. To determine this set-up some rules of thumb are introduced, but a detailed description is not available. Further investigation into this set-up should tell whether this set-up has a significant influence on the volume-exchange-model. This investigation should give insight into the influence of varying geometric properties of the breakwater material on this set-up.

Internal water level gradient

The influence of the core material on the external process is mainly determined by the permeability of the material. As previously mentioned, this effect is described by the Forchheimer equation. In its present form the volume-exchange-model requires an iteration of internal water level gradient. For a vertical transition, i.e. a horizontally directed flow, it is possible to determine iteratively the gradient. In case of sloped transition this iteration is not useful anymore, because here the flow is mainly

downwards. In this study a predefined maximum gradient is used to solve the iteration problem. The value of this maximum gradient is based on VAN GENT ET AL. [1994]. However, in the research of VAN GENT ET AL. [1994] no justification is given for the value of this limit. Presumably this maximum is based on the maximum vertical gradient. Given the significant influence of this gradient on the determination of body volume an accurate determination is required. Through experiments insight can be obtained into the value of these limits or even better an expression for this gradient.

References

BAART, S.A. [2008] Toe structures for rubble mound breakwaters, MSc thesis, Delft University of Technology, Delft, The Netherlands

BATTJES J.A. [2006] Short waves combined lecture notes of DUT (2001) and IHE (1984), CT4320, Delft University of Technology, Delft, The Netherlands

BURCHARTH H.F. [1993] The design of breakwaters, In: Coastal, estuarial and harbour engineering's reference book, *Chapman & Hall*, London (UK), pp. 381-424

BURCHARTH, H.F., CHRISTENSEN, M., JENSEN, T. AND FRIGAARD, P. [1998] Influence of core permeability on Accropode armour layer stability, *Proc. Int. Conf. Coastlines, Structures and breakwaters '98, Institution of Civil Engineers*, London, March 1998, pp. 34-45

BURCHARTH, H.F.; LIU, Z.; TROCH, P. [1999] Scaling of core material in rubble mound breakwater model tests. *Proceedings 5th International Conference on Coastal and Port Engineering in Developing Countries (COPEDEC)*, Cape Town, South Africa, pp. 1518-1528.

CARRIER, G.F. AND GREENSPAN, H.P. [1958] Water waves on finite amplitude on a sloping beach. *Journal of Fluid Mechanics*, *Pierre Hall*, Harvard University,Vol.4, pp. 97-109

CIRIA, CUR, CETMEF [2007] The rock manual, The use of rock in hydraulic engineering, C683 CIRIA, London

FÜHRBÖTER, I.A. [1993] Wave loads on sea dikes and sea-walls. In: Coastal, estuarial and harbour engineering's reference book, *Chapman & Hall*, London (UK), pp. 351-367

HALL K.R. AND HETTIARACHCHI S.[1992] Mathematical modeling of interaction with rubble mound breakwaters, Coastal structures and breakwaters, *Thomas Telford*, London, pp.123-147

HEIJ, J. DE [2001] The influence of structural permeability on armour stability of rubble mound breakwaters, MSc-thesis, Delft University of Technology, Delft, The Netherlands

HUGHES, S.A. AND FOWLER, J.E. [1995] Estimating wave-induced kinematics at sloping structures, *J. of Waterway, Port, Coastal and Ocean Engineering*, ASCE, vol. 121, no. 4, pp. 209-215

HUGHES, S.A. [2004] Estimation of wave run-up on smooth, impermeable slopes using the wave momentum flux parameter, *Coastal Engineering 51*, pp. 1085– 1104

JUANG, J-T, JIUN-YAN YOU, C.-F. L. [2009] Prediction of the Wave Run-up on Step Dike*, Proceedings of the Nineteenth International Offshore and Polar Engineering Conference*, Osaka, Japan, June 21-26, pp. 1069-1074

LATHAM, J-P, MANNION, M.B., POOLE A.B, BRADBURY, A.P. AND ALLSOP, N.W.H [1988] The influence of armour stone shape and rounding on the stability of breakwater armour layers, *Coastal Engineering Research Group*, Queen Mary College, University of London, Research report 1, September 1988

LE ROUX, J.P. [2003] Wave friction factor as related to the Shields parameter for steady currents, *Sedimentary Geology*, 155, pp. 37–43

LI, Y., [2000] Tsunamis: non-breaking and breaking solitary wave run-up, *Q Report No. KH-R-60,W. M. Keck Laboratory of Hydraulics and Water Resources*, California Institute of Technology, Pasadena, California.

LIN P. [2008] Numerical modeling of water waves*, Taylor & Francis*, London, England

MUTTRAY, M. [2000] Wellenbewegung in einem geschütteten Wellenbrecher, PhD thesis, Technical University Braunschweig, Braunschweig, Germany

MUTTRAY, M, OUMERACI, H ,REEDIJK, J [2004] Wave damping in rubble mounds, *Proc. Int. Conf. Coastal Eng*., Vol. 29, Lisbon, Portugal, pp. 4494-4506

MUTTRAY, M. OUMERACI, H. [2005] Theoretical and experimental study on wave damping inside a rubble mound breakwater, Coastal engineering, Vol. 52, pp. 709-725.

MUTTRAY, M., OUMERACI, H, TEN OEVER, E [2006] Wave reflection and wave run-up at rubble mound breakwaters, *Proc. Int. Conf. Coastal Eng.,* Vol. 30, San Diego, California, USA

SYNOLAKIS, C.E. [1986] The run-up of solitary waves, Ph.D. Thesis, California institute of Technology

TROCH, P. [2000] Experimentele studie en numerieke modellering van golfinteractie met stortsteen-golfbrekers, Proefschrift, Gent University, Gent, Belgium

VAN DER MEER, J.W. [1988] Rock slopes and gravel beaches under Wave attack, PhD thesis, Delft University of Technology, Delft, The Netherlands

VAN DER MEER, J.W. [1990] Measurement and computation of wave induced velocities on smooth slope*,* ASCE, *Proc. 22th ICCE*, Delft, pp. 191-204

VAN DER MEER, J.W. [2002] *Invloedsfactoren voor de ruwheid van toplagen bij golfoploop en overslag*, *bijlage bij het Technisch Rapport Golfoploop en Golfoverslag bij dijken*, Rijkswaterstaat, Dienst Weg- en Waterbouwkunde, publicatienummer DWW-2002-112

VAN GENT M.R.A. [1993] Stationary And Oscillatory Flow Through Coarse Porous Media, *Communications on hydraulic and geotechnical engineering*, Report No. 93-9. Delft University of Technology, Delft.

VAN GENT M.R.A., TÖNJES P., PETIT H.A.H., VAN DEN BOSCH P., [1994] Wave action on and in permeable coastal structures*, Proceedings 24th International Conference on Coastal Engineering*, Kobe, Japan, Vol.2, pp.1739-1753.

VAN GENT M.R.A., [1995]. Wave interaction with permeable coastal structures. Ph.D. Thesis TU Delft, Nederland, ISBN 90-407-1182-8.

VERHAGEN, H.J. D'ANGREMOND, K. AND VAN ROODE, F. [2009] Breakwaters and closure dams, *VSSD,* Delft

WITTEMAN, E.F.C, [1999] Run-up test on a permeable slope, MSc thesis, Delft University of Technology, Delft, The Netherlands

Appendix A

Roughness reduction factors according to VAN DER MEER [2002]* (in Dutch)

Table A.6 - Invloedsfactoren voor de ruwheid bij golfoploop en golfoverslag

Code	Omschrijving	invloedsfactor
1	Asfaltbeton	1,0
2	Mastiek	1,0
3	Dicht steenasfalt	1,0
4	Open geprefabriceerde steenasfaltmatten	0,9
5	Open steenasfalt	0,9
6	Zandasfalt (tijdelijk of in onderlaag)	1,0
7	**Breuksteen, gepenetreerd met asfalt (vol en zat)**	**0,8**
8	Baksteen/betonsteen, gepenetreerd met asfalt (vol en zat)	1,0
9	**Breuksteen, gepenetreerd met asfalt (patroonpenetratie)**	**0,7**
10	Betonblokken met afgeschuinde hoeken of gaten erin	0,9
11	Betonblokken zonder openingen	1,0
11.1	Haringmanblokken	0,9
11.2	Diaboolblokken	0,8
12	Open blokkenmatten, afgestrooid met granulair materiaal	0,9
13	Blokkenmatten zonder openingen in de blokken	0,95
14	Betonplaten van cementbeton of gesloten colloidaal beton, (in situ gestort)	1,0
15	Colloidaal beton, (open structuur)	1,0
16	Betonplaten, (prefab)	1,0
17	Doorgroeisteen, beton	0,95
18	Breuksteen, gepenetreerd met cementbeton of colloidaal beton, (vol en zat)	0,8
19	Breuksteen, met patroonpenetratie van cementbeton of colloidaal beton	0,7
20	Gras, gezaaid	1,0
21	Gras, zoden of gezaaid, in kunststofmatten	1,0
22	Bestorting van grof grind en andere granulaire materialen	0,8
23	Grove granulaire materialen c.q. breuksteen verpakt in metaalgaas	0,7
24	Fijne granulaire materialen c.q. zand/grind verpakt in geotextiel, zandzakken	0,9
25	Breuksteen, (stortsteen)	0,55
26	Basalt, gezet	0,9
26.01	Basalt, gezet, ingegoten met gietasfalt	0,95
26.02	Basalt, gezet, ingegoten met colloidaal beton of cementbeton	0,95
27	Betonzuilen en andere niet rechthoekige blokke	
27.1	Basalton	0,9
27.2	PIT Polygoon zuilen	0,9
27.3	Hydroblock	0,9
27.01	Betonzuilen of niet rechthoekige blokken, ingegoten met gietasfalt	1,0
27.11	Basalton, ingegoten met gietasfalt	1,0
27.21	PIT Polygoon zuilen, ingegoten met gietasfalt	1,0
27.31	Hydroblock, ingegoten met gietasfalt	1,0
27.02	Betonzuilen of niet rechthoekige blokken, ingegoten met beton	1,0
27.12	Basalton, ingegoten met beton	1,0
28	Natuursteen, gezet	
28.1	Vilvoordse	0,85
28.2	Lessinische	0,85

28.3	Doornikse	0,9
28.4	Petit graniet	0,90
28.5	Graniet	0,95
28.6	Noordse of Drentse steen	0,75
28.01	Natuursteen, gezet, en ingegoten met gietasfalt	
28.11	Vilvoordse, ingegoten met gietasfalt	0,95
28.21	Lessinische, ingegoten met gietasfalt	1,0
28.31	Doornikse, ingegoten met gietasfalt	1,0
28.41	Petit graniet, ingegoten met gietasfalt	1,0
28.51	Graniet, ingegoten met gietasfalt	1,0
28.61	Noordse of Drentse steen, ingegoten met gietasfalt	0,85
28.02	Natuursteen, gezet, en ingegoten met beton	
28.12	Vilvoordse, ingegoten met beton	0,95
28.22	Lessinische, ingegoten met beton	1,0
28.32	Doornikse, ingegoten met beton	1,0
28.42	Petit graniet, ingegoten met beton	1,0
28.52	Graniet, ingegoten met beton	1,0
28.62	Noordse of Drentse steen, ingegoten met beton	0,85
29	Koperslakblokken	1,0
30	Klei onder zand	
31	Bestorting van natuursteenmassa	0,55
32	Klinkers, beton of gebakken.	1,0
33	zand	
34	steenfundering, gebonden	

*****This table is published as appendix in the technical report: Golfoploop en Golfoverslag bij dijken, published by Rijkswaterstaat in September 2002, created by J.W. VAN DER MEER (see references).

Appendix B

Calculation values for the shape factors α and β for a Forchheimer flow

Table B.7 - Calculation values for the shape factors α and β for a Forchheimer flow, adapted to the use of the Forchheimer Equation (3.15) in the laminar Forchheimer flow type. Reference: BURCHARTH AND CHRISTENSEN [1991] taken from TROCH [2000]

Researcher	Material	Porosity n [-]	D_{50} [mm]	Re [-]	α [-]	β [-]
BURCHARTH AND CHRISTENSEN [1991] from TROCH [2000]	Uniform, spherical particles				~190	~1.8
	Uniform rounded sand grains				~240	~2.8
	Irregular, angular grains				to 360 or more	to 3.6 or more
FAND ET AL. [1987]	Uniform glass spheres	0.360	2-4	5-80	~182	~1.92
LINDQUIST* [1933]	shot	0.383	1-5	4-263	184	1.82
DUDGEON** [1966]	Uniform glass spheres	0.415 0.385	16 29	<400 <180	164 193	1.7 2.4
	River gravel	0.367 0.406	16 110	<85 <7000	329 922	4.7 2.0
	Angular rock	0.455 0.515 0.438 0.483	16 14 25 37	<400 <200 <400 <500	622 479 425 92	5.4 4.0 5.3 10.8
ENGELUND [1953]	Flinty, Calcareous sand and of uniform size	0.395	1.4-2.6	24-150	335	3.57

* Data taken from Ahmed et al., 1969.
** Data calculated from Dudgeon's graphs, not from the data points.

Note B.1: *In the volume-exchange-model a continuous shape factor of β is used. In reality these coefficients are not constants and should in principle be treated as instantaneous values, see Appendix D.*

Appendix C

Modifications for the volume-exchange-model

C.1 Distance d calculated according the linear wave theory

According to the linear wave theory, a wave has a lower propagation speed in shallow water $\left(\sqrt{gh(x)}\right)$. In a wave-structure-interaction, the wave is influenced by the shallower water, therefore the intersection of the wave profile and SWL (P2) will propagate towards the slope with a somewhat larger velocity than the wave crest (P1), see Figure C.1. The assumption that is made in Section 5.1, for determining the distance d, is therefore not completely conclusive.

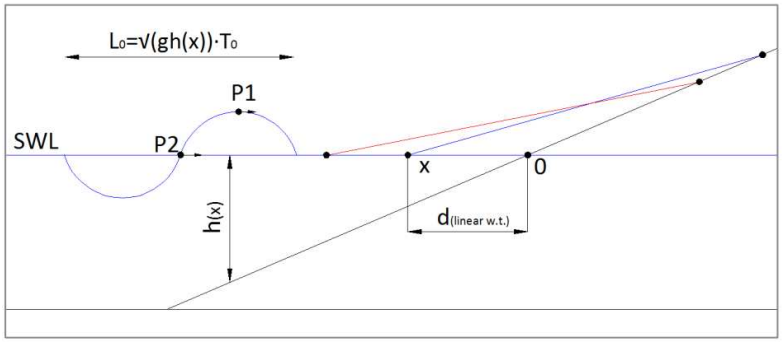

Figure C.1 - Schematization of the theory behind the distance d calculation according L.W.T

The following method describes an approach for determing a new distance d according to the linear wave theory. If one quarter of the wave is considered, then the following can be applied:

$$\frac{2\pi}{4} = \int_0^x k\,dx = \int_0^x \frac{2\pi}{T\sqrt{gh(x)}} \tag{C.1}$$

The water depth $h(x)$ can be expressed as follows:

$$h(x) = \frac{\mathrm{x}}{\cot\alpha} \tag{C.2}$$

With this expression, Equation C.1 can also be written as:

$$\frac{2\pi}{4} = 4\pi \frac{\sqrt{cot\alpha}}{T\sqrt{g}}\sqrt{x} \tag{C.3}$$

By rewriting this equation, x can be expressed as:

$$x = \left[\frac{1}{8}\frac{T\sqrt{g}}{\sqrt{cot\alpha}}\right]^2 = \frac{gT^2}{64}\cdot\frac{1}{cot\alpha} \tag{C.4}$$

Distance d according to the linear wave theory can now be calculated as:

$$d = L_0 \cdot \frac{\pi}{32}\cdot\frac{1}{cot\alpha} \tag{C.5}$$

C.2 Determination of a internal water level gradient for a fully turbulent porous flow

According to BURCHARTH AND CHRISTENSEN [1991], described in TROCH [2000], the porous flow is always fully turbulent in a prototype rubble mound breakwater for a design wave. They stated that in case of a fully turbulent flow, a physically more correct form of the Forchheimer model (Eq. 5.31) is:

$$I = I_c + b'(V - V_c)^2 \tag{C.6}$$

Where indices *c* stands for critical and V stands for velocity. The figure below shows the transition from a Forchheimer flow (not to be confused with the Forchheimer model mentioned above) into a given turbulent flow.

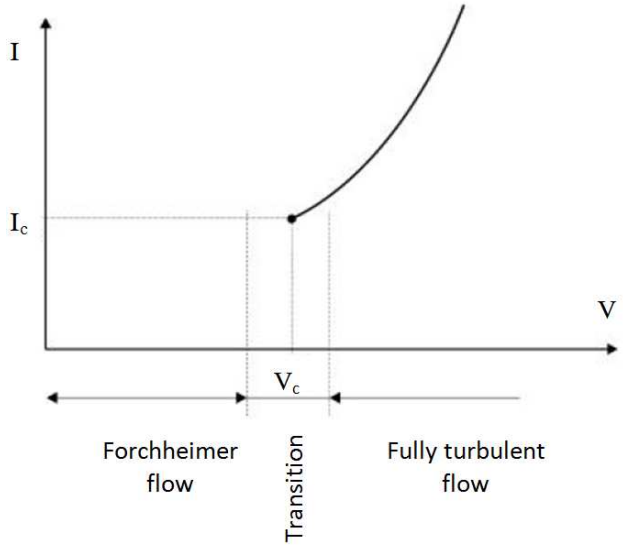

Figure C.2 - Presentation of the turbulent flow type according to BURCHARTH AND CHRISTENSEN [1991] (reference TROCH [2000])

Figure C.2 shows that the transition zone is relatively wide. The following table from TROCH [2000], based on GU EN WANG [1991], provides for various porous materials a magnitude for the characteristic values of the grain diameter D, the filter velocity V, the Reynolds number R, and related porous flow types. This table also shows that the transition zone between a Forchheimer flow and a fully turbulent flow is very wide. This emphasizes that in practice it is not easy to determine which type of flow should be considered.

Note C.1: *TROCH [2000] about the values in the table below: "The values show a certain range depending on the specific situation, but are valid (and intended) as a rule of thumb" (a translated quote).*

Table C.8 - Magnitude for the characteristic values for various porous materials. Values of the grain diameter D, the filter velocity V, the Reynolds number Re, and related porous flow types. Based on GU EN WANG [1991] from TROCH [2000]

Type of Material	Grain diameter D [m]	Filter velocity V [m/s]	*Re* =VD/ν [-]	Type of porous flow
sand	< O(10^{-3})	<O(10^{-3})	<O(1)	Darcy
Fine gravel	0.01	O(10^{-2})	O(10^{2})	Laminar Forchheimer
Rubble mound 2-300kg	0.1-0.3	O(10^{-1})	O(10^{4})	Fully Turbulent
Rubble mound 1-6 ton	0.7-1.2	O(1)	O(10^{6})	Fully Turbulent
Armour layer unit/ Large rock	>1.2	>O(1)	>O(10^{6})	Fully turbulent

BURCHARTH AND CHRISTENSEN [1991] (described in TROCH [2000]) calculate that for breakwaters made of rubble mound with a diameter d greater than 0.03 m, the I_c and V_c are both negligible (< O(10^{-2})), so equation C.6 reduces to $I = b'V^2$. The conclusion which can be drawn from this, is that in almost all practical cases (scale models and prototypes), when the grain diameter is greater than 0.03 and a continuous flow is assumed, it is justified to take only the turbulent term into account and the Forchheimer Equation 5.31 can be used:

$$I = b'V^2 \tag{5.31}$$

Below follows a table of calculated values for a' and b' from different researchers, valid for the Forchheimer Equation 5.31, for a fully turbulent flow (BURCHARTH AND ANDERSEN [1995], reference TROCH [2000]). It is clear that under the above proposition essentially the β'-term is important, instead of the α'.

Table C.9 - List of β'coefficients for fully turbulent flow

Material	Packing	d_{85}/d_{15}	α'	β'	Re	Data source*
Spheres	Cubic	1.0	900-6000	1.0-1.3	630-	Sm
	Rhomb	1.0	640-900	0.47-1.1	14000	Sm
	Random	1.0	410-1700	1.1-1.5	630-	D
	Random	1.8	3100	1.6	14000	D
	Random	1.0	220	1.5	180-9000	F
	Random	2.0	240	1.6	3700-	F
					7700	
					120-410	
					120-410	
Round rock	Random	1.4	~10000	2.2	<2100-	B
		1.7	1400-	2.2-2.9	8050	D

		?	15000	1.7	500-3600	H
		1.3	160-9800	1.9	?	W
			?		750-7500	
Semi-round	Random	1.9	~3000	2.7	800-2100	B
rock		1.3	?	2.4	750-7500	W
Irregular	Random	1.4-1.8	1400-	2.4-3.0	600-	B
rock		1.6	13000	4.1-11	10300	D
		?	270-1400	3.0-3.7	400-8200	H
		1.3-1.4	90-540	2.5-2.9	?	Sh
		1.3	980-2100	3.7	300-5700	W
			?		750-7500	
Equant rock	Random	1.2	?	3.6	750-7500	W
Tabular	Random	1.4	3000	1.5	1500-	Sm
rock		1.2	?	3.7	18000	W
					750-7500	

*B: BURCHARTH AND CHRISTENSEN [1991]; D: DUDGEON [1966]; F: FAND ET AL. [1987]; H: HANNOURA AND MC-CORQUODALE [1978]; Sh: SHIH [1990]; Sm: SMITH [1991]; W: WILLIAMS [1992].

Note C.2: *In the volume-exchange-model, a continuous shape factor of β is used. In reality these coefficients are not constants and should in principle be treated as instantaneous values, see Appendix D.*

C.3 The sea water surface in a concave shape

As already mentioned, CROSS AND SOLLITT [1972] (reference JUANG AND JIUN-YAN YOU [2009]) proposed that at maximum run-up, the shape of the run-up wedge is assumed to be a parabola with its is vertex at the bottom of the first wave trough (Fig. C.3). The corresponding equation is:

$$Y = MX^N - A \tag{5.32}$$

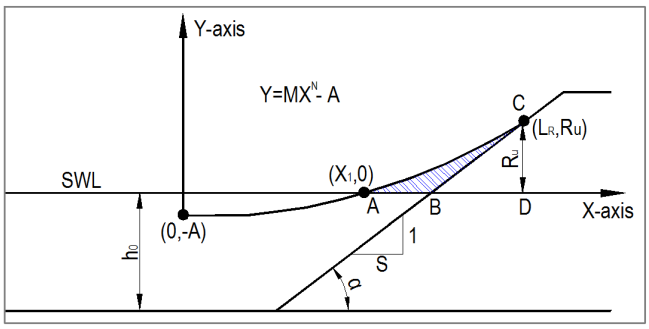

Figure C.3 - Wave run-up wedge according CROSS AND SOLLITT [1972] (reference: JUANG AND JIUN-YAN YOU [2009]

In which Y = the water surface elevation above the sea water level; X = the distance from the trough shoreward; A=the amplitude at the trough; M= a constant coefficient in a parabola equation; N= the exponent in the parabola equation. The area $A_{(ABC)}$ of the parabola run-up wedge area can be calculates by the following equation (Fig. C.3):

$$A_1 - A_2 = A_{(ACD)} - A_{(BCD)} = \int_{X_1}^{L_r}(MX^N - A)dx - \frac{{R_u}^2}{2}cot\alpha \quad \text{(C.7)}$$

After integration, the area of the run-up wedge is:

$$A_{(ABC)} = \frac{M}{N+1}(L_R^{N+1} - X_1^{N+1}) - A(L_R - X_1) - \frac{{R_u}^2}{2}cot\alpha \quad \text{(C.8)}$$

However, several unknown factors as M, N, L_R and X_1, still need to defined. HUGHES [2004] described: "Following the lead of ARCHETTI AND BROCCHINI [2002], a simple physical argument is that the weight of the fluid contained in the hatched wedge area $W_{(ABC)}$ is proportional to the maximum depth integrated wave momentum flux of the wave before it reached the toe of the structure slope". It can therefore be obtained that the proportionality factor can be described as follows:

$$K_m = \frac{K_p \cdot (M_F)_{max}}{W_{(ABC)}} \quad \text{(C.9)}$$

For calculating $(M_F)_{max}$, HUGHES [2004] established an empirical equation for estimating the wave momentum flux parameter for finite amplitude. The $(M_F)_{max}$ can be estimated by using the following empirical equation, established by HUHGES [2004] for a finite amplitude. The resulting, purely empirical equation, was given as:

$$\left(\frac{M_F}{\rho g h^2}\right) = A_0\left(\frac{h}{gT^2}\right)^{-A_1} \quad \text{(C.10)}$$

$$A_0 = 0.6392\left(\frac{H}{h}\right)^{2.0256} \quad \text{(C.11)}$$

$$A_1 = 0.1804\left(\frac{H}{h}\right)^{-0.391} \quad \text{(C.12)}$$

The value of $W_{(ABC)}$ can be estimated by multiplying Eq. C.8 with ρg. For the computation of the unknown factors in Eq. C.8, JUANG AND JIUN-YAN YOU [2009] suggested to re-write the run-up equation in a dimensionless form. By using the basic equations for M and L_R, physical laws, and some assumptions, the unknown factors can be described as follows:

$$\mathrm{M} = \frac{\mathrm{R_u} + a}{\mathrm{L_R^N}} \quad \text{(C.13)}$$

$$\mathrm{L_R} = \mathrm{X_1}(\mathrm{r}+1)^{\frac{1}{\mathrm{N}}} \quad \text{(C.14)}$$

$$(\mathrm{N}+1)\left[\frac{a \cdot \mathrm{s} \cdot \mathrm{r}^2}{2\mathrm{X_1}(\mathrm{r}+1)^{1/\mathrm{N}}}\right] + \mathrm{N} - \mathrm{r} = 0 \quad \text{(C.15)}$$

Where *r* is R_u/a. In JUANG AND JIUN-YAN YOU [2009] it is assumed that X_1 is the one-fourth of incident wave length and *a* is the amplitude of the incident wave. An estimation of the run-up height can be done with the use of an existing run-up approach (for example the approach of ALLSOP ET AL. [1985], described in the CUR / CIRIA [2007]). With these considerations the unknown N can be calculated.

Appendix D

Non-fixed shape factors

(Parts of this Appendix are based on or taken from MUTTRAY & OUMERACI [2005])

For the sake of simplicity, in this research, a fixed value for the form factor is assumed. This value depends on the type of flow and the material properties. However, in reality these coefficients are not constants and should in principle be treated as instantaneous values, even for oscillatory flow conditions. The following approaches for the resistance coefficient a and b, which include the non-dimensional coefficient K_a and K_b (see Table D.10), have been proposed for stationary flow:

$$a = K_a \frac{(1-n)^2}{n^3} \frac{\upsilon}{gd^2} \tag{D.1}$$

$$b = K_b \kappa_o \frac{1-n}{n^3} \frac{1}{gd} \tag{D.2}$$

The coefficient κ_o is 1 for stationary flow. If coefficient b accounts for viscous and turbulent shear stresses, the Forchheimer equation will be applicable not only for combined laminar–turbulent flow, but also for fully turbulent flow (VAN GENT [1992a] (reference MUTTRAY & OUMERACI [2005]). The hydraulic resistance of a uniform non-stationary flow is described by the extended Forchheimer equation (Eq. (3.11)). For oscillatory flow the additional resistance with regard to the convective acceleration has to be considered by a quadratic resistance term. Hence, the resistance coefficient b will be increased. VAN GENT [1993] determined experimentally a coefficient κ_o of $1 + 7.5\ /KC$ for an oscillatory flow. The Keulegan–Carpenter number $KC = \tilde{v}_f T\ /\ (nd)$ characterises the flow pattern (with velocity amplitude $\tilde{v}_f$ and period T) and the porous medium (particle size n and diameter d).

Table D.10 - Empirical coefficients and characteristic particle d for the Forchheimer coefficients $\boldsymbol{a}$ and $\boldsymbol{b}$ (stationary flow), reference MUTTRAY & OUMERACI [2005]

Author	Characteristic particle diameter	Dimensionless K_a	Coefficient K_b
Kozeny (1927), Carman (1937)	d_{eq} [a]	180	_c
Ergun(1952), Ergun and Orning (1994)	d_{n50} [b]	150	1.75
Engelund (1953)	d_{eq}	_c	1.8-3.6
Koenders (1985)	d_{n15}	250-330	_c
Den Adel (1987)	d_{n15}	75-350	_c
Shih (1990)	d_{n15}	>1684	1.72-3.29
Van Gent (1993)	d_{n50}	1000	1.1

a) The equivalent diameter d_{eq} is the diameter of a sphere with mass m_{50} and specific density ρ_s of an average actual particle: $d_{eq}=(6m_{50}/\pi\rho_s)^{1/3}$.

b) The nominal diameter D_{n50} is the diameter of a cube with mass m50 and specific density ρ_s of an average actual particle.$D_{n50}=(m_{50}/\rho_s)^{1/3}$

c) Authors proposed a different approach from Eqs. (D.1) and (D.2).

The inertia coefficient *c* will not be affected by the convective acceleration and reads:

$$c = \frac{1}{ng}\left(1 + K_m \frac{1-n}{n}\right) \tag{D.3}$$

The added mass coefficient K_m will be 0.5 for potential flow around an isolated sphere and for a cylinder it will be 1.0. In a densely packed porous medium the coefficient K_m cannot be determined theoretically; most probably it will tend to zero (MADSEN [1974] (reference MUTTRAY & OUMERACI [2005])). VAN GENT [1993] proposed the following empirical equation for the added mass coefficient of a rubble mound. His approach may lead for small velocity amplitudes $\tilde{v}_f$ and long periods T to negative values of K_m, which are physically meaningless and have to be excluded:

$$K_m = max.\left\{0.85 - 0.015\frac{ngT}{\tilde{v}_f}; 0\right\} \tag{D.4}$$

It is clear that mainly the turbulent term *b* is important, but for completeness the other friction terms are also described.

Note D.1: *Instantaneous values of b are too complicated to deal with in practice, for this reason the turbulent friction term is based on time invariant coefficients within a cycle.*

Appendix E

Sensitivity analysis of the volume-exchange-model

In this appendix, the calculation results of the sensitivity analysis of the volume-exchange-model is analyzed. This sensitivity analysis is done by applying the volume exchange method to a homogeneous structure with a vertical transition. Below the results are shown of the volume-exchange-model, where each parameter varies once. Values of the environmental and structural parameter used in this example, are related to a model test of the Zeebrugge breakwater (reference BURCHARTH ET AL. [1999]).

Case 1: varying wave period

Porosity:	0.38 m.
D_{n50}:	0.262 m.
Shape factor β	3.6
Wave height:	2.91 m
Cot α:	1.5
Roughness reduction:	0.75

Table E.11 - Sensitivity for varying wave period

Period	I_b	U_b	V_b	V_{ru}	c_r
7.9 sec	2.03	0.36	2.17	33.85	**0.94**
8.9 sec	1.89	0.35	2.38	42.96	**0.94**
9.9 sec	1.77	0.33	2.58	53.15	**0.95**
10.9 sec	1.66	0.32	2.77	64.43	**0.96**
11.9 sec	1.57	0.32	2.95	76.80	**0.96**

Case 2: varying wave height

Porosity:	0.38 m.
D_{n50}:	0.262 m.
Shape factor β	3.6
Wave period:	7.9 s
Cot α:	1.5
Roughness reduction:	0.75

Table E.13 - Sensitivity for varying wave height

Height	I_b	U_b	V_b	V_{ru}	c_r
1.0 m	1.01	0.25	0.54	11.63	**0.95**
1.5 m.	1.32	0.29	0.91	17.45	**0.95**
2.0 m.	1.59	0.32	1.33	23.26	**0.94**
2.5 m.	1.84	0.34	1.78	29.08	**0.94**
3.0 m.	2.07	0.36	2.26	34.89	**0.94**

Case 3: varying porosity

Wave period	7.9 s
D_{n50}:	0.262 m.
Shape factor β	3.6
Wave height:	2.91 m
Cot α:	1.5
Roughness reduction:	0.75

Table E.12 - Sensitivity for varying porosity

Porosity	I_b	U_b	V_b	V_{ru}	c_r
0.1	3.72	0.05	0.35	33.85	**0.99**
0.2	2.81	0.14	0.89	33.85	**0.97**
0.3	2.32	0.25	1.56	33.85	**0.95**
0.4	1.97	0.39	2.33	33.85	**0.93**
0.5	1.69	0.55	3.21	33.85	**0.91**

Case 4: varying D_{n50}

Wave period	7.9 s
Porosity:	0.38
Shape factor β	3.6
Wave height:	2.91 m
Cot α:	1.5
Roughness reduction:	0.75

Table E.14 - Sensitivity for varying D_{n50}

D_{n50}	I_b	U_b	V_b	V_{ru}	c_r
0.10 m	2.83	0.26	1.61	33.85	**0.95**
0.15 m	2.46	0.30	1.83	33.85	**0.95**
0.20 m	2.23	0.33	2.00	33.85	**0.94**
0.25 m	2.06	0.35	2.14	33.85	**0.94**
0.30 m	1.94	0.37	2.26	33.85	**0.93**

Appendix F

The volume-exchange-model for the 'P-structures' with vertical transition

In this appendix, for each defined 'notional permeability structure' the volume-exchange-model is elaborated. Below the volume-exchange-model is described with corresponding schematization of the tested structure. This elaboration assumes a vertical transition and therefore the schematization of the tested structures are only shown to give the grading of each layer.

F.1 Homogeneous and permeable structure with respectively a P-factor of 0.6 and 0.5

As already noted, the notional permeability expresses the influence of the core (and filter) permeability on the armour layer stability. Therefore, only the volume inflow in the core and filter should be determined. In a homogeneous structure this layer is not present. However, on behalf of a proper comparison between the 'Van der Meer structures', the homogeneous structure should include an 'imaginary' armour layer in the elaboration. In this way the volume-exchange-model works the same for a homogeneous structure (P is 0.6) and a permeable structure (P is 0.5). First, the two tested structures by VAN DER MEER [1988] are shown. The grading rate, the D_{n50} and the structures slope are given in the figure. The summary in Table 6.3 is based on these values.

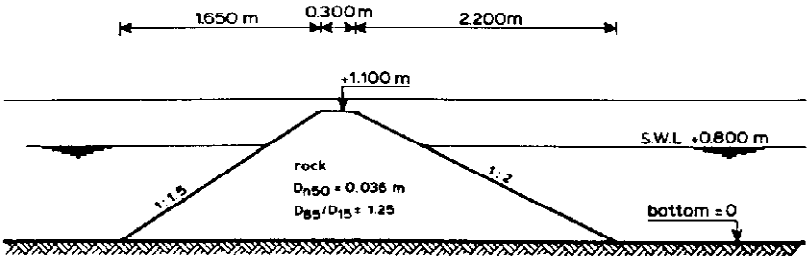

Figure F.1 - Schematization of the tested homogeneous structure by VAN DER MEER [1988]

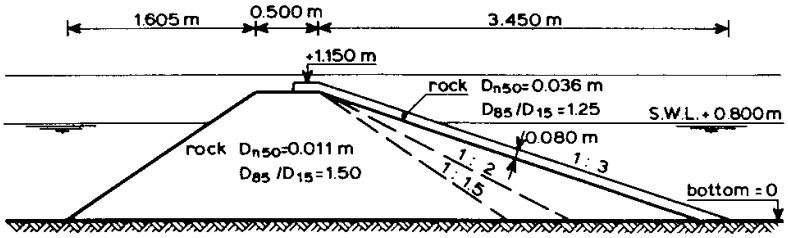

Figure F.2 - Schematization of the tested structure with a permeable core by VAN DER MEER [1988]

The volume-exchange-model, as described in Chapter 5, is able to calculate the volume inflow for one homogeneous material. However, for a notional permeability of 0.6 and 0.5, the structure consists of two parts (core and armour). In this case, the water level decrease in the armour layer should also be included. The following figure illustrates the volume-exchange-model for these two structures.

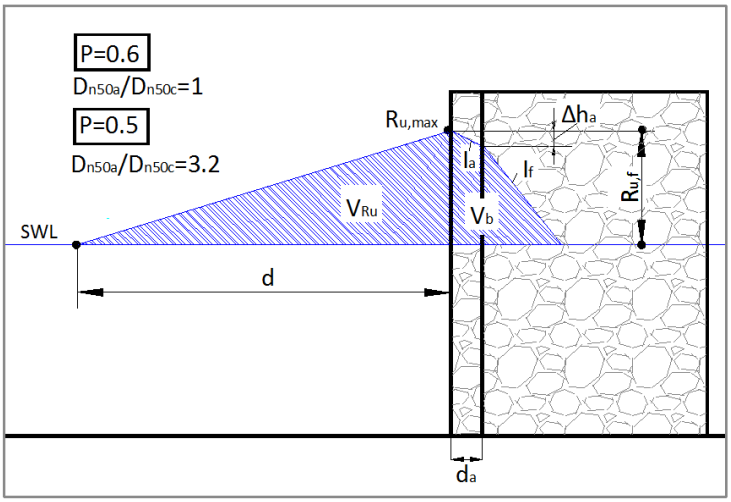

Figure F.3 - Volume inflow for a notional permeability factor of 0.5 and 0.6 (vertical transition)

The formulae for the volume inflow according to the volume-exchange-model, in case of a notional permeability of 0.5 and 0.6, can be described as:

Armour layer

Determination of the gradient $\frac{1}{2} \cdot n \cdot \left(\frac{1}{I_a}\right) \cdot R_{u,f}^2 = \frac{1}{\omega}\sqrt{\mathrm{I_a/b}} \cdot \mathrm{R_{u,f}} \cdot \left(1 - \cos\left(\omega \cdot \frac{\mathrm{T0}}{4}\right)\right)$

Base of the armour layer: $d_a = 2D_{n50a}$

Phreatic water level decrease in armour layer: $\Delta h_a = d_a \cdot I_a$

Core

Reduced run-up in core: $R_{u,core} = (R_{u,f} - \Delta h_a)$

Determination of the gradient $\frac{1}{2} \cdot n_c \cdot \left(\frac{1}{I_c}\right) \cdot R_{u,c}^2 = \frac{1}{\omega}\sqrt{\mathrm{I_c/b_c}} \cdot \mathrm{R_{u,c}} \cdot \left(1 - \cos\left(\omega \cdot \frac{\mathrm{T0}}{4}\right)\right)$

Volume in the core/ total: $V_{core} = \frac{1}{2} \cdot n_c \cdot \left(\frac{1}{I_c}\right) \cdot R_{u,c}^2$

It is clear that in case of P is 0.6 the water inflow is larger than with P is 0.5, because both the porosity n and D_{n50} in the core are larger.

F.2 Filter structure with a notional permeability of 0.4

The so-called 'filter structure' is not tested by VAN DER MEER [1988] and has therefore an assumed notional permeability factor. This structure type is widely used in practice and is for that reason included as a model structure. Since this structure type is not tested, an illustration for the geometry and the applied grading cannot be shown. The next figure shows the volume-exchange-model in case of this 'filter structure'.

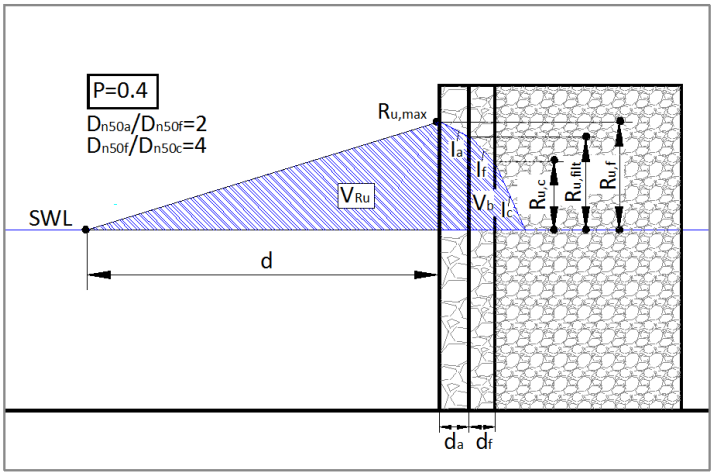

Figure F.4 - Volume inflow for a notional permeability factor of 0.4 (vertical transition)

The formulae for the volume inflow according to the volume-exchange-model, in case of a notional permeability of 0.4, can be described as:

Armour layer

Determination of the gradient $\frac{1}{2}\cdot n\cdot\left(\frac{1}{I_a}\right)\cdot R_{u,f}^2=\frac{1}{\omega}\sqrt{\mathrm{I_a/b}}\cdot \mathrm{R_{u,f}}\cdot\left(1-\cos\left(\omega\cdot\frac{\mathrm{T0}}{4}\right)\right)$

Base of the armour layer: $d_a=2D_{n50a}$

Phreatic water level decrease in armour layer: $\Delta h_a=d_a\cdot I_a$

Filter layer

Reduced run-up in filter: $R_{u,filt}=(R_{u,f}-\Delta h_a)$

Determination of the gradient $\frac{1}{2}\cdot n_f\cdot\left(\frac{1}{I_f}\right)\cdot R_{u,filt}^2=\frac{1}{\omega}\sqrt{\mathrm{I_f/b_f}}\cdot \mathrm{R_{u,filt}}\cdot\left(1-\cos\left(\omega\cdot\frac{\mathrm{T0}}{4}\right)\right)$

Base of the filter layer: $d_f=1.5\cdot D_{n50f}$

Phreatic water level decrease in filter layer: $\Delta h_f=d_f\cdot I_f$

Volume in the filter layer: $V_{filter}=n_f\cdot d_f\left(R_{u,filt}+\frac{1}{2}\cdot d_f\cdot I_f\right)$

Core

Reduced run-up in core: $R_{u,core}=(R_{u,f}-\Delta h_f-\Delta h_a)$

Determination of the gradient $\frac{1}{2}\cdot n_c\cdot\left(\frac{1}{I_c}\right)\cdot R_{u,c}^2=\frac{1}{\omega}\sqrt{\mathrm{I_c/b_c}}\cdot \mathrm{R_{u,c}}\cdot\left(1-\cos\left(\omega\cdot\frac{\mathrm{T0}}{4}\right)\right)$

Volume in the core: $V_{core}=\frac{1}{2}\cdot n_c\cdot\left(\frac{1}{I_c}\right)\cdot R_{u,c}^2$

Total volume

Total volume inflow: $V_{in,total}=V_{filter}+V_{core}$

F.3 Impermeable structure with a notional permeability of 0.1

In VAN DER MEER [1988] a practical lower boundary is found for a two diameters thick armour layer on a thin filter layer and with an impermeable core. The only storing capacity is in the small filter layer. Below an illustration of the tested structure.

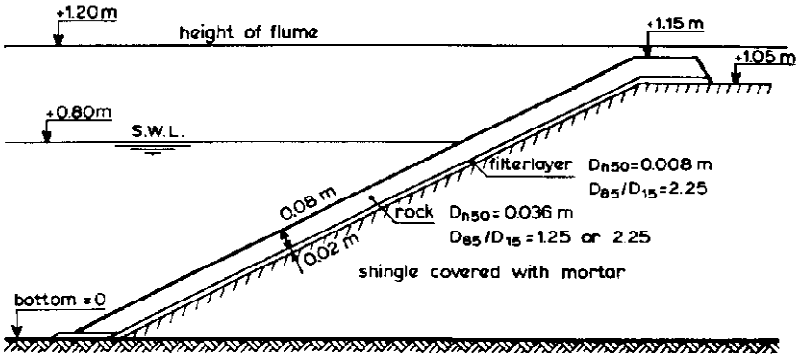

Figure F.5 - Schematization of the tested structure with impermeable core by VAN DER MEER [1988]

In practice, the influence of the filter layer on the run-up process is almost negligible, but for completeness, the influence of this layer is still included. Below follows an overview of the volume-exchange-model.

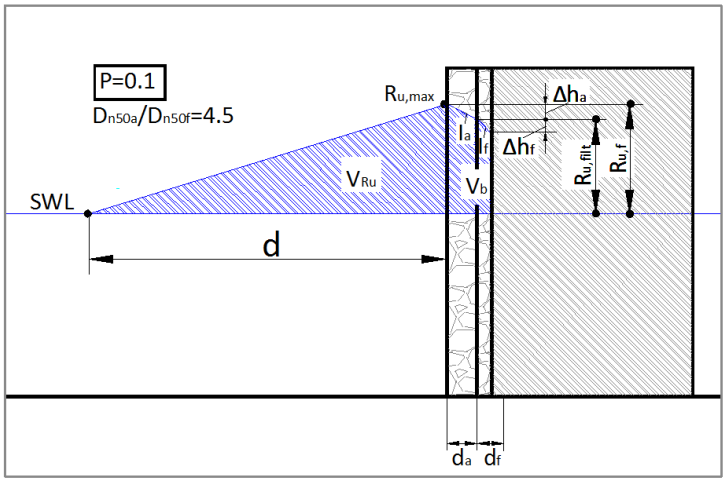

Figure F.6 - Volume inflow for a notional permeability factor of 0.1 (vertical transition)

The formulae for the volume inflow according to the volume-exchange-model, in case of a notional permeability of 0.1, can be described as:

Armour layer

Determination of the gradient $\frac{1}{2} \cdot n \cdot \left(\frac{1}{l_a}\right) \cdot R_{u,f}^2 = \frac{1}{\omega}\sqrt{\mathrm{I_a/b}} \cdot \mathrm{R_{u,f}} \cdot \left(1 - \cos\left(\omega \cdot \frac{\mathrm{T0}}{4}\right)\right)$

Base of the armour layer: $d_a = 2D_{n50a}$

Phreatic water level decrease in armour layer: $\Delta h_a = d_a \cdot I_a$

Filter layer

Reduced run-up in filter: $R_{u,filt} = (R_{u,f} - \Delta h_a)$

Determination of the gradient $\frac{1}{2} \cdot n_f \cdot \left(\frac{1}{I_f}\right) \cdot R_{u,filt}^2 = \frac{1}{\omega}\sqrt{\mathrm{I_f/b_f}} \cdot \mathrm{R_{u,filt}} \cdot \left(1 - \cos\left(\omega \cdot \frac{\mathrm{T0}}{4}\right)\right)$

Base of the filter layer: $d_f = 0.5 \cdot D_{n50f}$

Phreatic water level decrease in filter layer: $\Delta h_f = d_f \cdot I_f$

Volume in the filter layer / total volume: $V_{filter} = n_f \cdot d_f \left(R_{u,filt} + \frac{1}{2} \cdot d_f \cdot I_f\right)$

The inflow volume into the core of the structure is zero. There is only a flow into the filter layer. Given the small size of the filter layer this inflow is limited.

F.4 Calculation output of the volume-exchange-model

Below the calculation results of the above mentioned volume-exchange-models are given. The values of the porosity and grading are given in Table 6.5 in Chapter 6. The other used parameters are:

Slope angle (cot(α)): 2
Shape factor β: 3.6
D_{n50} of the armour layer: 0.262 m.
Wave height (in case of varying wave period): 2.91 m.
Wave period (in case of varying wave height): 14 s.

Table F.15 - Calculation values of the volume-exchange-models for the four defined 'P-structures'

				Notional permeability factor P														
				0.6	0.5	0.4	0.1	0.4	0.4	0.4	0.6	0.5	0.4	0.1	All	0.6	0.5	0.4	0.1
				I_c	I_c	I_f	I_f	V_f	I_c	V_c	V_b	V_b	V_b	V_b	V_{ru}	c_r	c_r	c_r	c_r
Wave period T_0	12	steepness	0.0130	1.36	2.02	1.78	2.36	0.58	2.83	0.67	2.56	1.76	1.25	0.21	78.1	**0.967**	**0.977**	**0.984**	**0.997**
	13		0.0110	1.30	1.93	1.70	2.25	0.59	2.72	0.73	2.75	1.89	1.32	0.21	91.7	**0.970**	**0.979**	**0.986**	**0.998**
	14		0.0095	1.24	1.85	1.63	2.15	0.60	2.62	0.78	2.93	2.01	1.38	0.21	106.3	**0.972**	**0.981**	**0.987**	**0.998**
	15		0.0083	1.20	1.77	1.57	2.07	0.61	2.53	0.84	3.11	2.14	1.45	0.21	122.0	**0.975**	**0.983**	**0.988**	**0.998**
Wave height H_s	2	steepness	0.0065	0.96	1.42	1.25	1.65	0.40	1.98	0.45	1.73	1.19	0.85	0.14	73.1	**0.976**	**0.984**	**0.988**	**0.998**
	3		0.0098	1.27	1.89	1.67	2.20	0.62	2.68	0.82	3.06	2.10	1.44	0.22	109.6	**0.972**	**0.981**	**0.987**	**0.998**
	4		0.0131	1.55	2.30	2.04	2.69	0.85	3.32	1.25	4.55	3.14	2.10	0.30	146.1	**0.969**	**0.979**	**0.986**	**0.998**
	5		0.0164	1.81	2.69	2.38	3.15	1.07	3.90	1.73	6.19	4.27	2.81	0.38	182.6	**0.966**	**0.977**	**0.985**	**0.998**

*The indices used in the table: f and c represent the layer in the structures, resp. filter and core. The index b represents the total body of the structure.

F.5 Derivation of a notional permeability formula for vertical transition

In this section a relation is given for the notional permeability coefficient. This relation is based on a curve fitting of the calculation results from Table F.15. For an example of the curve fitting see Figure F.7. The curve fitting is elaborated with the following equation:

$$P = a_1 \cdot (1 - c_r)^{b_1} \tag{F.1}$$

Table F.16 - Curve fitting results for equation F.1 (vertical transition)

Steepness	a_1	b_1	Correlation
0.0065	6.93	0.65	0.996
0.0083	5.86	0.61	0.996
0.0095	5.71	0.62	0.996
0.0098	5.62	0.62	0.996
0.0110	5.69	0.63	0.996
0.0130	5.68	0.65	0.996
0.0131	4.89	0.60	0.997
0.0164	4.51	0.59	0.997

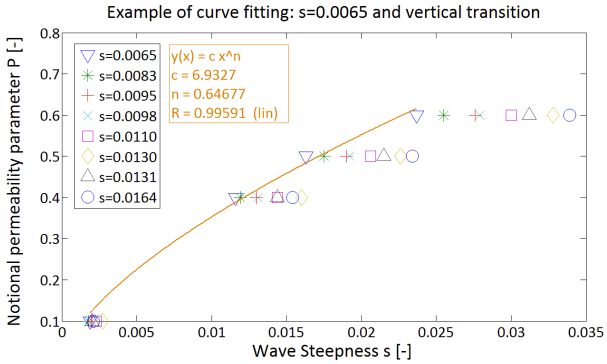

Figure F.7 - Example of a curve fitting (vertical transition)

Given these fitting results, the power coefficient is fixed with a value of 0.6. The equation for the second curve fitting becomes:

$$P = a_2 \cdot (1 - c_r)^{0.6} \tag{F.2}$$

Table F.17 - Curve fitting results for equation E.10 (vertical transition)

Steepness	a_2	Correlation
0.0065	5.74	0.994
0.0083	5.53	0.996
0.0095	5.27	0.996
0.0098	5.23	0.996
0.0110	5.00	0.995
0.0130	4.72	0.994
0.0131	4.91	0.997
0.0164	4.68	0.997

From Table F.17 follows that a_2 is related to the wave steepness. The next curve fitting has therefore the following form:

$$a_2 = d_1 \cdot \left(\frac{1}{s}\right)^{e_1} = 1.67 \cdot \left(\frac{1}{s}\right)^{0.25} \approx 1.7 \cdot \left(\frac{1}{s}\right)^{0.25} \tag{F.3}$$

This curve fitting gives a correlation coefficient of 0.976. Finally the equation becomes:

$$P = 1.7 \cdot s^{-0.25} \cdot (1 - c_r)^{0.6}$$

Appendix G

The volume-exchange-model for the 'P-structures' with a sloped transition

G.1 Calculation of the volume-exchange-model for a sloped transition

In this section the volume-exchange-model is elaborated for a sloped transition. A schematization of the volume exchange is given in Figure G.1.

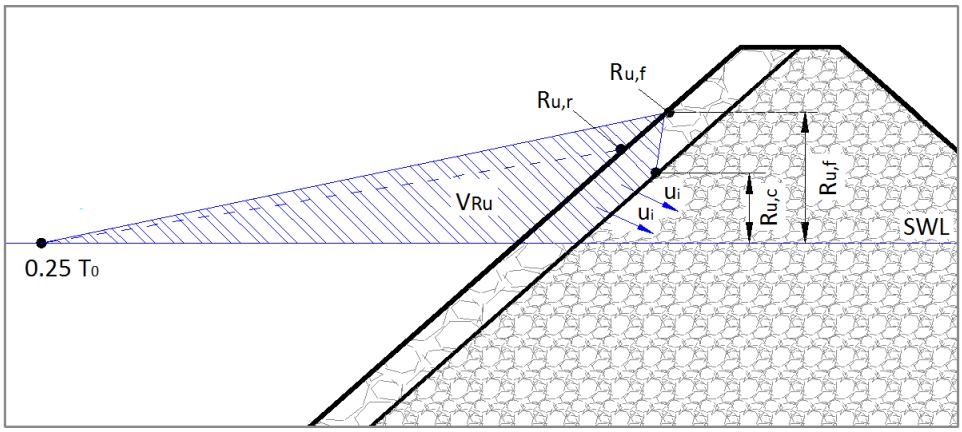

Figure G.1 - Schematization of the volume exchange for a sloped transition with two layers

Below a summary of the equations is used for a double layered sloped transition. The predefined maximum internal water level gradient is one, this assumption is based on the maximum gradient for vertical velocity. First, the general formulae of the volume-exchange-model follows here:

Volume exchange $V_{Ru,r} = V_{Ru,f} - V_b$

Run-up volume: $V_{Ru,f} = \frac{1}{2} \cdot d \cdot R_{u,f}$

Run-up with friction $R_{u,f} = \gamma_f \cdot R_u$

Base of the run-up triangle $d = \frac{4L_0}{3\pi^2}$

Turbulent term: $b = \beta \frac{1-n}{n^3} \frac{1}{gD}$

The formulae for the volume inflow according to the volume-exchange-model, in case of a notional permeability of 0.5 and 0.6, can be described as:

Imposed core run-up: $R_{u,c} = 0.5 \cdot R_{u,f}$

Determination of the gradient: $\frac{1}{2} \cdot n \cdot \left(\frac{1}{I}\right) \cdot (R_{u,c})^2 = \frac{1}{\omega}\sqrt{\frac{I}{b}} \cdot \frac{R_{u,c}}{\sin(\alpha)}\left(1 - \cos\left(\omega \cdot \frac{T_0}{4}\right)\right)$

Body volume when $I \leq 1$: $V_b = \frac{1}{\omega}\sqrt{\frac{I}{b}} \cdot \frac{R_{u,c}}{\sin(\alpha)}\left(1 - \cos\left(\omega \cdot \frac{T_0}{4}\right)\right)$

Body volume when $I > 1$: $V_b = \frac{1}{\omega}\sqrt{\frac{1}{b}} \cdot \frac{R_{u,c}}{\sin(\alpha)}\left(1 - \cos\left(\omega \cdot \frac{T_0}{4}\right)\right)$

With the calculation of the volume inflow, the reduced run-up volume can be calculated. The run-up reduction factor is the relation between the run-up reduced by friction (Ru, f) and the run-up reduced by friction and permeability ($R_{u,r}$).

Reduced run-up: $$R_{u,r} = \frac{(V_{Ru,f} - V_b)}{V_{Ru,f}} \cdot R_{u,f}$$

Run-up reduction factor: $$c_r = \frac{Ru,r}{Ru,f}$$

With these formulae and with the structure properties given in Table 6.5, the volume exchange can be calculated. The volume inflow for an impermeable structure is based on a fully saturated filter layer volume. In Table G.18 and G.19, the calculation results of the volume-exchange-model for a sloped transition are given.

Input:
Cot(α) = 1.5
H_s =2.91m (varying wave period)
T_0 =11 sec (varying wave height)
D_{n50a} =0.262m

Table G.18 - Calculations results of the volume-exchange-model with a slope angle of cot(α) is 1.5

						0.6	0.5	0.6	0.5	0.1	All	0.6	0.5	0.1
						I_c	I_c	V_{tot}	V_{tot}	V_{tot}	V_{ru}	c_r	c_r	c_r
Period T_0	**8**	**Steepness s**	**0.029**	**ξ-factor**	**3.90**	0.84	1.00	1.43	0.89	0.23	34.71	**0.959**	**0.975**	**0.993**
	9		**0.023**		**4.39**	0.78	1.00	1.56	1.00	0.23	43.93	**0.964**	**0.977**	**0.995**
	10		**0.019**		**4.88**	0.73	1.00	1.69	1.11	0.23	54.23	**0.969**	**0.980**	**0.996**
	11		**0.015**		**5.37**	0.69	1.00	1.81	1.23	0.23	65.62	**0.973**	**0.981**	**0.997**
Height H_s	**2**	**Steepness s**	**0.011**	**ξ-factor**	**6.48**	0.54	0.80	1.10	0.76	0.16	45.10	**0.976**	**0.983**	**0.997**
	3		**0.016**		**5.29**	0.70	1.00	1.88	1.27	0.24	67.65	**0.972**	**0.981**	**0.997**
	4		**0.021**		**4.58**	0.85	1.00	2.75	1.69	0.32	90.20	**0.970**	**0.981**	**0.997**
	5		**0.027**		**4.10**	0.99	1.00	3.69	2.11	0.40	112.75	**0.967**	**0.981**	**0.997**

Input:
Cot(α) = 2
H_s =2.91m (varying wave period)
T_0 =14 sec (varying wave height)
D_{n50a} =0.262m

Table G.19 - Calculations results of the volume-exchange-model with a slope angle of cot(α) is 2

						0.6 I_c	0.5 I_c	0.6 V_{tot}	0.5 V_{tot}	0.1 V_{tot}	All V_{ru}	0.6 c_r	0.5 c_r	0.1 c_r
Period T_0	**12**	**Steepness s**	**0.013**	**ξ-factor**	**4.39**	0.56	0.84	2.21	1.52	0.29	78.10	**0.972**	**0.981**	**0.996**
	13		**0.011**		**4.76**	0.54	0.79	2.34	1.61	0.29	91.65	**0.975**	**0.983**	**0.997**
	14		**0.010**		**5.12**	0.51	0.76	2.47	1.69	0.29	106.30	**0.977**	**0.984**	**0.997**
	15		**0.008**		**5.49**	0.49	0.72	2.59	1.77	0.29	122.02	**0.979**	**0.986**	**0.998**
Height H_s	**2**	**Steepness s**	**0.007**	**ξ-factor**	**6.18**	0.40	0.59	1.50	1.03	0.20	73.06	**0.979**	**0.986**	**0.997**
	3		**0.010**		**5.05**	0.52	0.77	2.57	1.76	0.30	109.58	**0.977**	**0.984**	**0.997**
	4		**0.013**		**4.37**	0.63	0.93	3.76	2.58	0.39	146.11	**0.974**	**0.982**	**0.997**
	5		**0.016**		**3.91**	0.73	1.00	5.04	3.33	0.49	182.64	**0.972**	**0.982**	**0.997**

G.2 Derivation of a notional permeability formula for sloped transition (cot(α) is 1.5)

Below a relation is given for the notional permeability coefficient. This relation is based on a curve fitting of the calculation results from Table G.18. The curve fitting is elaborated with the following equation:

$$P = a_1 \cdot (1 - c_r)^{b_1} \quad \text{(G.1)}$$

The values of c_r are given in Table G.18 for the three defined notional permeability structures. Table G.16 gives the fitting results.

Table G.20 - Curve fitting results for Eq. G.1 with cot (α) is 1.5

Steepness	a_1	b_1	Correlation
0.0291	7.79	0.79	0.984
0.0230	8.66	0.79	0.989
0.0187	9.43	0.78	0.992
0.0154	8.69	0.73	0.996
0.0106	12.95	0.82	0.994
0.0159	9.71	0.77	0.994
0.0212	7.21	0.70	0.990
0.0265	5.94	0.66	0.986

Given these fitting results, the power coefficient is fixed with a value of 0.8. The equation for the second curve fitting becomes:

$$P = a_2 \cdot (1 - c_r)^{0.8} \quad \text{(G.2)}$$

Table G.21 - Curve fitting results for Eq. G.2 with cot (α) is 1.5

Steepness	a_2	Correlation
0.0291	8.15	0.984
0.0230	9.11	0.989
0.0187	10.11	0.992
0.0154	11.12	0.996
0.0106	12.13	0.994
0.0159	11.03	0.994
0.0212	10.48	0988
0.0265	10.06	0.982

From Table G.21 follows that a_2 is related to the wave steepness. The next curve fitting has therefore the following form:

$$a_2 = d_1 \cdot \left(\frac{1}{s}\right)^{e_1} = 3.13 \cdot \left(\frac{1}{s}\right)^{0.3} \quad \text{(G.3)}$$

This curve fitting gives a correlation coefficient of 0.882. Finally the equation becomes:

$$P = 3.13 \cdot \left(\frac{1}{s}\right)^{0.3} \cdot (1 - c_r)^{0.8} \quad \text{(G.4)}$$

G.3 Derivation of a notional permeability formula for sloped transition (cot(α) is 2)

In this section a relation is given for the notional permeability coefficient. This relation is based on a curve fitting of the calculation results from Table G.19. The curve fitting is elaborated with the following equation:

$$P = a_1 \cdot (1 - c_r)^{b_1} \quad \text{(G.1)}$$

For a better curve fitting, a notional permeability coefficient of 0 is included, this coefficient has a run-up reduction value of 1.

Table G.22 - Curve fitting results for Eq. G.1 with cot (α) is 2

Steepness	a_1	b_1	Correlation
0.013	10.29	0.79	0.994
0.011	10.38	0.77	0.996
0.0095	10.64	0.75	0.996
0.0083	10.57	0.74	0.996
0.0065	13.21	0.79	0.995
0.0098	10.55	0.75	0.996
0.0131	8.92	0.73	0.997
0.0164	7.54	0.70	0.996

Given these fitting results the power coefficient is fixed with a value of 0.8. The equation for the second curve fitting becomes:

$$P = a_2 \cdot (1 - c_r)^{0.8} \quad \text{(G.5)}$$

This curve fitting results in the following table:

Table G.23 - Curve fitting results for Eq. G.5 with cot (α) is 2

Steepness	a_2	Correlation
0.0130	10.81	0.995
0.0110	11.77	0.996
0.0095	12.70	0.996
0.0083	13.68	0.996
0.0065	13.94	0.995
0.0098	12.61	0.996
0.0131	11.73	0.996
0.0164	11.19	0.994

From Table G.23 follows that a_2 is related to the wave steepness. The next curve fitting has therefore the following form:

$$a_2 = d_1 \cdot \left(\frac{1}{s}\right)^{e_1} = 3.13 \cdot \left(\frac{1}{s}\right)^{0.3}$$

This curve fitting has a correlation coefficient of 0.935. Finally the equation becomes:

$$P = 3.13 \cdot \left(\frac{1}{s}\right)^{0.3} \cdot (1 - c_r)^{0.8} \qquad \text{(G.6)}$$

Appendix H

Replacing the P-factor in the stability formula of VAN DER MEER [1988]

In this section the non-physical permeability description (P-coefficient) in the stability formula of VAN DER MEER [1988] is replaced by the run-up reduction coefficient. First, a summary is given of the assumptions made in the volume exchange model. Thereafter, the run-up reduction coefficients are calculated for the test program of VAN DER MEER [1988]. With these calculation results an alternative stability relation is derived by curve fitting the results.

H.1 Normative assumptions in the volume-exchange-model

Below the assumptions in the volume-exchange-model are summarized. This is done to indicate that the present form of the volume-exchange model still needs refinement.

- The roughness reduction factor is 0.75.
- No water flow below SWL.
- The imposed core run-up is 50% of the external maximum run-up.
- Internal water set-up is neglected.
- Regular waves instead of irregular waves.
- Triangular shaped wave run-up wedge instead of a concave shaped.
- In calculating the volume inflow only the turbulent friction term is included.
- Fixed shape factor β instead of an instantaneous value, as proposed by VAN GENT [1993].
- The time span of run-up from SWL till maximum external wave run-up is $\frac{1}{4}T_0$.
- The maximum gradient of the volume inflow in the case of a slope transition is 1.

H.2 Coupling the test results of VAN DER MEER [1988] with the volume-exchange-model

Below, the test results of VAN DER MEER [1988] are coupled with the volume-exchange-model. This coupling is elaborated by calculating the run-up reduction coefficient for the test conditions. The same procedure as the one used by VAN DER MEER has been used to fit the variables in the stability relation. Besides, it is assumed that the slope angle α, the number of waves *N* and the damage level *S* are correctly fitted in the derivation of VAN DER MEER [1988]. Under this consideration, without taking into account the permeability of the structure, the general form of the stability formula can be described as:

$$\frac{H_S}{\Delta D_{n50}} = \boldsymbol{a_0} \cdot \boldsymbol{\xi_m^{n_0}} \cdot \sqrt{cot\alpha} \cdot \left(\frac{S}{\sqrt{N}}\right)^{0.2} \tag{H.1}$$

From the calculation results in Appendix F and G follows that the run-up reduction coefficient is inversely proportional to the wave steepness, and presumably to the Iribarren number as well. In that case the dual permeability notation in the stability formula can be replaced by 1 parameter (c_r). The form of the formula H.1, for permeable structures, can now be expressed as follows:

$$\frac{H_S}{\Delta D_{n50}} = \boldsymbol{a_1} \cdot \boldsymbol{\xi_m^{n_0}} \cdot (c_r)^{n_1} \cdot \sqrt{cot\alpha} \cdot \left(\frac{S}{\sqrt{N}}\right)^{0.2} \tag{H.2}$$

Where n_0 is the fitting coefficient for all structure types. In VAN DER MEER [1988] this coefficient is 0.1, 0.5 or 0.6. Replacing the notional permeability coefficient P with the run-up reduction factor, the coefficient n_0 is equal to the power coefficient for an impermeable structure. In VAN DER MEER [1988] a value of 0.1 is fitted, but considering the doubtfulness of this curve fitting, the value should be further investigated. This is done by additional curve fitting of the test results for impermeable structures. For this curve fitting, only the surging waves are considered and the Iribarren range is assumed to be larger than 3.5. This fitting is executed for 4 different damage levels.

Note H.1 & H.2:

- *a_0 and n_0 are fitting coefficients for the stability relation <u>without</u> considering the permeability.*
- *a_1 and n_1 are fitting coefficients for the stability relation <u>with</u> considering the permeability.*

<u>Damage level 2</u>

Table H.24 - Test results of VAN DER MEER [1988] with a fixed damage level of 2.

Test nr.	Perm.	$\sqrt{cot\alpha}$	$\left(\frac{S}{\sqrt{n}}\right)^{0.2}$	Δ	T_m	D_{n50}	ξ_m (N=3000)	$H_s/\Delta D_{n50}$ (N=3000)
11	Imp.	1.41	0.52	1.7	1.16	0.0164	4.05	1.15
21	Imp.	1.41	0.52	1.7	1.31	0.0164	4.37	1.26
33	Imp.	1.41	0.52	1.63	1.85	0.0360	4.41	1.17
37	Imp.	1.41	0.52	1.63	2.19	0.0360	5.25	1.16
41	Imp.	1.41	0.52	1.63	2.69	0.0360	6.06	1.31
45	Imp.	1.41	0.52	1.63	3.11	0.0360	6.96	1.33

Curve fitting of above test results (Table H.24) gives the following equation:

$$\frac{H_S}{\Delta D_{n50}} = a_0 \cdot \xi_m^{\mathbf{0.25}} \cdot \sqrt{cot\alpha} \cdot \left(\frac{S}{\sqrt{N}}\right)^{0.2} \quad \text{(H.3)}$$

<u>Damage level 3</u>

Table H.25 - Test results of VAN DER MEER [1988] with a fixed damage level of 3

Test nr.	Perm.	$\sqrt{cot\alpha}$	$\left(\frac{S}{\sqrt{n}}\right)^{0.2}$	Δ	T_m	D_{n50}	ξ_m (N=3000)	$H_s/\Delta D_{n50}$ (N=3000)
12	Imp.	1.41	0.56	1.7	1.16	0.0164	3.92	1.23
22	Imp.	1.41	0.56	1.7	1.31	0.0164	4.22	1.35
34	Imp.	1.41	0.56	1.63	1.85	0.0360	4.25	1.26
38	Imp.	1.41	0.56	1.63	2.19	0.0360	5.03	1.26
42	Imp.	1.41	0.56	1.63	2.69	0.0360	5.91	1.38
46	Imp.	1.41	0.56	1.63	3.11	0.0360	6.88	1.36

Curve fitting of above test results (Table H.25) gives the following equation:

$$\frac{H_S}{\Delta D_{n50}} = a_0 \cdot \xi_m^{\mathbf{0.15}} \cdot \sqrt{cot\alpha} \cdot \left(\frac{S}{\sqrt{N}}\right)^{0.2} \quad \text{(H.4)}$$

Damage level 5

Table H.26 - Test results of VAN DER MEER [1988] with a fixed damage level of 5

Test nr.	Permea-bility	$\sqrt{cot\alpha}$	$\left(\frac{S}{\sqrt{n}}\right)^{0.2}$	Δ	T_m	D_{n50}	ξ_m (N=3000)	$H_s/\Delta D_{n50}$ (N=3000)
23	Imp.	1.41	0.62	1.7	1.31	0.0164	4.09	1.44
35	Imp.	1.41	0.62	1.63	1.85	0.0360	4.08	1.37
39	Imp.	1.41	0.62	1.63	2.19	0.0360	4.85	1.36
43	Imp.	1.41	0.62	1.63	2.69	0.0360	5.82	1.42
47	Imp.	1.41	0.62	1.63	3.11	0.0360	6.69	1.44

Curve fitting of above test results (Table H.26) gives the following equation:

$$\frac{H_S}{\Delta D_{n50}} = a_0 \cdot \xi_m^{\mathbf{0.12}} \cdot \sqrt{cot\alpha} \cdot \left(\frac{S}{\sqrt{N}}\right)^{0.2} \tag{H.5}$$

Damage level of 8

Table H.27 - Test results of VAN DER MEER [1988] with a fixed damage level of 8

Test nr.	Permea-bility	$\sqrt{cot\alpha}$	$\left(\frac{S}{\sqrt{n}}\right)^{0.2}$	Δ	T_m	D_{n50}	ξ_m (N=3000)	$H_s/\Delta D_{n50}$ (N=3000)
24	Imp.	1.41	0.68	1.7	1.31	0.0164	4.00	1.50
40	Imp.	1.41	0.68	1.63	2.19	0.0360	4.76	1.41
44	Imp.	1.41	0.68	1.63	2.69	0.0360	5.80	1.43
48	Imp.	1.41	0.68	1.63	3.11	0.0360	6.55	1.50

Curve fitting of above test results (Table 27) gives the following equation:

$$\frac{H_S}{\Delta D_{n50}} = a_0 \cdot \xi_m^{\mathbf{0.01}} \cdot \sqrt{cot\alpha} \cdot \left(\frac{S}{\sqrt{N}}\right)^{0.2}$$

From above fitting results follows that the direction (i.e. the power coefficient) of the Iribarren number is between 0.01 and 0.25. The fitting for a damage level of 2 and 3 is considered to be the most reliable, because this fitting contains more data points. Therefore, in this research a value of 0.2 is selected for the power coefficient of the Iribarren number. The above curve fitting results highlight again that the used value of 0.1 for impermeable structures in VAN DER MEER [1988] is not conclusively. With a power coefficient of 0.2 the general formula for permeable structures becomes:

$$\frac{H_S}{\Delta D_{n50}} = a_1 \cdot \boldsymbol{\xi_m^{0.2}} \cdot \sqrt{cot\alpha} \cdot \left(\frac{S}{\sqrt{N}}\right)^{0.2} \cdot (c_r)^{n_1} \tag{6.9}$$

Note H.3:

By considering a fixed power coefficient for the Iribarren number, the c_r should also include the influence of the Iribarren number on the permeability. In other words, in the test results of VAN DER MEER [1988] the power coefficient for permeable and homogeneous structures is respectively 0.5 and 0.6. Consequently, a fixed power coefficient of 0.2 leads to underestimations in case of permeable and homogeneous structures. Therefore, the introduced c_r-coefficient should also take the dependency of the influence of the Iribarren number (for changing permeability's) into account.

Table H.28 shows the run-up reduction coefficients of the test results for homogeneous and permeable structures. Using these c_r-values, the power coefficient n_1 is determined. It is assumed that a_1 has a value of 1.

Table H.28 - c_r-coefficients for the tested permeable and homogeneous structure types by VAN DER MEER [1988].

Test nr.	$\left(\frac{S}{\sqrt{n}}\right)^{0.2}$	$\sqrt{cot\alpha}$	Permea-bility	Δ	T_m	D_{n50}	ξ_m (N=3000)	$H_s/\Delta D_{n50}$ (N=3000)	H_s (N=3000)	Core pemeability	c_r	n_1
262	0.52	1.41	Perm.	1.615	2.16	0.036	4.44	1.59	0.092	0.4	0.9693	**7**
267	0.52	1.41	Perm.	1.615	2.89	0.036	5.43	1.90	0.110	0.4	0.9776	**17**
299	0.52	1.41	Hom.	1.615	2.18	0.036	4.21	1.80	0.105	0.4	0.9545	**13**
304	0.52	1.41	Hom.	1.615	2.86	0.036	5.17	2.06	0.120	0.4	0.9662	**20**
263	0.56	1.41	Perm.	1.615	2.16	0.036	4.28	1.71	0.099	0.4	0.9686	**9**
268	0.56	1.41	Perm.	1.615	2.89	0.036	5.26	2.03	0.118	0.4	0.9771	**18**
300	0.56	1.41	Hom.	1.615	2.18	0.036	4.09	1.91	0.110	0.4	0.9536	**12**
305	0.56	1.41	Hom.	1.615	2.86	0.036	4.85	2.34	0.136	0.4	0.9547	**17**
264	0.62	1.41	Perm.	1.615	2.16	0.036	4.09	1.87	0.109	0.4	0.9676	**10**
269	0.62	1.41	Perm.	1.615	2.89	0.036	4.99	2.25	0.131	0.4	0.9763	**22**
301	0.62	1.41	Hom.	1.615	2.18	0.036	3.88	2.12	0.123	0.4	0.9521	**12**
306	0.62	1.41	Hom.	1.615	2.86	0.036	4.74	2.45	0.142	0.4	0.9643	**20**
265	0.68	1.41	Perm.	1.615	2.16	0.036	3.92	2.04	0.118	0.4	0.9781	**14**
270	0.68	1.41	Perm.	1.615	2.89	0.036	4.79	2.45	0.142	0.4	0.9841	**25**
302	0.68	1.41	Hom.	1.615	2.18	0.0360	3.73	2.30	0.134	0.4	0.9508	**12**
307	0.68	1.41	Hom.	1.615	2.86	0.0360	4.48	2.74	0.159	0.4	0.9630	**20**

- The range of n_1 for permeable structures is: $7 \leq n_1 \leq 25$
- The range of n_1 for homogeneous structures is: $12 \leq n_1 \leq 20$

This range indicates that a general stability relation (for all structures types) cannot be derived by using the current expression for c_r. The reason of the wide range is that the calculated run-up reduction coefficients are not sufficiently dependent on the Iribarren number. This is contradictory to the test results of VAN DER MEER [1988] and the Van-der-Meer-formula, which clearly shows a more dependent relation between the Iribarren number and the influence of the core permeability (P is 0.1, 0.5 and 0.6). Since the run-up reduction coefficient is less dependent on the Iribarren number, the stability relation for permeable and homogeneous structure types should be described separately:

Homogeneous structures:
$$\frac{H_S}{\Delta D_{n50}} = 3.1 \cdot \xi_m^{\mathbf{0.2}} \cdot \sqrt{cot\alpha} \cdot \left(\frac{S}{\sqrt{N}}\right)^{0.2} \cdot (c_r)^{11} \qquad \text{(H.7)}$$

Permeable structures:
$$\frac{H_S}{\Delta D_{n50}} = 2.7 \cdot \xi_m^{\mathbf{0.2}} \cdot \sqrt{cot\alpha} \cdot \left(\frac{S}{\sqrt{N}}\right)^{0.2} \cdot (c_r)^{15} \qquad \text{(H.8)}$$

Note H.4: *For this curve fitting the calculation results of test 265, 270, 302, and 307 are used.*

To indicate the considerable influence of the assumption on the model, some reasonable changes are made in the next elaboration. The concerning changed assumptions are:

- The imposed core run-up is 60% of the external maximum run-up (instead of 50%).

- The roughness reduction factor is 0.8 (instead of 0.75).
- The time span of run-up from SWL till maximum external wave run-up is $\frac{1}{3}T_0$ (instead of $\frac{1}{3}T_0$)

Table H.29 shows the run-up reduction coefficients when above assumptions are included. It is assumed that a_1 has a value of 1.

Table H.29 - c_r-coefficients for the tested permeable and homogeneous structure types by VAN DER MEER [1988], with changed assumptions

Test nr.	$\left(\frac{S}{\sqrt{n}}\right)^{0.2}$	$\sqrt{cot\alpha}$	Perma-bility	Δ	T_m	D_{n50}	ξ_m (N=3000)	$H_s/\Delta D_{n50}$ (N=3000)	H_s (N=3000)	Perm. core n_c	c_r	n_1
265	0.68	1.41	Perm.	1.615	2.16	0.036	3.92	2.04	0.118	0.4	0.9560	**11**
270	0.68	1.41	Perm.	1.615	2.89	0.036	4.79	2.45	0.142	0.4	0.9620	**13**
302	0.68	1.41	Hom.	1.615	2.18	0.036	3.73	2.30	0.134	0.4	0.9366	**9**
307	0.68	1.41	Hom.	1.615	2.86	0.036	4.48	2.74	0.159	0.4	0.9433	**12**

- The range of n_1 for permeable structures is: $11 \leq n_1 \leq 13$
- The range of n_1 for homogeneous structures is: $9 \leq n_1 \leq 12$

Fitting above calculation results in Eq. 6.9, the stability formulae can described as:

Homogeneous structures:
$$\frac{H_S}{\Delta D_{n50}} = 3.1 \cdot \xi_m^{\mathbf{0.2}} \cdot \sqrt{cot\alpha} \cdot \left(\frac{S}{\sqrt{N}}\right)^{0.2} \cdot (c_r)^9 \quad \text{(H.8)}$$

Permeable structures:
$$\frac{H_S}{\Delta D_{n50}} = 2.7 \cdot \xi_m^{\mathbf{0.2}} \cdot \sqrt{cot\alpha} \cdot \left(\frac{S}{\sqrt{N}}\right)^{0.2} \cdot (c_r)^{12} \quad \text{(H.9)}$$

These curve fitting results indicate that changes in above assumptions have a considerable influence on the value of the run-up reduction coefficient. Besides, the influence of the Iribarren number is increasing. Therefore, the calculation results are promising when the assumptions are changed. In other words, when some assumptions in the volume-exchange-model are changed, the formulae (H.8 and H.9) show an increasing similarity. For that reason, it is assumed that refinement of the c_r-calculation and expansion of the data set of VAN DER MEER [1988] should lead to a general stability relation in the proposed form (Eq. 6.9). Examples of refining the c_r-calculation are: including the internal water set-up, including the water flow below SWL, and taken the laminar and inertia term into account. Other recommendations for refining the calculation of the c_r-value are described in Chapter 6.5 and 7.3.